NASA/CR—2001-211160

Human Health Effects of Ozone Depletion From Stratospheric Aircraft

U.S. Environmental Protection Agency
Washington, DC

Prepared under Interagency Agreement Reference #80938647,
NASA Reference #C–30039–J

National Aeronautics and
Space Administration

Glenn Research Center

September 2001

Acknowledgments

EPA greatly appreciates input received from invited experts and others who participated in two technical workshops held in November 1999 and August 2000 by EPA, and/or who provided input on drafts of the report. These experts include:

Dr. Donald E. Anderson, National Aeronautics and Space Administration (NASA)
Dr. Steven L. Baughcum, The Boeing Company
Dr. John E. Frederick, The University of Chicago
Mr. Warren Gillette, Federal Aviation Administration (FAA)
Dr. Charles Jackman, NASA
Dr. S. Randolph Kawa, NASA
Dr. Malcolm Ko, Atmospheric and Environmental Research (AER), Inc.
Dr. Ronald D. Ley, University of New Mexico
Dr. Sasha Madronich, National Center for Atmospheric Research (NCAR)
Dr. Hugh Pitcher, Battelle Pacific Northwest National Laboratories
Dr. Ian C. Plumb, Commonwealth Scientific and Industrial Research Organization (CSIRO)
Dr. José M. Rodriguez, University of Miami
Ms. Karen Sage, Science Applications International Corporation (SAIC)
Mr. Howard L. Wesoky, FAA (retired)
Dr. Donald Wuebbles, University of Illinois

EPA would also like to particularly thank two independent peer reviewers who evaluated this report: Dr. Edward De Fabo, The George Washington University and Dr. Douglas Kinnison, NCAR.

Special appreciation is given to Dr. Frank Arnold, Dr. Janice Longstreth, Ms. Erin Meyer, Ms. Hyatt Nolan, Ms. Katrin Peterson, and Mr. Mark Wagner of ICF for their role in preparing this report and in supporting the two technical workshops.

EPA personnel participating in this effort include: Ms. Cindy Newberg, Dr. Reva Rubenstein (retired), Mr. Bryan Manning, Ms. Tia Sutton, and Mr. Stephen Seidel.

The NASA Project Officer for this IAG is Dr. Chowen Wey. The EPA Project Officer for this IAG is Dr. Lisa Chang.

Available from

NASA Center for Aerospace Information
7121 Standard Drive
Hanover, MD 21076

National Technical Information Service
5285 Port Royal Road
Springfield, VA 22100

Available electronically at http://gltrs.grc.nasa.gov/GLTRS

Preface

This report was prepared by the U.S. Environmental Protection Agency (EPA) to fulfill commitments under an Inter-Agency Agreement (IAG) with the National Aeronautics and Space Administration (NASA) (EPA IAG Reference #80938647, NASA Reference #C-30039-J). The methods used in this report reflect input from invited experts and others who participated in two technical workshops held in November 1999 and August 2000 by EPA, and/or who provided input on drafts of the report. EPA's contractor supporting this effort is ICF Consulting, Inc. (ICF). ICF also arranged for independent scientific review of this study, conducted in March-April of 2001. Two reviewers were selected as recognized experts in the relevant atmospheric sciences and health sciences fields, based upon recommendations from workshop participants. In addition to the independent review, ICF also provided the invited experts who participated in the two workshops mentioned above, as well as other relevant experts, an opportunity to provide additional comments during March-April of 2001.

As a critical part of the technology development process that focused on the commercial development of high-speed (i.e., supersonic) civil transport (HSCT), the National Aeronautics and Space Administration (NASA) requested that the United States Environmental Protection Agency (EPA) advise on potential environmental policy issues associated with the future development of supersonic flight technologies. This report presents EPA's initial response to NASA's request, through the evaluation of expected environmental and health effects related to the stratospheric ozone impacts of a hypothetical HSCT fleet. The report also provides a comparison of the estimated health impacts to those expected under previous and current control regimes for protecting stratospheric ozone.

Studies already completed under both national and international programs indicated that a future fleet of stratospheric aircraft may contribute to stratospheric ozone depletion and global climate change (e.g., IPCC 1999 and NAS 1975). However, this study is significantly different in that it draws from updated assessments of the atmospheric impacts of a future fleet of HSCT (Kawa *et al.* 1999) and updated data on the relationship between ultraviolet radiation (UVR) exposure and health effects; and it calculates impacts for health endpoints that more readily allow for comparison of the HSCT risks with those arising from previous international policies on ozone-depleting substances (ODS).

The authors of this report consulted with experts from government, industry, and academia in the fields of atmospheric chemistry and dynamics, health effects of UVR, HSCT technology, atmospheric modeling, and health effects modeling (see Acknowledgments section). In two EPA-sponsored workshops (in November 1999 and August 2000) these experts focused on choosing appropriate state-of-the-art methodology for this assessment. Throughout the study implementation period discussion continued among the experts via conference calls and other correspondence. Meeting participants reviewed an early draft of the document in August 2000, ensuring proper implementation of the methodology, adequate treatment of uncertainty, and consideration of relevant scientific and/or technological advances since project initiation.

The penultimate document was peer reviewed for its technical content by Dr. Edward DeFabo of The George Washington University and by Dr. Douglas Kinnison of the National Center for Atmospheric Research. The peer reviewers were asked to draw upon their expertise in UVR biological effects assessment and atmospheric science, respectively, to comment on whether the methods, tools, and approach used in the study reflect sound scientific practice and adequately address the questions at hand. Throughout the process of preparing this report, workshop participants also provided vital input that substantially improved the document.

Written comments were received from peer reviewers and several experts who participated in the workshops. In these comments, all reviewers who commented on the overall methodology stated that the methodology used in this study represents a sound, state-of-the-art approach to assessing the ozone-related health effects of a potential HSCT fleet. A number of comments identified areas for clarification of specific technical items, all of which have been considered by the authors. The reviewers and several experts stated that the report provides solid analysis and discussion of results, given the scope of the work and the large number of uncertainties that currently exist in the areas of ozone depletion and UVR health impacts estimation.
Several areas were highlighted during peer review of this report where additional research would enhance relevant assessment capabilities. Dr. DeFabo indicated that one of the greatest sources of uncertainty in estimating UVR-

induced health impacts is the lack of adequate experimental data from which biological action spectrum for malignant melanoma (as well as basal cell carcinoma) can be developed. Due to this lack of information, this study predicts cases of malignant melanoma based on the SCUP-h action spectrum for squamous cell carcinoma. However, this analysis should be reconsidered if future studies aimed at developing an action spectrum for malignant melanoma reveal that its shape is not congruent with the SCUP action spectrum for squamous cell carcinoma (i.e., it does not have similar shape). He also pointed out that until more data on the mechanism of UVB radiation on cataract induction becomes available (via action spectrum studies, additional epidemiological data, etc.), risk assessment regarding cataract formation and ozone depletion is also "subject to the uncertainties as properly addressed in the report." Dr. Kinnison stated that the study is limited by its assessment of UVR effects only in the population of light-skinned individuals in the United States. Indeed, data is needed for additional population skin-types in other regions of the world to complete a more comprehensive assessment of health effects resulting from UVR changes that could occur world-wide. EPA acknowledges that further scientific research in these and other areas could complement and significantly enhance the information presented in this report.

Workshop participants who reviewed the report conveyed similar points. Most other comments were editorial remarks generally intended to enhance the clarity of the report. All comments of the reviewers and workshop participants were considered, and the document was modified appropriately.

EPA wishes to acknowledge everyone involved in this report and thank all reviewers for their extensive time, effort, and expert guidance. The involvement of peer reviewers, workshop participants, and other scientific and industry contacts greatly enhanced the technical soundness of this report. EPA accepts responsibility for all information presented and any errors contained in this document.

Global Programs Division (6205J)
Office of Atmospheric Programs
U.S. Environmental Protection Agency
Washington, DC 20460

Table of Contents

Executive Summary 1

Chapter 1. Introduction and Background 11

1.1 Potential atmospheric and biological impacts of stratospheric flight 11
1.1.1 How HSCT may contribute to ozone depletion 11
1.1.2 Current assessment of atmospheric impacts from stratospheric aircraft 12
1.1.2.a. NASA's *Assessment of the Effects of High-Speed Aircraft in the Stratosphere* 13
1.1.2.b. *Aviation and the Global Atmosphere* (IPCC 1999) 15
1.1.3 Biological effects of stratospheric ozone depletion 16

1.2 Relevant U.S. and international authorities and agencies 18
1.2.1 U.S. Environmental Protection Agency (EPA) 18
1.2.2 National Aeronautics and Space Administration (NASA) 20
1.2.3 Federal Aviation Administration (FAA) 20
1.2.4 International Civil Aviation Organization (ICAO) 21
1.2.5 Montreal Protocol 22
1.2.6 UN Framework Convention on Climate Change (UNFCCC) 23

1.3 Commercial interest in supersonic technologies 25
1.3.1 Civil supersonic transport 25
1.3.2 Space and defense 26
1.3.3 Supersonic business jets 26

Chapter 2. Methods 27

2.1 Modeling overview 29

2.2 Estimated HSCT-induced ozone change 31
2.2.1 NASA assessment selection of source of central values 31
2.2.2 Adaptation of CSIRO data and fleet growth schedule 32
2.2.2.a. Adaptation of CSIRO data 32
2.2.2.b. Specification of fleet growth schedule 34

2.3 Calculation of UVR change 36

2.4 Calculation of health impacts 38
2.4.1 Human health endpoints 41
2.4.2 Other human health and environmental effects 44
2.4.3 Action spectra 45
2.4.4 Dose metrics 47

2.5 Model implementation 48

2.6 Uncertainty in estimated impacts 49
2.6.1 Uncertainties associated with change in ozone estimates 50
2.6.2 Uncertainties associated with change in UVR estimates 53
2.6.3 Uncertainties associated with change in health effect estimates 55
2.6.3.a. Uncertainty in the BAF 55
2.6.3.b. Uncertainty in population projections 55
2.6.3.c. Latency 56
2.6.4 Other sources of uncertainty 57
2.6.4.a. Contributions to unknown uncertainties in change in ozone estimates 57
2.6.4.b. Contributions to unknown uncertainties in change in health effect estimates 58

2.7 Sensitivity of estimated health impacts to technological and operational change 60

Chapter 3. Results and Discussion 63

3.1 HSCT impacts of stratospheric ozone concentrations 63
3.1.1 Annual percent change in ozone 63
3.1.2 Seasonal patterns 65
3.1.3 Latitudinal patterns 67

3.2 HSCT impacts on UVR 67
3.2.1 Seasonal patterns 70
3.2.2 Latitudinal patterns 70

3.3 HSCT impacts on human health 70
3.3.1 Total incidence and mortality due to HSCT operation 71
3.3.2 Seasonal patterns 72
3.3.3 Latitudinal patterns 73
3.3.4 Estimates of annual changes in health effects 74

3.4 Uncertainty analyses 79
3.4.1 Uncertainties associated with change in ozone estimates 81
3.4.2 Uncertainties associated with change in UVR estimates 81
3.4.3 Uncertainties associated with change in health effects estimates 82
3.4.3.a. Uncertainty in population projections 82
3.4.3.b. Latency 83
3.4.4 Summary of uncertainty analyses 85

3.5 Sensitivity to technological and operational change 86

Chapter 4. Synthesis 89

4.1 Findings in context of past ODS regulatory activities 89
4.1.1 Description of the Montreal Protocol: Amendments and adjustments 89
4.1.2 Comparison of HSCT with ODS policy scenarios 91
4.1.3 Other stratospheric protection actions within and beyond Montreal Protocol requirements 95

4.2 Applicability of results to other scenarios 97

Chapter 5. References 99

Appendix A - Overview of Evaluation Methodology 105

Appendix B - Description of the CSIRO Model 107

Appendix C - Methodological Sensitivity: Use of Relative Versus Absolute Ozone Change 109

Appendix D - Background Information on RAFs 111

Appendix E - Information and Future Directions for Cataract Methodology 115

Appendix F - Sensitivity to Choice of Reference Scenario 119

Appendix G - Summary of ODS Policy Controls 121

Executive Summary

Introduction

The National Aeronautics and Space Administration (NASA) has asked the United States Environmental Protection Agency (EPA) to advise on potential environmental policy issues associated with the future development of supersonic flight technologies. Studies undertaken under national and international programs indicate that a future fleet of stratospheric aircraft may contribute to stratospheric ozone depletion and global climate change (Kawa *et al.* 1999, IPCC 1999). NASA's request was initiated in 1998 by its High-Speed Research (HSR) program, a focused technology development program intended to enable the commercial development of high-speed (i.e., supersonic) civil transport (HSCT). Environmental policy concerns are a critical element of the technology development process (Shaw *et al.* 1997). Although the HSR program was terminated in fiscal year (FY) 1999 due to a changing market outlook for HSCT, interest both domestically and internationally persists regarding potential future supersonic aviation technology applications, including a supersonic business jet (SSBJ) aircraft.

This report presents EPA's initial response to NASA's request. Consistent with the scope of the study to which NASA and EPA agreed, EPA has evaluated only the environmental concerns related to the stratospheric ozone impacts of a hypothetical HSCT fleet, although recent research indicates that a fleet of HSCT is predicted to contribute to climate warming as well. The report first briefly reviews the considerable existing literature related to this topic. Biological and environmental concerns related to stratospheric ozone depletion are summarized, and recent assessments of HSCT's atmospheric effects are described. EPA's present evaluation relies heavily on these recent atmospheric assessments, which have been extensively reviewed by the atmospheric sciences community (Kawa *et al.* 1999, IPCC 1999). This report also briefly describes the international and domestic institutional frameworks established to address stratospheric ozone depletion, as well as those established to control pollution from aircraft engine exhaust emissions.

The main focus of this report is to address the following questions:

- What are the health impacts (and associated uncertainties) resulting from the projected atmospheric ozone changes associated with a potential future HSCT fleet?

- How do these estimated health impacts compare with those expected under previous and current control regimes for protecting stratospheric ozone?

This report also discusses the sensitivity of estimated health impacts to changes in assumptions regarding HSCT technology or operational parameters.

Overview of HSCT health impacts analysis approach

The approach to evaluating the health impacts from NASA's conceptual HSCT fleet was developed in consultation with experts from atmospheric science and health science communities. The methods and assumptions used in this study were formulated through an expert workshop hosted by EPA in November, 1999 (ICF 1999) and a meeting to review the preliminary implementation of these methods held in August, 2000 (ICF 2000*b*).

Several established sources of input and models were used to estimate the health impacts from HSCT-induced stratospheric ozone depletion. The results of a recent NASA scientific assessment (Kawa *et al.* 1999) were used to characterize a potential civil supersonic transport fleet's impacts on stratospheric ozone. These HSCT ozone impact estimates then served as inputs to the Tropospheric Ultraviolet-Visible (TUV) model, which computes the amount of ultraviolet radiation (UVR), or ultraviolet (UV) irradiance, reaching the earth's surface.[1] Estimated UV irradiance values produced by the TUV model, by month and latitude were input directly to the Atmospheric Health Effects Framework (AHEF). The AHEF, previously reviewed and used by EPA for over a decade, produces estimates of changes in skin cancer incidence and mortality, as well as cataract incidence, for given changes in UV irradiance. The AHEF was then used to generate estimates of incremental health effects from HSCT-induced ozone depletion and change in UV irradiance.

[1] TUV data tables are calculated for cloud-free conditions.

HSCT fleet scenario

The estimates of HSCT ozone impacts used in the present study are associated with a highly specific scenario of atmospheric, operational, and fleet technology parameters. The present study starts with an HSCT fleet scenario (or "base case") selected, in consultation with technology and assessment experts, from among the many scenarios evaluated by NASA (Kawa *et al.* 1999). This scenario (1,000 HSCT in 2050) differed from the NASA assessment "base case" scenario (500 HSCT in 2015), but was considered more appropriate to the present state of technology development. The aircraft is specified as a 300 passenger, 5,000 nautical mile range aircraft flying at Mach 2.4 (cruise altitude in the 17-20 km range). The engine NO_x emission index (EI) was specified at 5 g/kg, the EI(SO_2) at 0.4 g/kg, and the amount of fuel sulfur converted to particles in the wake was specified at 10 percent. Emissions inventories (based on fuel use along flight paths) were developed in consultation with industry experts based on detailed assumptions regarding future air traffic demand and HSCT market capture.

Output for this scenario (Scenario 36 in Kawa *et al.* 1999), as used in this study, was produced by the same atmospheric model selected to provide the NASA assessment base case central value. The absolute value of the uncertainty range for the NASA base case central value was also adopted as the uncertainty range around the HSCT ozone impact central value used in this study. The central value for the 1,000 HSCT, year 2050 scenario is -0.6 percent change in total column ozone (annual average value for the Northern Hemisphere). The -0.6 percent change represents the change in column ozone when a projected subsonic fleet in 2050 is replaced by a modified fleet consisting of 1,000 HSCT and fewer subsonic aircraft (to account for expected replacement of some subsonic flights by supersonic flights). The accompanying uncertainty range is defined by a range of -2.7 percent to +0.3 percent around a central value of -0.6 percent.

Furthermore, for the present study, the estimated steady-state ozone impact values for this fleet scenario were extrapolated to provide a time-dependent estimate of HSCT-induced ozone change. This extrapolation assumed linear growth from 0 in-service HSCT in 2015 to 1,000 aircraft in 2050. A linear relationship between fleet size and estimated ozone impact is also assumed. Fleet size (and also ozone impact) was held constant from 2050 to 2100, the last year examined in this study.

Estimate of health impacts from HSCT-induced ozone change

Data presented in Table 1a can be used to calculate the central values of total skin cancer incidence (i.e., the sum of CMM, BCC, and SCC incidence estimates), total skin cancer mortality (i.e., the sum of CMM and NMSC mortality estimates), and total cataract incidence resulting from this hypothetical HSCT fleet scenario. Those values are 1.5 million cases of skin cancer, 7,100 cases of skin cancer mortality, and 360,000 cases of cataracts. These values represent the incremental health effects expected when a projected subsonic fleet is replaced by a modified fleet (i.e., including 1,000 HSCT and a slightly reduced subsonic fleet). Also shown in parentheses in Table 1a are upper and lower uncertainty bounds around the estimated central value. These upper and lower uncertainty bounds are based only on consideration of the uncertainty range in the estimated HSCT atmospheric impacts. All values in Table 1a are subject to an additional uncertainty (approximately a factor of 2) due to uncertainties related to the estimation of biological effects of UVR. All values in Table 1a are subject to further uncertainty due to factors which are presently difficult to quantify, such as long-term changes in atmospheric opacity and human UVR exposure behavior. For all values in Table 1a, incidence and mortality estimates were created for model cohorts in the U.S. light-skinned (skin cancer) population[2] born between 1890 and 2100.

Table 1a. Estimated Incremental U.S. Health Impacts due to HSCT Fleet among People Born between 1890 and 2100 (thousands of cases)

Numbers in parentheses are upper and lower bounds, based only on the uncertainty range in estimated HSCT ozone impacts. All values, including those in parenthesis, are subject to additional uncertainty (approximately a factor of 2) due to uncertainties related to the estimation of biological effects of UVR. See text for additional discussion of uncertainty.

	CMM Incidence	CMM Mortality	BCC Incidence	SCC Incidence	NMSC Mortality	Cataract Incidence
HSCT	36 (-25 to 180)	4.5 (-3 to 23)	970 (-690 to 4,900)	520 (-380 to 2,700)	2.6 (-2 to 13)	360 (-270 to 1,900)

CMM = Cutaneous Malignant Melanoma, **BCC** = Basal Cell Carcinoma, **SCC** = Squamous Cell Carcinoma, **NMSC** = Non-Melanoma Skin Cancer (SCC + BCC)

[2] The term "light-skinned" reflects the degree of skin pigmentation in people most sensitive to UVR. "Light-skinned" refers to people with Type I skin (very pale skin that burns often and never tans) and Type II skin (skin that burns often and tans minimally). The population of light-skinned individuals in the U.S. is the population segment for which sufficient data exists to perform the quantitative modeling exercises used in this evaluation.

Health effects under previous stratospheric protection control regimes

Rows (a) through (d) of Table 1b show the number of "excess" health effects cases that were estimated to occur under several ozone-depleting substance (ODS) policy scenarios relative to 1979 -1980 ("baseline") levels of ozone depletion. The same UVR and health effects models were used for all scenarios presented in Tables 1a and 1b, and health effects estimates were based on consideration of the same baseline data and simulation period. The values in rows (a) - (d) are taken from an earlier study (ICF 2000*a*). As with the values in Table 1a, the values in Table 1b are subject to some uncertainty due to uncertainty in atmospheric inputs (discussed in WMO 1999), and they are subject to additional uncertainty (approximately a factor of 2) related to the estimation of biological effects of UVR.

Row (a) of Table 1b shows that according to previous model studies, about 6.3 million "excess" cases of CMM (i.e., in excess of baseline incidence of this malady) in the U.S. light-skinned population would have occurred under an atmosphere reflecting worldwide compliance with the controls set forth in the original 1987 Montreal Protocol. Row (d) shows that if all Parties (i.e., nations) to the Montreal Protocol fully implement the Protocol, including all amendments and adjustments (through the Montreal Adjustments), approximately 130,000 cases of CMM, in excess of baseline CMM incidence, would still occur in the U.S. light-skinned population.

Table 1b. Estimated Excess U.S. Health Impacts among People Born between 1890 and 2100 under Several Ozone-Depleting Substance (ODS) Policy Scenarios (thousands of cases)

Source: ICF 2000(a). See text for additional discussion.

	CMM Incidence	CMM Mortality	BCC Incidence	SCC Incidence	NMSC Mortality	Cataract Incidence
Montreal Protocol (row a)	6,300	820	160,000	80,000	380	140,000
London Amendments (row b)	330	41	8,100	4,100	18	3,500
Copenhagen Amendments (row c)	160	20	4,000	2,000	8.3	1,700
Montreal Adjustments (row d)	130	17	3,300	1,600	6.9	1,400

CMM = Cutaneous Malignant Melanoma, **BCC** = Basal Cell Carcinoma, **SCC** = Squamous Cell Carcinoma, **NMSC** = Non-Melanoma Skin Cancer (SCC + BCC)

"MONTREAL PROTOCOL" of 1987: Freeze of CFC production and consumption at 1986 levels; 50% reduction in CFC production by 1998 (for developed countries) and 2008 (for Article 5 (developing) countries); later production freezes on halons, other halogenated compounds, carbon tetrachloride (CCl_4), and methyl chloroform (CH_3CCl_3).

"LONDON AMENDMENTS" of 1990: Complete phase-out of CFCs, hydrochlorofluorocarbons (HCFCs), and CCl_4 by 2000 (developed countries) and by 2010 (Article 5 countries); complete phase-out of CH_3CCl_3 by 2005 (developed countries) and by 2015 (developing countries).

"COPENHAGEN AMENDMENTS" of 1992: Accelerated phase-out of CFCs, CCl_4, and CH_3CCl_3 by 1996 and halons by 1994 (developed countries); and accelerated reduction of HCFCs and hydrobromofluorocarbons (HBFCs) (Article 5 countries).

"MONTREAL ADJUSTMENTS" of 1997: Complete phase-out of methyl bromide by 2005 (developed countries) and 2015 (Article 5 countries); HCFC phase-out schedule (Article 5 countries).

Comparison of HSCT Impacts with health effects under previous stratospheric protection control regimes

A key manner in which the data in Table 1b can be read is to indicate the incremental health benefits (i.e., avoided health impacts) achieved by each set of amendments and adjustments to the Montreal Protocol. For example, data in rows (c) and (d) of the table indicate that the increase in the stringency of the Montreal Protocol through the Montreal Adjustments was expected to decrease CMM incidence by approximately 30,000 cases (relative to health impacts under the Montreal Protocol as amended and adjusted through the Copenhagen Amendments of 1992; i.e., row (d) subtracted from row (c)).

At the same time, the estimates in Table 1a indicate that the simulated incremental increase in CMM incidence due to operation of an HSCT fleet is about 36,000 additional cases relative to an atmosphere in the absence of this fleet (i.e. relative to the Montreal Adjustments). This comparison indicates that the negative human health impacts associated with operation of the proposed fleet of HSCT are of similar magnitude to the health benefits expected from recent increases in stringency agreed upon by the Parties to the Montreal Protocol.

The Protocol serves as the chief forum for the establishment of effective global control measures for protecting stratospheric ozone. Today, 175 countries have ratified the Montreal Protocol, and 48 have ratified the Montreal Adjustments. The Parties to the Protocol also meet regularly to consider further measures to protect stratospheric ozone, such as the "Beijing Amendments" to which the Parties agreed in 1999. Although Parties to the Protocol must align their domestic regulations with the control measures of the Protocol, any Party may adopt more stringent measures.

Uncertainties in estimated health impacts

The sources of uncertainty in the estimated health impacts from the modeled HSCT fleet originate at each modeling step in this assessment: (1) model calculations of the impact of the HSCT fleet scenario on atmospheric ozone, (2) translation of the atmospheric ozone changes to biologically-weighted UVR exposures, and (3) translation of weighted UVR exposures to skin cancer incidence, skin cancer mortality, and cataract incidence. The same uncertainties arising from (2) and (3) would also apply to the estimates of health impacts under ODS policy scenarios. In addition, uncertainty in estimated health impacts associated with ODS-induced ozone depletion also arises from uncertainties in projected atmospheric impacts of ODS policy scenarios, which have been discussed elsewhere (WMO 1999).

The estimated HSCT health impact is uncertain to a factor of -1.7 to + 4.1 about the central value due to uncertainties in estimated fleet atmospheric impacts (see Table 3-2). This is the uncertainty range that is indicated in Table 1a. It should be noted that this uncertainty range comprises not only the possibility for adverse health impacts of much larger magnitude than the central value, but also the possibility that the impacts may be *directionally* different; an atmosphere with HSCT-induced ozone change could lead to a *reduction* in skin cancer and cataract occurrences, relative to a reference atmosphere. This latter estimated possibility

arises from the uncertainty in the estimated column ozone response to HSCT. In addition to providing an estimate of how much larger than the central value the estimated HSCT ozone depletion could be, the NASA assessment concluded that there is a small possibility that the HSCT fleet could lead to an increase in column ozone.

The estimated health impacts due to HSCT-induced ozone depletion (as well as the estimated health impacts under the ODS policy scenarios) are estimated to be further uncertain to a factor of approximately 2 due to presently quantified uncertainties in health effects parameters. Finally, these uncertainty factors do not reflect consideration of all sources of uncertainty. Additional sources include long-term, systematic changes in atmospheric opacity; changes in human UVR exposure behavior; limited experimental data from which to derive certain effect-specific UVR weighting functions; and improvements in medical care and increased longevity. Assumptions have been made based on best available knowledge, but further quantitative tests are needed to understand the sensitivity of simulated results to each of the assumptions. Nevertheless, it can be seen that the estimated health impacts from the HSCT scenario modeled in this study may be considerably less, or far greater than, the central value.

Accurate prediction of future changes in health effects would require consideration of the net effect of all factors such as those listed above. This is a task that is beyond the ability of the current state of the science, both atmospheric and epidemiological. Furthermore, it should be recognized that no direct measurements (e.g., of future UV levels or skin cancer incidence) will be able to attribute explicitly observed changes to any specific factor, unless such a factor is far more important that all the others combined. Nevertheless, it is possible to examine one of these effects, the HSCT impact, in isolation, under the assumption that the other factors are maintained constant at current conditions. The validity of this principle is based on the assumption that the HSCT impacts are independent of the other factors (e.g., behavioral changes will occur regardless of whether an HSCT fleet is in place).

Sensitivity of estimated health impacts to technological and operational change

Previous work by NASA (Kawa *et al.* 1999) characterized the sensitivity of the predicted HSCT ozone impact to selected changes in assumptions regarding fleet technology and operational design options. For example, that study found that decreasing fleet cruise altitude by 2 km reduced the average annual Northern Hemisphere column ozone impact by 50 percent.

Elimination of fuel sulfur content decreased the column ozone response by 75 percent. Changes in atmospheric ozone of this magnitude are simulated to lead to health effects changes of similar proportion. For example, a 50 percent reduction in estimated ozone depletion is expected to lead to roughly 50 percent decreases in estimated skin cancer and cataract impacts. Thus, there may be some possibility to mitigate adverse health impacts of HSCT-induced ozone depletion through changes in technological and operational parameters.

Applicability of results to other scenarios

The present study has evaluated a single conceptual scenario for a large fleet of long-range supersonic commercial transport aircraft. The emissions inventory constructed to represent the chemical inputs to the atmosphere from this fleet were based upon specific aviation traffic and market scenario projections as well as narrowly-defined projections of aircraft performance and emissions. Simulated atmospheric impacts, in turn, are sensitive to the fleet's emissions, cruise altitude, and flight routes. The results of the present study should be considered highly specific to the single scenario considered in this evaluation because UVR exposure and health responses are sensitive to these simulated atmospheric impacts. Also, the results of this study should not be directly extrapolated to estimate the health impacts from substantially different future atmospheric or fleet operational or technological scenarios (e.g., a fleet of business jets that fly in the stratosphere).

For substantially different fleet scenarios (e.g., different aircraft, different routes, different altitudes, different emissions characteristics) the atmospheric impacts would likely have to be re-assessed, including re-evaluation of uncertainties in atmospheric impacts. In addition, as the scientific knowledge of stratospheric chemistry and dynamics, background atmosphere, global atmospheric change, and human health effects evolves, the models and assumptions used in future analyses should be updated accordingly. In contrast, the general methodology or sequence of modeling tools used in the present study should be applicable to a wide range of future stratospheric aviation scenarios, provided adequately updated and appropriate inputs are used.

Chapter summaries

Chapter 1 of this report provides a broad scientific and institutional context for the analyses presented. Chapter 2 describes the modeling method used to evaluate the impacts of estimated HSCT-induced column ozone changes on UVR and selected human health endpoints. Chapter 3 presents the results of modeling simulations, and discusses uncertainties and potential sensitivity of results to technological and operational factors. Chapter 4 discusses: 1) the results in the context of previous regulatory actions to protect stratospheric ozone and 2) the applicability of the methods and results of this study to scenarios other than the single HSCT fleet scenario evaluated in this report.

Chapter 1. Introduction and Background

This chapter provides background information on recent assessments of the potential impacts of stratospheric aircraft on the atmosphere, focusing on stratospheric ozone impacts and biological and human health concerns associated with stratospheric ozone depletion. This chapter also provides brief descriptions of institutional and regulatory bodies with authority or interest relative to the environmental impacts of stratospheric aircraft, and it briefly describes recent commercial interest in supersonic flight.

1.1 Potential atmospheric and biological impacts of stratospheric flight

Activities that may contribute to the depletion of stratospheric ozone are a matter of concern because lower levels of ozone can lead to adverse environmental and biological impacts. The following discussion provides a brief explanation of the main impacts.

1.1.1 How HSCT may contribute to ozone depletion

High-speed civil transport (HSCT) is a type of supersonic aircraft that would cruise in the stratosphere, carry approximately 300 passengers each, and travel at more than twice the speed of current commercial subsonic aircraft (Mach 2.4, 1,600 mph). The estimated impacts of HSCT on ozone depletion are based largely on three main constituents of the exhaust emissions of HSCT: oxides of nitrogen (NO_x), water vapor (H_2O), and oxides of sulfur (SO_x). In the middle and upper stratosphere, the primary process for ozone loss involves NO_x radicals (Kawa *et al.* 1999). As NO_x radicals from HSCT exhaust accumulate at altitudes above 22 kilometers (km), ozone depletion may be exacerbated. In the lower stratosphere, these emissions can have varying effects on ozone depletion since NO_x can moderate ozone loss caused by other radicals such as hydrogen oxides (HO_x), chlorine oxides (ClO_x), and bromine oxides (BrO_x). In addition, NO_x participates in the formation of polar stratospheric clouds (PSCs) that provide a substrate for ozone depletion reactions and that are responsible for large seasonal ozone loss in polar regions.

Water vapor in HSCT exhaust can affect stratospheric ozone depletion in several ways. First, as the source of HO_x radicals, increased water in the atmosphere leads to higher

concentrations of HO_x, which is as important as NO_x in exacerbating ozone loss. Second, increased water in the atmosphere affects the relative concentrations of radical species since it increases the reactivity of aerosols toward gases such as hydrogen chloride (HCl) and chlorine nitrate ($ClONO_2$). Also, water vapor increases the condensation temperature in the atmosphere and thus influences the composition and growth of aerosol particles (promoting the formation of PSCs) (Kawa *et al.* 1999).

Finally, SO_x in HSCT emissions may affect ozone loss by potentially increasing the aerosol surface area throughout the stratosphere. Current studies show that stratospheric aerosol surface area is sensitive to processes that convert SO_x to sulfate particles in the aircraft wake, although these processes are not well understood and large uncertainties remain. Increases in aerosol surface area suppress NO_x and enhance ozone loss caused by other radicals such as ClO_x and HO_x. The net effect of aerosol in HSCT emissions is uncertain, but atmospheric ozone is known to be sensitive to changing aerosol conditions (Kawa *et al.* 1999).

1.1.2 Current assessment of atmospheric impacts from stratospheric aircraft

Much of the evaluation of the impacts on human health presented in this document builds on two atmospheric assessments: the National Aeronautics and Space Administration's (NASA) *Assessment of the Effects of High-Speed Aircraft in the Stratosphere* published in 1999 (hereafter referred to as the NASA assessment) and the Intergovernmental Panel on Climate Change's (IPCC) special report, *Aviation and the Global Atmosphere* (IPCC 1999).

Both of these assessments focus on the effects of aviation on the atmosphere, but the analyses have a few key differences. The IPCC report emphasizes the aviation industry as a whole, whereas the NASA assessment focuses on evaluating the incremental impacts of supersonic aviation. Both assessments assumed that a fraction of the subsonic fleet was replaced by the supersonic fleet. The IPCC study also evaluates potential fleet impacts on erythemally weighted (i.e., sunburn-causing) ultraviolet radiation (UVR).[1] Both studies assume identical

[1] The term "ultraviolet" refers to a portion of the electromagnetic spectrum with wavelengths shorter than visible light. The sun produces UVR, which is by convention commonly split into three bands: UV-A, UV-B, and UV-C. Although artificial sources of UVR (e.g., sun lamps) have been associated with adverse health effects, the term is used in this document to refer exclusively to solar ultraviolet irradiance.

scenarios with respect to the development and operation of an HSCT fleet, but results from different atmospheric models were selected to provide the central-value estimates of ozone change. The following section presents a brief summary of findings from the two assessments.

1.1.2.a. NASA's *Assessment of the Effects of High-Speed Aircraft in the Stratosphere*

As part of the agency's Atmospheric Effects of Aviation Project, a component of its High-Speed Research (HSR) program, NASA performed a comprehensive assessment of the potential incremental impacts on atmospheric chemistry and climate when the projected subsonic fleet is modified to include HSCT. This effort served as a follow-up to a previous HSCT assessment performed by NASA (Stolarski *et al.* 1995). From 1989 to 1998, scientists from universities, industry, NASA, other federal research facilities, and international research programs carried out the assessment. The findings represent a broad consensus of the atmospheric research community, including the report's authors, reviewers, and other contributors.

The assessment assimilated current scientific understanding of the fundamental physics and chemistry of the atmosphere relevant to predicting HSCT impacts, including trends in major trace chemical constituents of the stratosphere and present understanding of atmospheric transport and photochemical processes. This understanding is based on recent observations by atmospheric measurement campaigns from a variety of research platforms, as well as laboratory studies of chemical reactions and rates. In conjunction with NASA and industry technologists, the assessment also developed estimates of the future distribution of HSCT emissions in the global atmosphere. In addition, the assessment integrated research on fluid dynamics, chemistry, and particle microphysics as they relate to aircraft near-field, aircraft far-field, and global scale dispersion.

The NASA assessment also addressed seasonal and geographic patterns in column ozone impacts, assumptions regarding the composition of the future atmosphere, and sensitivities to parameters that potentially could be controlled through regulation or technological and operational modifications (e.g., developments in NO_x combustor technology, fuel sulfur content and subsequent oxidation, and fleet cruise altitude). Results of these evaluations are presented in the NASA assessment (Kawa *et al.* 1999).

Overall, NASA predicted the annual average change in ozone for the Northern Hemisphere to be -0.4 percent, assuming a fleet of 500 HSCT in 2015, with an uncertainty range of -2.5 percent to +0.5 percent.[2] Both the estimated ozone impact and the uncertainty bounds used in the evaluation are based on a combination of model results and expert judgment. The uncertainty bounds were produced by listing uncertainties in the model (e.g., emissions to the atmosphere, transport of emissions, chemical effect of emissions) and then assigning qualitative confidence ratings and numerical uncertainty ranges to each contributing factor. The ratings and ranges are based on a combination of numerical tests, comparison with measurements, and theoretical expectations.

The assessment resulted in several key findings in addition to those described above:

- Water vapor, an inherent byproduct of jet fuel combustion, accounts for a major part of the estimated stratospheric ozone impact of a fleet of HSCT. Increased water vapor in the stratosphere may contribute to global climate warming as well.

- Production of sulfate aerosol particles in the wake makes a potentially significant contribution to the calculated ozone impact of a proposed HSCT fleet.

- NO_x emissions are an important parameter in the assessment of HSCT impacts on ozone depletion. Although current atmospheric models do not indicate a high level of sensitivity to very low emissions (EI_{NOx} = 5 g/kg to 10 g/kg), higher NO_x emissions clearly increase the impact on stratospheric ozone, especially in the case of larger fleets.

- Flying HSCT at lower altitudes reduces stratospheric ozone depletion.

- Exhaust build-up in polar regions presents additional concerns related to ozone depletion, both in winter and summer.

---

[2] These results are based on the scenario of 500 HSCT in the year 2015 flying Mach 2.4 with a NO_x emission index of 5 g/kg, an EI_{SO_2} of 0.4 g/kg, and 10 percent of fuel sulfur converted to particles.

- The total climate forcing (radiative forcing) from 1,000 HSCT is calculated to be +0.1 Watts per square meter (W/m^2) in 2050, with an uncertainty level approximated by a factor of at least 3 due to uncertainty in exhaust accumulation and temperature adjustment to a non-uniform perturbation of radiatively active gases in the stratosphere. This level of climate forcing is disproportionately large for the projected fuel use, and it is equivalent to approximately 50 percent of the predicted forcing from the entire subsonic fleet projected for 2050.

1.1.2.b. *Aviation and the Global Atmosphere* (IPCC 1999)

The IPCC's report addresses the impacts of both subsonic and supersonic aviation on atmospheric ozone, UVR at the ground, and climate change, in addition to analyzing regulatory and market-based mitigation responses. The IPCC evaluated a scenario in which a fleet of supersonic aircraft replaced a proportion of the subsonic fleet. The IPCC assumed that the supersonic fleet would begin operation in 2015, growing to a maximum of 1,000 aircraft by 2050. The NASA assessment used the same model (2-D or 3-D) to estimate the impacts of both subsonic and supersonic aviation on stratospheric ozone. In contrast, the IPCC methodology combined 3-D model estimates generated for subsonic aircraft with 2-D model estimates generated for HSCT to quantify the total impact of subsonic and supersonic aviation on stratospheric ozone.

The IPCC evaluation predicted a reduction in stratospheric ozone as a result of the combined fleet. The greatest effect was predicted for the month of July at 45°N, when the ozone column change in 2050 relative to the scenario without aircraft is -0.4 percent, with the supersonic component of the fleet contributing about -1.3 percent and the subsonic component contributing about +0.9 percent. The IPCC also addressed the impacts on erythemal dose rate (i.e., the irradiance on a horizontal surface adjusted to account for the sunburning effect of the radiation). As compared with a no-aircraft scenario, the combined fleet would change the dose rate at 45°N in July by +0.3 percent, with a two-thirds uncertainty range[3] of -1.7 percent to

[3] The IPCC report defines the two-thirds uncertainty range to mean that there is a 67 percent probability that the true value falls within this range. The IPCC report also states that the confidence interval was derived based in part on expert judgment of scientists contributing to each relevant chapter and may include a combination of objective statistical models and subjective expertise. It therefore does not imply one specific statistical model.

+3.3 percent. The IPCC report predicted that by 2050 this combined fleet would increase the radiative forcing under the reference scenario (0.19 W/m^2 assuming no supersonic aircraft) by an additional 0.08 W/m^2, primarily as a result of the accumulation of stratospheric water vapor.

1.1.3 Biological effects of stratospheric ozone depletion

One significant effect of stratospheric ozone depletion is the increased transmission of UVR to the Earth's lower atmosphere (the troposphere) and surface. Many biological and chemical processes are known to be affected by UVR, and individual organisms can be harmed considerably by UVR. As discussed in several United Nations Environment Programme (UNEP) documents (UNEP 1991, 1994, and 1998), specific concerns include increases in the incidence of skin cancer, ocular damage, and other health effects in humans and animals; damage to terrestrial and oceanic vegetation; damage to some outdoor materials; changes in the chemistry of the lower atmosphere (e.g., photochemical smog formation); and alterations of the biogeochemical cycles of 1) non-living, 2) organic, and 3) inorganic matter whose degradation depends on exposure to ambient solar radiation (Madronich *et al.* 1998).

Humans and animals are exposed to the UV-B rays in sunlight principally through the eyes and skin. Effects of exposure occur as certain molecules, or chromophores, present in the tissues and cells of these organs absorb solar energy. The absorption of this energy leads to molecular changes that eventually can result in a biological effect (Longstreth *et al.* 1998).

Chromophores absorb light energy from various wavelengths with varying efficiencies. Five of the chromophores present in skin and eye tissues that are key to the biological effects of UV-B in humans and animals are DNA, tyrosine and tryptophan (two amino acids that are largely responsible for UVR absorbance by proteins), trans-urocanic acid (a molecule present in quantity in the outermost layer of skin), and melanin (the principal skin pigment). Research has documented the effects of sunlight on health in three major organ systems: the eye, the immune system, and the skin (Longstreth *et al.* 1998).

One of the key parameters required to predict biological impacts associated with increased UVR is the action spectrum, which describes the relative effectiveness of UV-A and UV-B wavelength radiation in the induction of a particular health effect (see Section 2.4.3). Due to limited experimental data from which action spectra are derived, the best available action

spectra for health effects such as melanoma skin cancer and cataracts still include a significant degree of uncertainty. Uncertainties in action spectra are discussed in Sections 2.6.3 and 2.6.4 of this report.

Since the early 1970s, scientists have conducted research to better understand and characterize the relationships between UVR exposure and biological effects. Research on the relationships between UVR exposure and biological effects has been summarized in EPA (1987) and UNEP (1991, 1994, and 1998). Quantitative risk estimates are available for some UV-B-associated effects (e.g., cataract and skin cancer), but insufficient data are available to develop similar estimates for effects such as immunosuppression.

Several efforts have been made to assess the human health impacts from stratospheric flight and its atmospheric ozone effects. Cutchis examined relationships between human erythemal dose rates and changes in stratospheric ozone that could arise from a future stratospheric flight (Cutchis 1974). This work, however, did not consider specific aircraft fleet scenarios. The U.S. Department of Transportation (DOT) Climate Impact Assessment Program (CIAP) assessed the possible physical, biological, social, and economic effects that might result from future aircraft operations in the stratosphere. A National Academies of Sciences and Engineering committee (established to advise DOT on CIAP) reported on potential skin cancer and climate impacts of stratospheric aircraft. The report from this committee provided estimates of the percentage increases in the incidence of skin cancer likely to occur for given stratospheric aircraft fleet scenarios and discussed uncertainties in the estimates (NAS 1975).

More recently, as noted in Section 1.1.2.b., the IPCC evaluated the potential impacts of future worldwide aviation activity on atmospheric ozone and erythema. The scenarios of future aviation activity included fleets with 500 to 1,000 supersonic aircraft operating in the stratosphere. To project changes in UVR associated with fleet scenarios, the IPCC used ozone change data produced by a set of atmospheric models. Changes in erythemal dose under the world aircraft fleet, both with and without a supersonic component, were projected for the years 2015 and 2050.

The present study uses the recent assessment of the atmospheric impacts of a future fleet of HSCT (Kawa *et al.* 1999) as well as updated data on the relationship between UVR exposure and health effects to calculate impacts for health endpoints that more readily allow for

comparison of the HSCT risks with those arising from previous international policies on ozone-depleting substances (ODS).

1.2 Relevant U.S. and international authorities and agencies

Many organizations are or may potentially be interested in aircraft emissions as they pertain to air quality, stratospheric ozone depletion, and the potential effects on global warming. An understanding of the existing institutional framework is helpful to placing the findings of this study into the appropriate context (see Chapter 4). The following sections provide background information on this institutional framework, including these authorities:

- U.S. Environmental Protection Agency (EPA)
- National Aeronautics and Space Administration (NASA)
- Federal Aviation Administration (FAA)
- International Civil Aviation Organization (ICAO)
- Montreal Protocol
- United Nations Framework Convention on Climate Change (UNFCCC)

1.2.1 U.S. Environmental Protection Agency (EPA)

The mission of EPA is to protect human health and safeguard the natural environment – air, water, and land – upon which life depends. As the U.S. Congress has passed legislation to address environmental and human health threats, EPA has responded with a comprehensive set of regulations aimed largely at controlling risks. EPA also employs innovative environmental protection programs to achieve its goals. For example, EPA partners with the U.S. Department of Energy (DOE) in the voluntary ENERGY STAR® labeling program. In order to reduce carbon dioxide emissions, ENERGY STAR identifies and promotes energy-efficient products, including residential heating and cooling equipment, major appliances, office equipment, lighting, consumer electronics, and other product areas.

Section 231 of the Clean Air Act (42 U.S.C. §7571) authorizes EPA to set emissions standards for air pollutants emitted from aircraft engines that cause, or contribute to, air pollution endangering public health or welfare. Under the authority of Section 231, EPA issued emission standards in 1973 for air pollutants generated during the landing/take-off cycle of aircraft

operation by subsonic and supersonic aircraft engines. In 1976, EPA adopted hydrocarbon (HC), NO_x, and carbon monoxide (CO) standards for supersonic aircraft engines. These standards were revised in 1982 (by revision of HC standards and withdrawal of existing NO_x and CO standards).

At the international level, ICAO adopted HC, NO_x and CO standards for supersonic engines in 1981. EPA has worked with ICAO and the U.S. FAA to continue developing appropriate emission standards for aircraft engines. More recently, as directed by Section 231, EPA promulgated regulations that adopt the international standards established by ICAO for NO_x and CO emissions from subsonic aircraft engines. The regulations include emission standards for subsonic gas turbine engines, which power almost all of the U.S. commercial aviation fleet, as well as engines designed for aircraft that operate at supersonic flight speeds.

Title VI of the Clean Air Act (CAA) provides EPA with broad regulatory authority to protect the stratosphere. Under this title, EPA implements the requirements of the 1987 Montreal Protocol on Substances that Deplete the Ozone Layer (see Section 1.2.5 below). Section 614 (b) of the CAA (42 U.S.C. §7671 (m)) requires that in the case of any conflict "between any provision of [Title VI] and any provision of the Montreal Protocol, the more stringent provision shall govern." Section 615 of the CAA (42 U.S.C. §7671(n)) authorizes EPA to promulgate regulations to control any substance, practice, process, or activity that may reasonably be anticipated to affect the stratosphere, and especially ozone in the stratosphere, where the effect may endanger public health or welfare. Under Title VI, EPA has developed various regulatory programs to protect the ozone layer, including programs to phase-out of production many ODS such as CFCs and halons; product labeling programs; recycling programs for stationary and motor vehicle refrigerants; and programs to review substitutes for ODS. EPA also engages in communication and outreach activities related to the science and impacts of ozone depletion.

Section 103(a) of the CAA, 42 U.S.C. §7403(a), requires EPA to establish a national research and development program for the prevention and control of air pollution. As part of this effort, EPA is required to conduct and accelerate research, investigations, experiments, demonstrations, surveys, and studies relating to the causes, effects (including health and welfare effects), extent, prevention, and control of air pollution. Section 103(b), 42 U.S.C. §7403(b), authorizes EPA to cooperate with other federal departments and agencies on the research and other activities.

1.2.2 National Aeronautics and Space Administration (NASA)

Among NASA's core missions is the preservation of the pre-eminent position of the United States in the development and application of aeronautical science and technology. Given the projected growth in commercial air travel and the strong international competition in the sale of commercial aircraft, revolutionary aircraft technologies need to be developed rapidly in order to ensure the welfare of the traveling public and create new markets for the U.S. aircraft industry. The goal of such technologies will be to increase the safety and affordability of air travel and to minimize any resulting effects on the environment (NRC 1997).

The HSR program (a 10-year, $1.2 billion partnership between NASA, Boeing, McDonnell-Douglas, General Electric, and Pratt and Whitney) was one of two NASA programs designed to achieve these results. As stated earlier, the HSR program was a focused technology program intended to enable the commercial development of HSCT. Phase I (Technology Exploration) of the program was completed in fiscal year (FY) 95 and produced critical information regarding the ability of HSCT to satisfy environmental concerns (i.e., noise and engine emissions). Phase II (Technology Development) focused on development of specific technologies related to affordability, airframe durability, engine service life, engine emissions, aircraft manufacturing and production, and range.

Despite excellent progress (NRC 1997), changes in the market outlook for the HSCT led to termination of the focused HSR program in FY 1999. NASA continues work on supersonic technologies under programs distributed among several newer initiatives such as the Ultra-Efficient Engine Technology (UEET) program.

1.2.3 Federal Aviation Administration (FAA)

The primary responsibility of the FAA, an agency of the DOT, is to assure the safety of civil aviation. This mission includes overseeing the development and implementation of programs designed to control the environmental effects of civil aviation. Under Section 232 of the CAA, the Secretary of Transportation is responsible for the enforcement of the aircraft emission standards set forth by EPA under Section 231 of the CAA. Engine emissions certification testing is conducted by engine manufacturers, and enforcement is conducted through program administration and monitoring by the FAA. Within the FAA, the Office of Environment and

Energy develops, recommends, and coordinates national aviation policy as it relates to environment and energy matters.

1.2.4 International Civil Aviation Organization (ICAO)

ICAO, established in 1944 under the Convention on International Civil Aviation (the "Chicago Convention"), is the agency in the United Nations with global responsibility for the establishment of standards, recommended practices, and guidance on various aspects of international civil aviation, including the environment. In 1986, ICAO established the Committee on Aviation Environmental Protection (CAEP) to address noise and emission-related problems associated with aviation activities and to identify appropriate standards and recommended practices.[4] CAEP works closely with regional bodies and national airworthiness authorities to discuss and propose changes in recommended environmental standards. In the evaluation process, CAEP considers technical feasibility, economic reasonableness, and the environmental benefit of proposals. If standards and recommendations proposed by CAEP are adopted by ICAO, they are attached as Annexes to the Chicago Convention.

The Chicago Convention states that participating nations, such as the United States, have an obligation to adopt the ICAO established standards to the extent possible. A country that decides not to comply with the established standards must provide ICAO with a written explanation describing why compliance is impractical or how compliance would compromise its national interest. Most states take ICAO's international standards, recommended practices, and guidance material into account in regulating their domestic aviation. To date, ICAO efforts have focused on establishing standards for aircraft noise and emissions from subsonic and supersonic aircraft engines during landing and takeoff cycles.

ICAO/CAEP's technical working group on emissions has held discussions concerning the development of standards for a potential next-generation supersonic transport. Working papers submitted by the aviation industry (Gerstle 1996, Baughcum 1997) identified important considerations relative to potential emissions standards for a future supersonic transport:

[4] The Committee on Aircraft Engine Emissions and the Committee on Aircraft Noise were predecessor to CAEP.

- Emissions of concern would be those related to a supersonic transport's ground-level, climate, and stratospheric ozone impacts and would also include those already regulated under existing landing and take-off standards;

- Standards would be a key factor in the design of a future supersonic transport;

- Current standards for both subsonic and supersonic engines are based on emissions during the landing and take-off phases of the flight cycle, but a supersonic standard would need to consider cruise emissions as well;

- The Parties to the Montreal Protocol on Substances that Deplete the Ozone Layer ("Montreal Protocol") potentially could specify restrictions to limit the stratospheric impact; and

- The Parties to the UNFCCC also could elect to constrain supersonic transport emissions due to climate considerations.

With respect to addressing the contribution of aviation to climate change, in 1998 the 32nd ICAO Assembly recognized the work already done by CAEP in recent years. The CAEP work plan calls for working groups to study technical and operational approaches as well as market-based options for reducing greenhouse gas emissions. Furthermore, CAEP tasked the Secretariat with continued attention to help bridge the efforts of CAEP and the UNFCCC.

1.2.5 Montreal Protocol

On September 16, 1987, the United States, along with 23 other nations and the European Economic Community, signed the Montreal Protocol on Substances that Deplete the Ozone Layer. The Protocol was soon ratified by 34 countries and became effective on January 1, 1989. The Protocol originally placed limitations on the production and consumption of chlorofluorocarbons (CFCs) and halons. Over the past 12 years, the Protocol has been amended on several occasions to increase the array of ozone-depleting chemicals regulated under it and to increase the stringency of the control measures. To date, over 170 countries have ratified the original Protocol. Key provisions include the following:

- Developed countries must phase out CFCs, carbon tetrachloride, methyl chloroform, and hydrobromofluorcarbons (HBFCs) by 1996; halons by 1994; methyl bromide by 2005; and hydrochlorofluorocarbons (HCFCs) by 2020 (although 0.5 percent of production is permitted for maintenance purposes only until 2030);

- Developing countries have a grace period before they must start their phaseout schedules. The requirements for developing countries include a phaseout of CFCs, halons, and carbon tetrachloride by 2010, methyl chloroform and methyl bromide by 2015, HBFCs by 1996, and HCFCs by 2040.

- The import of controlled substances from countries that are not Parties to the Protocol is severely restricted, as is the export of such chemicals to non-Parties; and

- The Parties must regularly reassess the Protocol, making revisions to policies on controlled substances based on the latest scientific evidence. The Protocol also requires the Parties to evaluate the effectiveness of the implementation of the Protocol.

The Protocol has established assessment panels to evaluate, every four years, scientific, technical, and economic issues related to proposed controls on ODS (UNEP 1992). Each year, the panel of experts is convened by the Technology and Economic Assessment Panel (TEAP) of the Parties to the Montreal Protocol. Each Party is responsible for taking the necessary regulatory steps domestically to implement the requirements of the Protocol. Within the United States, authority to implement the provisions of the Protocol was granted to EPA under Title VI of the CAA.

1.2.6 UN Framework Convention on Climate Change (UNFCCC)

The UNFCCC, adopted in 1992, seeks to stabilize atmospheric concentrations of greenhouse gases at safe levels. More than 170 Parties have ratified the Convention. The Convention's principal policy body is the Conference of the Parties (COP), and the COP is supported by a number of subsidiary bodies and working groups. The COP relies on the IPCC for scientific and technical advice.

The Convention's ultimate objective is to achieve stabilization of greenhouse gas concentrations in the atmosphere at a level that would prevent dangerous anthropogenic interference with the climate system. To achieve this objective, the Convention requires all Parties to develop national inventories of greenhouse gas emissions; formulate national programs to mitigate climate change; and promote technologies, practices, and processes that control, reduce, or prevent emissions in all relevant sectors. The Convention initially had a general aim (non-binding commitment) for developed countries and countries with economies in transition (Annex I countries) to return greenhouse gas emissions to their 1990 levels by 2000.

In March 1995, at the First Session of COP (COP 1), the Parties adopted the "Berlin Mandate," which called for strengthened commitments by the Annex I countries. In December 1997 at COP 3, the Berlin Mandate led to the Kyoto Protocol, which if ratified, would require Annex I countries to reduce their collective emissions of greenhouse gases by approximately 5 percent below baseline levels by the period 2008-2012. The Protocol sets emission targets for Annex I nations but lets each nation determine its own strategies for achieving its target. The Kyoto Protocol was opened for signature on March 16, 1999, and would enter into force if it is ratified by at least 55 countries representing 55 percent of the total 1990 carbon dioxide emissions from Annex I countries.

The Convention does not specifically refer to civil aviation. Instead it applies to all sources of emissions of the specified greenhouse gases and therefore includes aviation. International civil aviation currently is excluded from the Kyoto targets. Instead, a provision was included that refers to ICAO and its role. The relevant text (Article 2, paragraph 2 of the Kyoto Protocol) reads as follows:

> The Parties included in Annex I shall pursue limitation or reduction of emissions of greenhouse gases not controlled by the Montreal Protocol from aviation and marine bunker fuels, working through the International Civil Aviation Organization and the International Maritime Organization, respectively.

This provision clearly recognizes ICAO's leadership role in coordinating activities aimed at reducing or limiting international emissions of greenhouse gases from civil aviation. ICAO already has been active in addressing emissions from aviation that affect local air quality by setting standards that appear in Annex 16 to the Chicago Convention.

1.3 Commercial interest in supersonic technologies

This section offers a brief description of some recent commercial activities related to supersonic technology.

1.3.1 Civil supersonic transport

Civil supersonic transport aircraft were first produced in the 1970s in Europe and the former Soviet Union, but due to economic and environmental concerns, the number of commercial supersonic aircraft in regular service has remained low (fewer than 20 aircraft). The chief example is the Concorde aircraft (developed in Europe), which has a 3,000 nautical mile range with a payload of 128 passengers (Shaw *et al.* 1997).

In the 1980s and 1990s, developments in aviation technology and passenger demand indicated that a substantially larger fleet of civil supersonic transport might be environmentally and economically feasible in the early part of the 21st century. More specifically, in the 1990s, studies indicated that opportunity existed for a second-generation supersonic commercial airliner to become a key part of the international air transportation system in the 21st century. Projections indicated that by the year 2015, due to strong increases in long-distance air travel, more than 600,000 passengers per day would be traveling substantial distances, predominantly over water. These routes would be among the most appropriate for HSCT, and beyond the year 2000 this segment of the international air transportation market is expected to be the fastest-growing. The potential market for an HSCT was then projected to be between 500-1,500 aircraft over the 2005-2030 time period, depending on available technology and other factors (Shaw *et al.* 1997).

Consequently, as previously described (Section 1.2.2), the HSR program was formulated to provide U.S. industry with the critical technologies needed to support an informed industry

decision about whether to launch a HSCT early in the 21st century. Despite successful completion of the first phase of this program, the HSR program was terminated in FY 1999 due to changes in the commercial outlook for HSCT.

1.3.2 Space and defense

Supersonic flight also has further potential future applications in the space and military sectors. Demilitarized supersonic aircraft have been considered as potential airborne launchers of commercial space vehicles (Scott 1999). In addition, the U.S. military formulated a research program to explore quiet supersonic aircraft technologies for potential applications such as high-speed reconnaissance (Anonymous 2000, Wall 2000, Wall and Scott 2000).

1.3.3 Supersonic business jets

Another potential supersonic platform is a smaller "business" jet. Presently, the estimated potential market for a supersonic business jet (SSBJ) is between 150-400 aircraft (Sparaco 1998), and a development program for such aircraft could be launched by 2015. Companies such as Dassault, Lockheed Martin, Gulfstream, and Boeing have expressed interest in SSBJ technology.

Chapter 2. Methods

This chapter describes the methodology used to address the health impacts associated with a proposed HSCT fleet. The first three of the following questions were considered in the analysis developed for this assessment. The answers to the questions are discussed in this chapter and then compared with the results of other analyses to address the fourth question below:

1. What are the health impacts resulting from the projected atmospheric ozone changes associated with a potential future HSCT fleet?

2. How large is the uncertainty in the estimated health impacts, and what are the major sources of this uncertainty?

3. How sensitive are the estimated health impacts to changes in projected ozone concentrations arising from different assumptions regarding future technological or operational parameters?

4. How do the health impacts predicted to result from an HSCT fleet compare with those expected under previous and current control regimes for protecting stratospheric ozone?

The methods used to address these questions were developed in consultation with experts from the atmospheric science, medical, and risk assessment disciplines, as well as with participants in the NASA (Kawa *et al.* 1999) and IPCC (IPCC 1999) assessments of the effects of HSCT on the atmosphere (ICF 1999, 2000*b*). To answer the fourth question, results of earlier modeling studies of human health impacts under previous and current stratospheric ozone protection policies were compared with the HSCT results estimated in this study.

As discussed in Chapter 1, past estimates are available for the stratospheric ozone, climatic, and human health effects of supersonic aircraft (e.g., NAS (1975)). Since those earlier studies, however, the atmospheric assessments of the impacts of stratospheric flight, as well as the tools used to relate changes in UVR to human health impacts, have evolved greatly. In particular, the NASA assessment described earlier in Section 1.1.2.a reported the results of a

major, decade-long assessment of the projected impacts of HSCT on the atmosphere (Kawa *et. al* 1999). The NASA assessment was able to draw upon the atmospheric science advances of the 1970s through 1990s produced by national and international programs to understand and assess stratospheric perturbations caused by compounds such as CFCs. Similarly, the modeling tools used by EPA to relate ozone protection policies to human health effects have been updated to reflect the best available information. The methods described in this chapter make the best and most appropriate use of these state-of-the-art modeling tools and output.

This chapter is organized in the following sections:

- Section 2.1 provides an overview of the modeling sequence used to project health impacts from HSCT-induced ozone change;
- Section 2.2 describes the data sources and methods used to estimate time-dependent HSCT-induced ozone change;
- Section 2.3 describes the calculation of associated UVR changes;
- Section 2.4 details the steps followed to produce estimates of skin cancer incidence, skin cancer mortality, and cataract incidence that could result from the proposed fleet of HSCT;
- Section 2.5 discusses the development of a health effects baseline estimate for comparing the proposed HSCT fleet's impact on human health endpoints;
- Section 2.6 describes the steps taken to evaluate the uncertainties that accompany the results reported in this document; and
- Section 2.7 describes the approach used to explore the impact of changes in technological, atmospheric, or other parameters on predictions of future excess cases of skin cancer and cataract, as well as skin cancer mortality.

2.1 Modeling overview

This assessment is based on output from a series of models that analyze changes in atmospheric ozone, changes in ground-level UVR, and human health effects attributable to the proposed HSCT fleet. As described in Section 2.2, calculations of these ozone changes are based on results from the Commonwealth Scientific and Industrial Research Organization (CSIRO) model, which is one of the models that was used in the NASA assessment.[1] This study uses archived CSIRO model results that provide estimates of changes in zonal-mean total column ozone[2] that would result when a standard subsonic fleet is replaced by a hybrid fleet containing 1,000 HSCT. These estimates are provided for each month by 5-degree latitude increments across the US for the year 2050. These estimates are then converted to fractional changes in ozone, as discussed in Section 2.2.2.a., and scaled back to the year 2015 according to the fleet growth schedule detailed in Section 2.2.2.b.

Subsequently, the Tropospheric Ultraviolet-Visible (TUV) model is employed to estimate the change in ground-level UVR resulting from CSIRO ozone change estimates, and finally the Atmospheric Health Effects Framework (AHEF) is used to project the incremental health effects associated with a growing fleet of HSCT.

Figure 2-1 depicts the dependence of predicted changes in human health effects on inputs generated from these and other models, as well as data supplied from other sources.[3] The modular structure of the AHEF is such that each set of inputs is separate and each set of outputs is dependent on the inputs from the previous module. See Section 2.4 for a more complete discussion of these input variables. This structure also allows for substitution of individual modules without the need to reconfigure the entire modeling framework. This flexibility is important for two reasons: (1) The framework can be tailored specifically to the

[1] See section 2.2.1 for a description of NASA analysis leading to the selection of the CSIRO model to assess HSCT ozone impacts.

[2] The comparison of total column ozone estimates (tropospheric plus stratospheric ozone) is an accurate way to assess the impact of supersonic aircraft on stratospheric ozone levels because operation of a fleet of HSCT is not expected to affect tropospheric ozone significantly (ICF 1999).

[3] Appendix A provides additional information on the relationship between the various inputs used in this human health impact evaluation.

needs of an HSCT risk assessment, and (2) When more accurate model algorithms or sources of data become available, revisions can be incorporated easily into the AHEF.

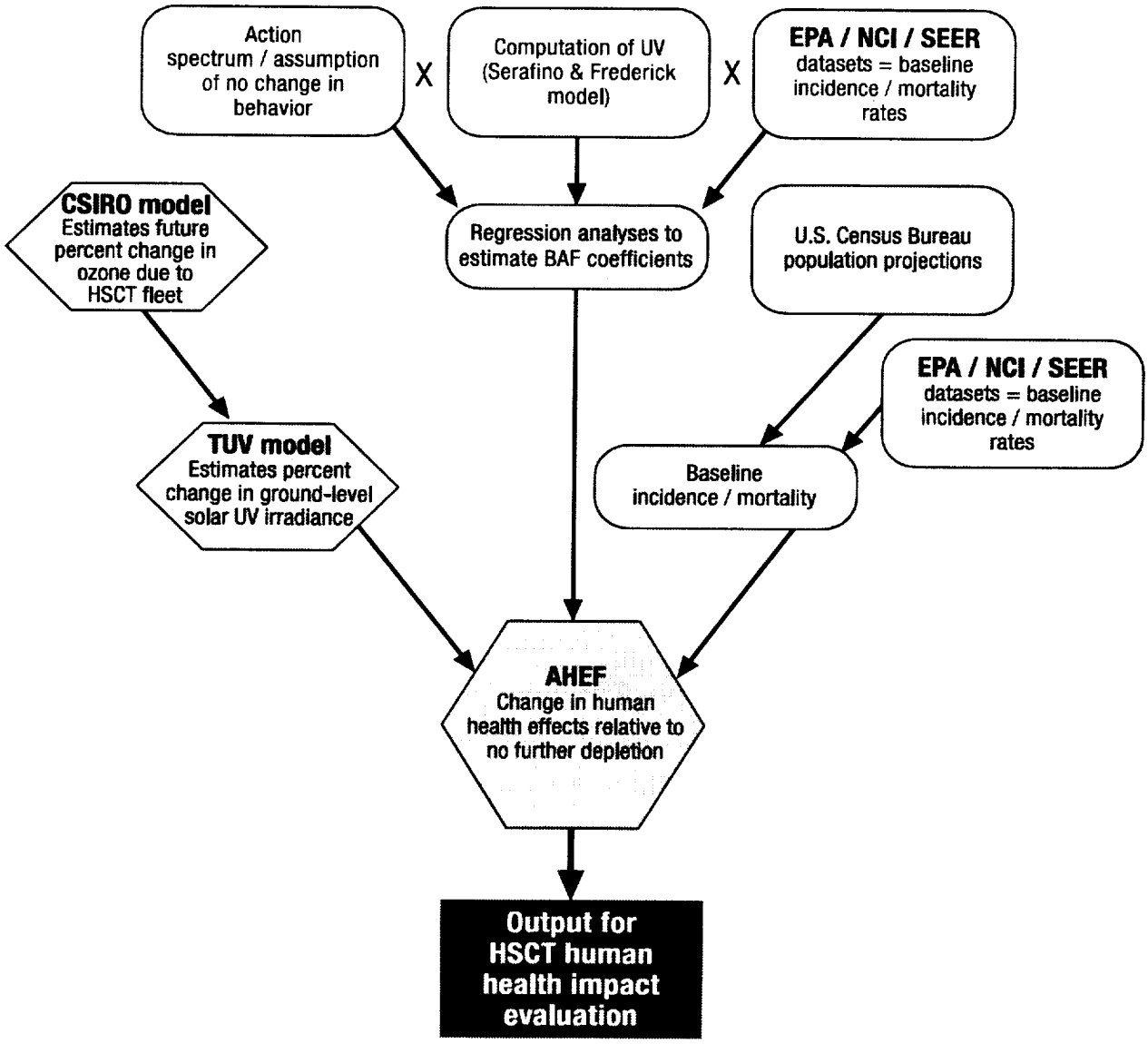

Figure 2-1. Relationship between the models used for this evaluation of human health impacts. The symbols used in this diagram do not correspond to traditional flow chart notation. BAF = biological amplification factor. NCI = National Cancer Institute. SEER = Surveillance, Epidemiology, and End Results Program.

2.2 Estimated HSCT-induced ozone change

This section describes the source of estimates of the ozone changes associated with an HSCT fleet and the adaptation of these estimates for application in the present study.

2.2.1 NASA assessment selection of source of central values

The CSIRO model was selected through the NASA assessment process as the source of central HSCT ozone response predictions for the baseline scenario in the report of the NASA assessment (Kawa *et al.* 1999).[4] For the present study, the results of this model were also chosen to provide central ozone response outputs for the baseline scenario after consultation with atmospheric scientists who participated in both the NASA and IPCC assessments.

Briefly, the NASA assessment evaluated eight models that predict the change in ozone resulting from HSCT engine emissions. The models included five two-dimensional (2-D) models and three three-dimensional (3-D) models. The ozone change estimates generated by these models exhibited a substantial degree of variability, mainly due to different model representations of atmospheric transport (e.g., polar processes and the representation of polar stratospheric clouds (PSCs)) (Kawa *et al.* 1999).

When estimates generated by the 2-D and 3-D models were compared with measurements, the CSIRO model was considered to provide the most representative results among the eight models evaluated, because it displayed better agreement with measured atmospheric conditions for two important parameters: (1) the prediction of background NO_y[5] levels in the lower stratosphere and (2) the age of stratospheric air. On the basis of these two diagnostics the CSIRO model was considered likely to have provided a more realistic simulation of the accumulation of HSCT exhaust in the stratosphere. Additional detail on the CSIRO model,

[4] Scenario 4 assumes EI_{NOx} = 5 g/kg, 500 aircraft, 2015 conditions, and no sulfur conversion in the aircraft wake.

[5] NO_y denotes total reactive nitrogen in the atmosphere. It includes NO, NO_2, NO_3, HNO_3, $ClONO_2$, N_2O_5, HO_2NO_2, $BrONO_2$, and others. It does not include N_2 or N_2O. NO_x, a term commonly used in atmospheric chemistry, denotes the sum of reactive nitrogen oxides NO + NO_2, which are the primary aircraft engine exhaust species, and it is a subset of NO_y.

including assumptions regarding the effect of zonal asymmetries on temperature distribution, heterogeneous processes in the northern hemisphere, and representations of PSCs, are provided in Appendix B.

2.2.2 Adaptation of CSIRO data and fleet growth schedule

The specific fleet scenario considered by this study (i.e., 1,000 in-service HSCT by the year 2050, described in more detail below) was selected from a limited number of fleet scenarios analyzed in the NASA assessment. The following sections describe the specific scenario used and how the outputs from the CSIRO model simulation of this scenario were adapted for use in this study.

2.2.2.a. Adaptation of CSIRO data

Outputs were used from a CSIRO run for the year 2050 that includes a hybrid fleet with 1,000 HSCT flying at Mach 2.4, with an NO_x emission index (EI_{NOx}) of 5 g/kg, an EI_{SO_2} of 0.4 g/kg, and 10 percent fuel sulfur converted to particles. Cruise altitude (i.e., in the lower stratosphere, between 17 and 20 km) is assumed to be identical to that of the NASA Technology Concept Airplane, a 300-passenger aircraft projected to travel at Mach 2.4 with a range of 5,000 nautical miles. These parameters correspond to Scenario 36 on Table 4-6 of the NASA assessment (Kawa *et al.* 1999).[6]

The CSIRO data were provided by NASA through its contract with Science Applications International Corporation (SAIC). The data consist of steady state monthly ozone column estimates for two simulations, generated by 5-degree latitude bands for the Northern Hemisphere. The first simulation is intended to reflect atmospheric conditions expected to be present in 2050 with the operation of a projected subsonic fleet. In the second simulation, the subsonic fleet is modified to include 1,000 HSCT while preserving the number of passenger-

[6] It is important to note that changes in parameters such as different choices of Mach number (which could change cruise altitude), aircraft design technology (which changes fuel burn and total mass of emissions), combustor technology, route structure (the scenarios were based on a projection of air traffic passenger demand in 2015), and aircraft utilization (the scenarios assumed very high (average of 16 block hours/day) utilization by the entire HSCT fleet) could result in significant changes in the ozone impact resulting from a fleet of HSCT.

kilometers.[7] For simplicity, the ozone estimates generated from these simulations are referred to as "$O_{3\ \text{without an HSCT fleet}}$" and "$O_{3\ \text{with an HSCT fleet}}$", respectively.

These 5-degree latitude band ozone estimates are aggregated and averaged to form three 10-degree latitude bands that span the United States (i.e., 20 to 30°N, 30 to 40°N, and 40 to 50°N) to enable the data to be input into the AHEF.[8] These ozone estimates then are used to produce the fractional change in ozone per month by latitude band for 2050. The following equation describes this process:

(Equation 2-1)

$$(O_{3\ \text{with an HSCT fleet}} - O_{3\ \text{without an HSCT fleet}}) / O_{3\ \text{without an HSCT fleet}} = \text{Fractional change in } O_3$$

The fractional change in ozone then is multiplied by 100 to obtain an estimate of percent change in ozone. The percent change in ozone estimates for 2050 were scaled linearly to correspond with the estimated percentage of the HSCT fleet in operation per year from 2015 to 2050 as described in Section 2.2.2.b. From 2050 to 2100, the estimated HSCT-induced percent column ozone change is held constant (ICF 1999). These estimates of future changes in stratospheric ozone levels from operation of an HSCT fleet from 2015 to 2100 then serve as inputs to the TUV model.

It is also possible to use the absolute value (in Dobson units) of the CSIRO-produced estimates of HSCT-induced ozone change, rather than the fractional value, as has been done in this evaluation. The sensitivity of estimated health impacts to the use of the absolute value (Equation 2-2), instead of the fractional value, for ozone change was explored:

$$(O_{3\ \text{with an HSCT fleet}} - O_{3\ \text{without an HSCT fleet}}) = \text{Absolute change in } O_3 \qquad \text{(Equation 2-2)}$$

[7] No estimates exist (over the time period assessed) for ozone concentrations expected when there is global compliance with the Montreal Adjustments and a projected subsonic fleet is in operation. Thus, health effects estimates derived from the ozone results of these scenarios are calculated relative to health effects estimated under the assumption of global compliance with Montreal Adjustments, without the presence of a subsonic fleet.

[8] While an analysis of ozone change for all latitude bands is not presented graphically in this document, the variation in ozone estimated to occur for each latitude band is similar to the variation in the annual average around the Northern Hemisphere central value of -0.6 percent. Figure 3-2 presents ozone depletion by month for a representative latitude band (20 to 30°N).

See Appendix C for additional explanation of this analysis. Briefly, small differences (less than 1.5 percent) were observed in estimated health impacts when the absolute value for ozone change was used instead of the fractional value. The results therefore are judged to be relatively insensitive to the choice of absolute or relative ozone change, and this study employs the approach based on the relative ozone change as described in Equation 2-1.

2.2.2.b. Specification of fleet growth schedule

Current evaluations of the impact of HSCT on the ozone layer (i.e., the IPCC and NASA assessments) focus on total fleet size in a given future year but do not specify the annual rate of deployment for HSCT needed to reach this total fleet size (IPCC 1999, Kawa *et al.* 1999). Hence, creating a fleet growth schedule is the first step in modeling the impact that a growing HSCT fleet will have on future changes in human health effects.

Based on discussions among an expert group, a linear fleet size ramp-up was assumed (ICF 1999). The ultimate fleet size of 1,000 aircraft in passenger-service in 2050 is based on projections of future demand and analyses of market capture (Kawa *et al.* 1999). Passenger-kilometers per year follow subsonic market projections and are replaced from subsonic to supersonic aircraft on a one-to-one ratio, with subsonic aircraft being phased out as more HSCT enter passenger service. Figure 2-2 illustrates the in-service schedule used in this evaluation.

The approach described above is somewhat different from either of those used in the NASA and IPCC reports (Kawa *et al.* 1999, IPCC 1999). For example, the NASA assessment envisioned a fleet of 500 HSCT in operation in 2015. However, full-scale fleet production requires technological and design innovations that will not be available for commercial use for a number of years. Therefore, it is no longer realistic to assume that a fleet of 500 HSCT would exist in 2015, given the state of technology plus research and development activities. With these limitations, 2015 was chosen as an earliest starting point for the HSCT fleet.

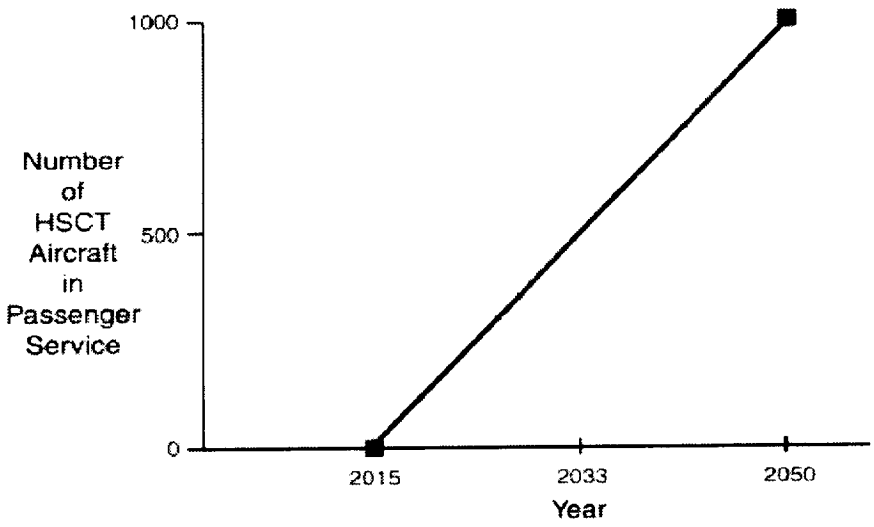

Figure 2-2. HSCT fleet size. The operation of HSCT is assumed to begin in 2015 and ramp up linearly until 1,000 aircraft are in operation in 2050. This evaluation then assumes that 1,000 aircraft are in operation from 2050 to 2100.

The present study estimates time-dependent fractional ozone changes by scaling CSIRO data for the year 2050 linearly back to 2015 whereas the NASA and IPCC reports base their ozone change estimates on steady-state emissions of mature HSCT fleets in a given year (Kawa *et al.* 1999, IPCC 1999). The time-dependent analysis used in this evaluation does not attempt to account for possible geographic changes in HSCT utilization, instead assuming that global air traffic patterns for HSCT would grow incrementally. This incremental growth assumption was selected for ease of modeling, and actual HSCT growth patterns may be different.

Moreover, the time-dependent ozone changes developed and used in this analysis do not attempt to account for any departures from a linear relationship between fleet size and ozone change that might occur due to a changing background atmosphere (e.g., changing background NO_x). The effects of changing background NO_x on this assumption are expected to be second order in magnitude and, thus, the assumption of a linear relationship was selected as a reasonable initial approximation. The sensitivity of results to this assumption could be evaluated in future work.

2.3 Calculation of UVR change

The amount of UVR reaching the Earth's surface is computed using the TUV radiation model (Madronich 1992, 1993b; Madronich and de Gruijl 1993; Madronich *et al.* 1996, 1998). The TUV model is widely regarded as an accurate tool for calculating surface UVR levels and has been updated many times to reflect current science. The accuracy of the TUV model has been demonstrated in a number of comparisons to direct measurements of UVR at the Earth's surface (e.g., Shetter *et al.* 1992, 1996; Kirk *et al.* 1994; Lantz *et al.* 1996). Since 1989, the TUV model has been used in the scientific evaluations of ozone depletion (WMO 1989, 1991, 1995, 1999) and related environmental consequences (UNEP 1989, 1991, 1994, 1998) as mandated under the Montreal Protocol.

The TUV model computes the radiation levels at any height in the atmosphere including the Earth's surface. The spectral irradiance, $F(\lambda, x, t)$, incident at the Earth's surface, at time t, location x, and wavelength λ, may be represented symbolically as the product of the solar spectral irradiance at the top of the atmosphere, $F_{toa}(\lambda)$, and an atmospheric transmission factor, T.

$$F(\lambda, x, t) = F_{toa}(\lambda)\, T(\lambda, x, t; \theta_o, O_3, \text{clouds, aerosols, } \ldots) \qquad \text{(Equation 2-3)}$$

Values of $F_{toa}(\lambda)$ are known from direct observations of the Sun by satellite-, balloon-, and ground-based instruments. The values of T depend on parameters such as the solar zenith angle, θ_o, and the seasonal variation in Earth-Sun distance. They also depend on atmospheric optical properties, specifically absorption by ozone, possibly some pollutant gases (NO_2, SO_2), and scattering by air molecules (known as Rayleigh scattering). Atmospheric particles (clouds and aerosols) can contribute to both absorption (e.g., soot) and scattering (mathematically described by the Mie theory) and may be used optionally in TUV. Surface reflections also are included, as they can contribute substantially to the radiation incident at the surface (see for example McKenzie *et al.* (1998)). Many of these factors are functions of location (latitude, surface elevation, altitude above the surface) and time (day, year, and long-term trends), so that $F(\lambda, x, t)$ is also a strong function of time and geographic site. The TUV model calculates T by first subdividing the atmosphere into vertical layers (typically 1 km thick), each having an

assumed uniform composition. The model uses vertical profiles of air density, temperature, and ozone from the United States Standard Atmosphere[9] (USSA 1976).

When different ozone column values are considered (e.g., under different future Montreal Protocol scenarios), the changes in ozone are applied to the reference scenario at each altitude in proportion to the ratio of new to reference ozone column values, so that the shape of the profile is conserved. Thus, since approximately 90 percent of the total ozone column is in the stratosphere, most of the ozone changes are also located in the stratosphere.

In principle, not only changes in total ozone columns, but also the altitude at which ozone perturbations occur, can have some effect because of the coupling between ozone absorption and scattering by air molecules. In practice these considerations are important only when the ozone perturbations occur in the lower-to-middle troposphere and are relatively insensitive to perturbations that occur in the stratosphere (i.e., well above the region where scattering occurs). The figure provided in Appendix D indicates that compared to the more complex altitude-dependent effect, the simple scaling method is approximately accurate to better than 10 percent for perturbations occurring in the upper troposphere and lower stratosphere. For example, ozone perturbation occurring near 20 kilometers reveals an RAF near 1.12, while an assumption of uniform column ozone change results in an RAF of 1.17. See Appendix D for further discussion.

Within each uniform layer, the equation of radiative transfer is solved using an accurate numerical scheme, a modified version of the discrete ordinates method developed by Stamnes *et al.* (1988). The modifications, made by Madronich and co-workers, removed numerical instabilities and improved accuracy at low Sun (when atmospheric curvature becomes important) through the use of a pseudo-spherical technique. The solutions for each layer then are matched at the interfaces to adjoining layers, and the entire system (the matching equations for all 80 layers) is solved using matrix inversion methods. The result is the spectral irradiance at any location and time, $F(\lambda, x, t)$.

[9] The US Standard Atmosphere (USSA) provides average values for a number of atmospheric parameters at different altitudes.

The TUV model also calculates biologically weighted radiation, UV_{bio}, defined as:

$$UV_{bio} = \int F(\lambda, x, t)\, B(\lambda)\, d\lambda \qquad \text{(Equation 2-4)}$$

where $B(\lambda)$ is a spectral sensitivity function (also known as an action spectrum or weighting function) for the biological endpoint of interest. (See Section 2.4.3 for additional information on action spectra.) For example, the action spectrum for erythema (i.e., sunburn), $B_{ery}(\lambda)$, has been determined from spectral exposure studies on humans, and the data have been characterized by the following expression (McKinlay and Diffey 1987):

$$\begin{aligned} \log_{10} B_{ery}(\lambda) &= 0.0 && \text{for } \lambda = (250\text{-}298 \text{ nm}) \\ &= 0.094\,(298\text{-}\lambda) && (298\text{-}328 \text{ nm}) \\ &= 0.015\,(139\text{-}\lambda) && (328\text{-}400 \text{ nm}) \end{aligned} \qquad \text{(Equation 2-5)}$$

Action spectra for a number of other biological endpoints have been estimated (e.g., DNA damage, ocular damage), and their sensitivity to UV changes associated with ozone depletion have been tabulated (most recently by Madronich *et al.* (1998)).

The TUV model provides "look-up tables" (calculated for cloud-free conditions) as a function of the total ozone column, solar zenith angle, and surface elevations. These tables are then used to calculate cumulative UVR for a given latitude, time of day, day of month,[10] and amount of ozone, as measured in Dobson units. These tables vary by action spectrum and serve as inputs to the AHEF.

2.4 Calculation of health impacts

The AHEF consists of a series of modules that estimate changes in the incidence and/or mortality of selected health effects resulting from past and future changes in stratospheric ozone concentrations. These changes in health effects (i.e., cataract incidence and melanoma

[10] The look-up tables estimate the average irradiance per hour for every hour between 4 am and 10 pm on the 15th day of a given month. These representative irradiance estimates then are multiplied by 30 to obtain an estimate of the average irradiance for the whole month.

and non-melanoma incidence and mortality) typically are expressed relative to health effects that would have occurred if ozone concentrations that existed in 1979-1980 had been maintained through the time period of interest. Currently, EPA uses the AHEF to estimate incremental changes in health effects associated with the Montreal Protocol, its subsequent amendments, and other ODS phaseout and release scenarios (ICF 2000*a*).

The AHEF first computes projections of incidence and mortality based on historical rates assuming ozone conditions identical to those existing in 1979-1980. The establishment of this 1979-1980 health effects baseline provides a standard from which all changes in health effects resulting from ozone perturbations (e.g., from a fleet of HSCT) can be quantified. (See Section 2.5 for an additional discussion of the baselines used in this evaluation of human health impacts.) Baseline health impact estimates are calculated by combining historical data on U.S. cataract incidence and skin cancer incidence and mortality (National Cancer Institute (NCI)/EPA, National Institute of Health (NIH), and/or SEER data sets), with U.S. Census Bureau age and sex group population projections. In developing the AHEF 1979-1980 baseline, only light-skinned populations are considered because baseline rates of responsiveness to UV exposure are not well documented in other populations. In addition, to account for latitudinal variations in UVR, baseline projections are estimated for three latitude bands that span the United States (i.e., 20 to 30°N, 30 to 40°N, and 40 to 50°N) (ICF 2000*a*).

Next, the health impacts arising from a particular ozone perturbation can be determined by first calculating an estimated UV dose for any location for the time periods encompassed by various dose metrics. These UV exposures are calculated using the appropriate action spectra and dose metrics, such as peak single day or cumulative annual exposures for either an individual's entire life or selected ages (ICF 2000*a*).

Next, estimates of UV dose are combined with dose-response relationships for the health effects to produce estimates of changes in health impacts due to the perturbation being studied. These estimates then are compared with the AHEF estimates of 1979-1980 baseline health effects to project future incremental levels of cataract incidence and skin cancer incidence and mortality. The dose-response relationships are calculated by plotting weighted UV exposures against data characterizing each health effect. The slopes of the resulting curves are referred to as BAFs and are estimated separately for each health effect from actual human incidence and mortality data (ICF 2000*a*).

BAFs can also be defined as the percentage variation in skin cancer incidence and mortality associated with a percentage change in UV exposure, controlling for factors such as age and birth year. Age must be considered due to the lag period between exposure and detection for skin cancer and cataracts and because skin cancer incidence and mortality depend upon cumulative UV exposure. Further discussion of BAFs and RAFs can be found elsewhere (UNEP 1994). An equation is used to generate BAF estimates since BAFs for the selected health endpoints examined in this evaluation have not yet been derived from experimental data. The following equation estimates the relationship between UV exposure and cutaneous malignant melanoma (CMM) mortality, controlling for birth year (CMM only) and for age while taking into account the intensity of UV exposure across different latitudes throughout the United States. This power function is obtained by deriving a best-fit equation that describes the appropriate dose-response curve:

$$R_{ij} = e^{\left[B_0 + \sum B_{C_i} C_i + \sum B_{A_j} A_j + B_{UV} \ln\left(UV_{ij}\right)\right] + \varepsilon_{ij}} \qquad \text{(Equation 2-6)}$$

where R_{ij} is the mortality rate for the ith cohort and the jth age group, and UV_{ij} is UV exposure for the ith cohort and the jth age group. The C_i and A_j terms are cohort and age group dummy variables, and B_{C_i} and B_{A_j} are the corresponding coefficients that control for the influence of these factors on CMM mortality.[11] B_0 is the regression coefficient, or intercept, and B_{UV} is the BAF for the health effect of interest (CMM, in this example). This equation is solved for each latitude band of interest.

The TUV calculates the future annual percentage change in UV dose across the latitudinal bands for the scenario based on the CSIRO model's outputs. This is multiplied by the BAF for each health effect and yields the percent change in future health effects attributable to changes in ozone concentration. Multiplying these percentages by the baseline projections for each appropriate health effect and age group produces the change in future cases or mortality attributable to the HSCT fleet scenario. The following equations summarize this process:

[11] This regression is run using the maximum likelihood non-linear Poisson method because the error term is no longer normally distributed after the natural log is applied to both sides of Equation 2-6.

(Equation 2-7)

(Percent change in weighted UV relative to UV_{ref}) x (BAF)	= or	Percent change in I/M relative to I/M_{ref}

Note: ref =reference scenario (e.g., Montreal Adjustments, 1979-1980 baseline); I/M = incidence or mortality

The remainder of this section highlights the human health endpoints analyzed in this evaluation and then discusses the action spectra and dose metrics used to quantify and predict each health effect. Table 2-1 presents a summary of the human health effects and their associated parameters used in this analysis.

2.4.1 Human health endpoints

As described above, the human health endpoints examined in this evaluation are basal cell carcinoma (BCC), squamous cell carcinoma (SCC), and CMM incidence; CMM and non-melanoma skin cancer (NMSC) mortality; and cataract incidence. BCC and SCC are collectively referred to as NMSC. These diseases were evaluated because their etiologies are fairly well understood. In addition, action spectra and dose-response relationships have been estimated for each of them, thus making it possible to quantitatively project potential changes in these health effects due to increases in UVR. These diseases are also some of the most serious human health impacts associated with UV exposure.

Humans develop three major forms of skin cancer thought to be etiologically related to UV exposure: CMM, BCC, and SCC. These UV-associated tumors develop principally in light-skinned individuals. Darker skinned individuals (e.g., Asians, Hispanics, and Blacks) also develop these tumors but at much lower rates. In NCI's 1978-1979 survey in the United States, for instance, the incidence of NMSC in African-Americans was nearly 100-fold less than that observed in Caucasians and the incidence in Hispanics in New Mexico was one-sixth (males) to one-eighth (females) of those observed in Anglos (Scotto *et al.* 1983).

Table 2-1. Summary of Health Effects Parameters Examined in this Human Health Impact Evaluation

Endpoint[a]	Action Spectrum
Melanoma Mortality	SCUP-h
Melanoma Incidence	SCUP-h
NMSC Mortality	SCUP-h
NMSC Incidence--BCC	SCUP-h
NMSC Incidence--SCC	SCUP-h
Cataract	DNA-h[b]

[a] These endpoints are evaluated on a cumulative annual basis over the lifetime of the individual.

[b] The action spectra for cataracts are currently being updated. The number of cataract cases predicted by the AHEF for this human health impact evaluation is not expected to change significantly as a result of these updates. See Appendix E for additional information.

SCUP-h = Skin Cancer Utrecht Philadelphia action spectrum, adjusted for human skin transmission.

CMM develops from melanocytes, the pigment-producing cells of the skin. These tumors often grow rapidly, frequently developing aggressive metastases. Although it is clear that exposure to the UV in sunlight is a major risk factor for CMM development, the dose-response relationship is not completely understood. There is some indication that intermittent high-dose exposure (i.e., sunburns) may be important and that exposure early in life poses a greater health risk than exposure later in life (Elwood and Jopson 1997).

NMSCs arise from keratinocytes, the principal cell of the epidermis, the outermost living layer of the skin. BCCs develop from undifferentiated cells in the germinal, basal layer of the epidermis. They are the predominant skin cancer in light-skinned populations, representing, in the United States, about 80 percent of all skin cancer cases (Epstein 1996). BCCs tend to grow slowly and usually appear on the neck, hands, face, and trunk. In addition, they rarely metastasize and have a cure rate of greater than 95 percent if detected in the early stages (de Gruijl and Van der Leun 1993). SCC is a neoplasm[12] of keratinocytes as well, but it arises from a more differentiated cell higher up in the epidermis. It typically is found on the ears, face, or hands. SCC is much less common than BCC. However, SCC has the same cure rate as BCC, given early detection, and is two to three times more common in men than in women (Public Health Service 1996).

[12] A neoplasm is a quickly reproducing growth of the abnormal cells that create a tumor.

Although both BCC and SCC are tumors of keratinocytes, they appear to have somewhat different dose-response relationships to UV. SCC risks appear to be related to an individual's total accumulated exposure; populations at especially high risk are those with outdoor occupations (e.g., farmers, foresters). In contrast, BCC risks, similar to those associated with CMM, appear to be related to intermittent exposure with exposures in childhood being particularly important (Kricker 1992, Armstrong *et al.* 1997).

A cataract is an agglomeration of protein on (or in) the lens of the eye that prevents light from reaching the retina and thus interferes with vision. There are three major forms of cataract: nuclear, cortical, and posterior subcapsular, so named because of their location in the lens. Nuclear cataracts occur in the inner layers of the lens, cortical cataracts occur in the outer layers of the lens, and posterior subcapsular occur at the back (posterior) interface of the lens and its epithelial capsule. Frequently, these forms occur in combination (Longstreth *et al.* 1998).

In a 1991 study (Italian American Cataract Study Group 1991), pure cortical cataract represented slightly less than 50 percent of the cataracts occurring in individuals aged 45-79, and mixed cataracts represented about 40 percent, with most of the mixed forms including a cortical component. Although many factors such as poor nutrition, heavy drinking, diabetes, exposure to radiation, and genetic predisposition can also increase the risk of cataract, exposure to increased levels of UVR has been linked definitively to cortical cataract (Italian American Cataract Study Group 1991, Klein *et al.* 1995, West and Valmadrid 1995, West *et al.* 1998). Indeed, in the Klein *et al.* study (1995), heavy sun exposure was on a par with diabetes or heavy drinking as a risk factor for cataract.

The social and economic consequences of cataracts are enormous. Worldwide, it is the leading cause of blindness (West and Valmadrid 1995). In the United States, cataract surgery constitutes a significant component of the health care budget, amounting to approximately $3 billion in 1992 (Javitt and Taylor 1995). In this study, estimates of changes in cataract incidence resulting from a fleet of HSCT is provided based on the best available information. As technology evolves and researchers increase their ability to make quantitative predictions of cataract incidence based on changes in UVR, updates to the cataract modeling methodology can be made to increase the accuracy of the preliminary estimates presented in this evaluation. Appendix E discusses the methodology used in this evaluation to estimate changes in cataract

incidence and provides information on interim updates to the methodology as well as future directions for cataract modeling.

2.4.2 Other human health and environmental effects

In addition to the health effects featured in the AHEF, UVR has been associated with other human health consequences that are as yet unquantified. For example, UV exposure can produce immunosuppression in humans that could lead to increases in the incidence and severity of some infectious diseases or result in an increased failure rate of vaccination programs (Longstreth *et al.* 1998). Numerous studies in animals have shown that UV exposure depresses the immune responses to microorganisms (principally those that enter via the skin), and results in more severe infections. Human infectious diseases in which animal tests have shown such an effect include herpes, tuberculosis, leprosy, trichinosis, leishmaniasis, listeriosis, and Lyme disease (Longstreth *et al.* 1998).

Although action spectra (defined below) have been derived for immunosuppression (e.g., De Fabo and Noonan 1983), certain key data gaps would make it difficult to develop estimates of health effects changes for this endpoint. For example, sufficient epidemiological data do not presently exist that would allow the quantification of the number of affected individuals necessary to estimate baseline incidence. In addition, no commonly accepted method exists to measure the degree of UV-induced immunosuppression experienced by these individuals. Finally, the scientific community is not in agreement as to which dose metric should be used to assess the consequences of immunosuppression.

The first links between UVR and adverse human health impacts were discovered many years ago. Researchers continue their efforts to understand the complex mechanisms by which the Sun affects nearly every form of life on this planet. Many nonhuman impacts have been associated with UVR, such as damage to agricultural crops. Enhanced UV levels have varied repercussions on terrestrial ecosystems, ranging from decreased photosynthesis rates to changes in competitive balance and increased susceptibility to disease (Caldwell *et al.* 1998). Effects on aquatic ecosystems are predicted as well, including decreased species diversity and reduced larval survival rates (Hader *et al.* 1998). Increased UVR also may degrade polymeric

materials and thus reduce their useful life, which has far-reaching impacts on construction and manufacturing industries (Andrady *et al.* 1998).

2.4.3 Action spectra

An action spectrum describes the relative effectiveness of (i.e., is used as a weighting function for) UV-A and UV-B wavelength radiation in the induction of health effects (e.g., DNA damage, skin cancer, erythema, and cataract) (ICF 2000*a*). Action spectra are determined through controlled UV exposures on animal subjects to evaluate the effectiveness of a wavelength at inducing a specific health effect. Figure 2-3 depicts commonly used action spectra for the health effects examined in this evaluation.

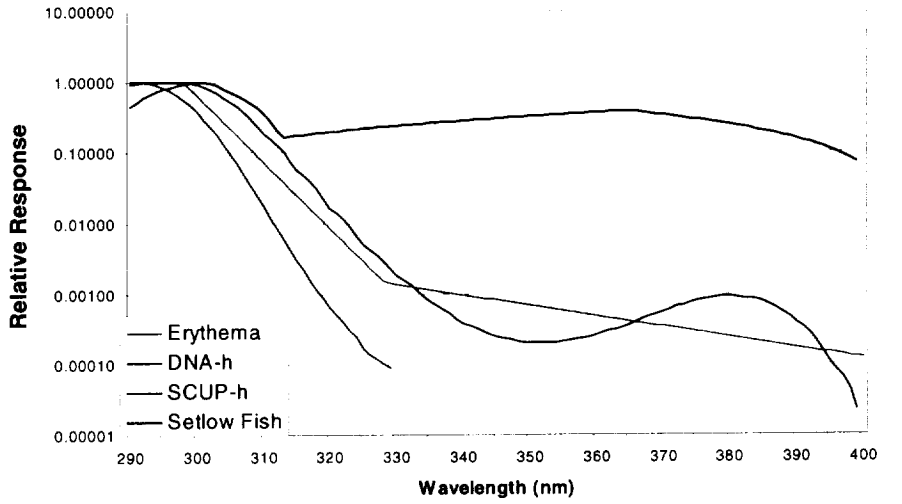

Figure 2-3. UV action spectra. SCUP-h has been selected for use in this study to assess skin cancer incidence and mortality, and DNA-h is used to evaluate cataract incidence. In this figure, the erythema (described in McKinlay and Diffey 1987) and Setlow fish melanoma action spectra (described in Setlow *et al.* 1993) are presented for comparison purposes.

If an action spectrum is known, it can be combined with exposure data to determine effective UV dose (i.e., the intensity at each wavelength weighted by effectiveness at producing the health effect of interest). Researchers then can perform studies quantifying the responses of organisms to particular doses of UVR, thus creating dose-response curves and BAFs for a particular health effect. As described in Equation 2-6 above, the BAF is used by the AHEF to relate changes in weighted ground-level UVR to changes in health effects.

Several action spectra were proposed to evaluate the various human health effects examined in this evaluation. The SCUP-h and DNA-h action spectrum were selected for further analysis. SCUP-h was derived on the basis of induction of SCC in hairless mice and then adjusted for human skin characteristics (de Gruijl *et al.* 1993), as described below. SCUP-h was chosen for use in this evaluation because it is widely accepted and is believed to be the appropriate action spectrum for SCC. SCUP-h also has been selected for BCC and CMM because both are cancers of the skin and action spectra specific to either of these tumors do not exist (Longstreth *et al.* 1998). The DNA-h action spectrum is a generalized DNA damage action spectrum (derived from studies on bacteria and viruses as described below) and was selected for cataract estimates because of research indicating that UV-induced damage in lens epithelia (thought to be a precursor to cataract) can be reversed via photoreactivation (i.e., repair of DNA in marsupials) (Tafoya *et al.* 1997).

This study, in using the SCUP-h action spectrum for CMM, has assumed that the action spectrum for one type of skin cancer (SCC) can be used to make predictions about another (CMM). This assumption introduces a presently unquantified source of uncertainty which may be substantial. The results of analyses (such as the present one) which use the SCUP-h action spectrum for CMM predictions are accurate to the extent that the shape of the as-yet unidentified CMM-specific action spectrum is congruent or similar to that of SCUP-h. Similar considerations apply to the use of the SCUP-h action spectrum for prediction of BCC, although differences between BCC and SCC are considered biologically less significant than those between melanoma and non-melanoma skin cancer. Similarly, as discussed in Appendix E, the use of the DNA-h action spectrum to make predictions about cataract incidence may introduce unquantified uncertainty. However, the information and tools used in this study represent the best available approach and are consistent with current practices in risk assessment.

As noted above, SCUP-h is the action spectrum for SCC in mice that has been corrected for transmission through human skin. Mouse skin and human skin have different absorption spectra for UV light, principally because mouse epidermis is thinner than human epidermis and thus more of the UVR gets through the layers of dead cells to the target at the base of the epidermis (the outer viable layer in which skin cancer develops). In order to adjust for these differences, the UV absorption spectra of mouse skin and human skin are compared across the relevant wavelengths and the differences between them are then corrected for by multiplication by the appropriate ratios. As an example, suppose that at 300 nanometers (nm), the thickness

of human skin prevents 5 percent less UVR from reaching the base of the epidermis than mouse skin does. To compensate for this difference in absorption between mouse and human skin, the dose plotted at 300 nm for mice would need to be reduced by 5 percent. Thus, the action spectrum would be modified by 5 percent at 300 nm to account for the relative efficiency of the incoming light in human skin.

A similar adjustment is made when Setlow's DNA action spectrum is corrected for human skin, except in this instance it is not the difference in two species, but the difference between no skin (i.e., in a petri dish) and what would be predicted for the same reaction occurring in human skin. Setlow's DNA action spectrum is a generalized action spectrum that was developed from *in vitro* experiments on a number of different microbial systems where the UV directly hits the affected microbial targets. In skin, the UV first has to pass through a number of cell layers before hitting DNA targets in live cells. These layers have a number of UV-absorbing molecules (e.g., *trans*-urocanic acid, proteins) that selectively filter out some wavelengths of UV; this filtration reduces the energy reaching the target so that the effective energy in skin is somewhat less than that in a petri dish.

2.4.4 Dose metrics

The AHEF can examine a variety of dose metrics, which allows for evaluation of exposure early in life. This early exposure is thought to be more important than cumulative exposures for some health endpoints. Exposures for CMM mortality and incidence, as well as BCC incidence, are approximated both as an average annual measure and as the exposure received on a peak day (i.e., June 21) for each year. These two methods of characterizing exposure then can be applied for every year of a person's life or only for exposures received at selected ages (e.g., from ages 1 to 20). The exposures in this study are based on estimates of cumulative annual lifetime exposure.

2.5 Model implementation

This section discusses development of the Montreal Adjustments baseline used as a reference scenario for this study.

The AHEF is designed to express changes in health effects due to a particular ozone perturbation relative to the health effects that would have occurred if the 1979-1980 ozone conditions were held constant through time. In the current application, however, the AHEF is used to predict the incremental health effects associated with an HSCT-induced stratospheric ozone perturbation relative to those that would have occurred in the absence of this perturbation. Thus, the appropriate "baseline" for this evaluation is the set of health effects expected under atmospheric conditions reflecting adherence to the Montreal Adjustments to the Montreal Protocol.[13]

Since the AHEF expresses health effects relative to 1979 -1980 ozone conditions, the incremental health effects for the Montreal Adjustments scenario in the absence of an HSCT fleet must be estimated first. The AHEF then is used to estimate the health effects associated with a fleet of HSCT relative to the 1979 -1980 ozone conditions. The incremental health effects associated with the presence of an HSCT fleet relative to the Montreal Adjustments are thus the difference between the results of these two AHEF model simulations. This concept is illustrated qualitatively for skin cancer and cataract incidence in Figure 2-4.

---

[13] The CSIRO model assumes global compliance with the Copenhagen Amendments to the Montreal Protocol. The AHEF, by contrast, generates estimates assuming compliance with the Montreal Adjustments to the Montreal Protocol. That is, the models assume a slightly different baseline or reference atmospheric scenario. The differing assumptions regarding reference scenario are not judged to significantly affect this study's results because only the incremental differences in ozone between the CSIRO results with and without an HSCT fleet are used to generate the percent change in UV using TUV-generated look-up tables (see Equation 2-1 and Section 2.3). To test this judgment, a sensitivity analysis was performed to determine if choice of reference scenario would affect the resulting health effect estimates. Reasonable perturbations to the reference scenario lead to between approximately 1 and 5 percent changes in estimated HSCT-induced health impacts. See Appendix F for a description of these sensitivity tests.

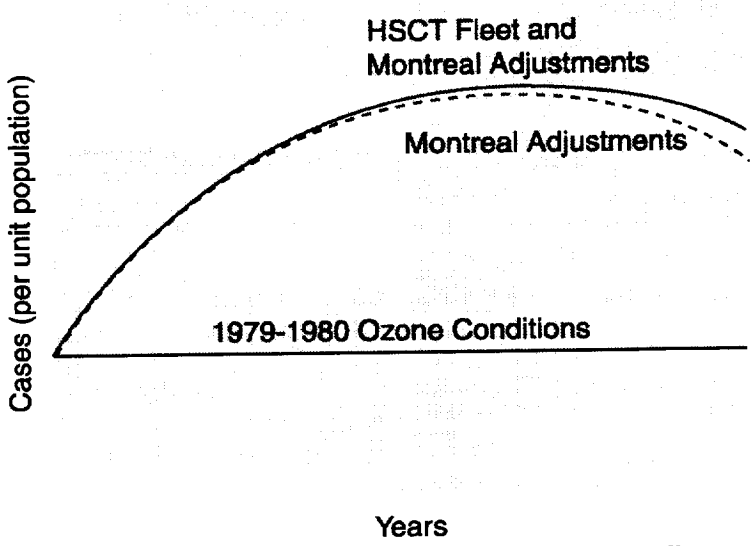

Figure 2-4. Incremental health effects due to an HSCT fleet. This figure depicts the method used by the AHEF to estimate the additional health effects associated with the operation of a fleet of HSCT relative to the Montreal Adjustments.
Note: The curves illustrate the relationship between various emission scenarios, but provide qualitative information only.

2.6 Uncertainty in estimated impacts

Several steps were taken to consider uncertainty in estimated HSCT health impacts. First, the key calculation steps required to estimate human health impacts arising from HSCT-induced ozone change were identified. The steps involved (1) the prediction, by atmospheric models, of the precise ozone column changes under HSCT scenarios, (2) the calculation of consequent changes in surface UVR, and (3) the quantification of the health impacts of the perturbed UVR levels (Madronich 1999). In consultation with experts, the sources and magnitudes of the major uncertainties associated with each step were identified. Table 2-2 summarizes these uncertainties. In many cases, it was not possible to quantify the impact of various sources of uncertainty. Some of the unquantified sources are presented in Table 2-3.

Second, for selected major individual sources of uncertainty (e.g., estimated changes in column ozone, BAFs), the error range estimate was run through the sequence of models to evaluate the uncertainty in the estimated health impact due just to the particular individual input uncertainty. Other sources of uncertainty are also qualitatively discussed. Although a comprehensive, integrated analysis of uncertainty in estimated health impacts due to all

sources was not performed, the results of the individual model runs were used to obtain an initial sense of the uncertainty in the results of this study.

Table 2-2. Factors Contributing Known Uncertainty

Factor	Parameter	Uncertainty	Explanation
Change in Ozone Estimates	General Atmospheric	a range of -2.7% to +0.3% around a central value of -0.6% column ozone depletion[a]	Estimated using information from NASA assessment (Kawa *et al.* 1999)[b]
Change in UVR Estimates	RAF	±10% radiation model <2% ozone absorption spectrum	(Koepke *et al.* 1998) (De More *et al.* 1997)
	Action Spectrum	50%[c]	(Table 11.8, UNEP 1998)
Changes in Health Effect Estimates	BAF	30%	(deGruijl *et al.* 1993, Longstreth *et al.* 1998)

[a] This corresponds to a -350 percent and +150 percent uncertainty range.
[b] Kawa *et al.* (1999) estimated that the uncertainty of the predicted change in Northern Hemisphere ozone content for a fleet of 500 HSCT in 2015 is given by +0.5% to -2.5% around the central value of -0.4%. This corresponds to an upper bound obtained by adding an additional -2.1% ozone decrease and a lower bound obtained by adding a +0.9% ozone increase to the central value, respectively. In this study, the uncertainty range for a fleet of 1,000 HSCT in 2100 was obtained by adding the same increments (-2.1% and +0.9%) to the central value of -0.6%.
[c] This estimate applies only if the action spectrum lies within the range of action spectra for biological effects in mammals.

2.6.1 Uncertainties associated with change in ozone estimates

An uncertainty range for the estimated HSCT column ozone impact was obtained from the NASA assessment. Briefly, that assessment evaluated sources of potential error in the modeling of processes controlling ozone impact. Sources addressed included exhaust particle production; model representation of atmospheric transport; long-term circulation; exhaust accumulation; chemical characteristics of the background atmosphere (halogen, NO_y, and H_2O distributions); and chemistry (reaction kinetics and treatment of heterogeneous processes).

Using a combination of tests of model prediction sensitivity to variations in these parameters, evaluations of existing model biases involving these parameters, and existing information on parameter uncertainty (e.g., measurement error in laboratory studies of reaction kinetics), an estimate of error in central value attributable to each source of uncertainty was developed.

Table 2-3. Factors with Unknown Contributions to Uncertainty

Factor	Parameter
Change in Ozone Estimates	Composition of Future Atmosphere
	Ability to Model Atmospheric Processes Accurately
	Response of Ozone Layer to ODS Phaseout
	Changes in Composition and Quantity of HSCT Emissions
Change in UVR Estimates	Long-term Systematic Changes in Atmospheric Opacity (e.g., clouds, aerosols, other pollutants)
Change in Health Effect Estimates	Changes in Human UV Exposure Behavior
	Improvements in Medical Care/Increased Longevity
	Changes in Socioeconomic Factors
	Latency
	Changes in Population Composition and Size

An estimate of the total uncertainty in the central-value estimate arising from all of these sources of uncertainty was derived by combining the root sums of squares of each of the individual sources of uncertainty (Kawa *et al.* 1999).

The NASA assessment total uncertainty range was developed around a central value of average annual Northern Hemisphere response to a fleet of 500 HSCT in the year 2015. Due to the fact that other uncertainty estimates were not available, this same total uncertainty range is applied in this study to the estimated ozone change for all latitudes and all months, even though estimated ozone changes may be more uncertain at some latitudes and in some seasons than others. Furthermore, the same total uncertainty range is used even though the central value employed in this study is based on a 1,000 aircraft, year 2050 scenario. The use of the 500-aircraft uncertainty range for the 1,000 aircraft scenario is reasonable for the following three reasons (ICF 1999):

- First, some of the modeled processes (e.g., transport or chemical kinetics and mechanisms) should not be very sensitive to the fleet size.

- Second, the estimated uncertainties are conservative and should be applicable to somewhat larger fleet sizes, as well.

- Finally, the assumption that the 500-aircraft uncertainty range can be applied to a fleet of 1,000 aircraft is consistent with the discussion in IPCC (1999) pointing out that the ranges of model-predicted depletion are similar for the 500 plane fleet and the 1,000 plane fleet.

In the evaluation presented here, the uncertainty range is therefore scaled linearly from zero to 500 aircraft and then assumed to remain constant from 500 to 1,000 aircraft. Although this scaling approach is different from the simple linear scaling from 0 to 1,000 aircraft adopted for the central value, it satisfies the decision to use the same uncertainty range for the 500 aircraft and 1,000 aircraft central value estimates.

Recent research has reinforced estimates that 10 percent or less of fuel sulfur will be converted to new particles (i.e., the lower end of the particle production range used in the assessment is most probable). Thus, the uncertainty in ozone depletion associated with the conversion processes, which was largely on the negative side, may be less than previously suspected. This reduction in risk is counterbalanced, however, by new research on the partitioning of NO_x/NO_y in the stratosphere, which suggests a greater effectiveness of aircraft NO_x emissions in destroying ozone. Because these new findings suggest offsetting changes in predicted ozone impacts, no modifications in the uncertainty range were deemed necessary (ICF 2000*b*). The uncertainty in estimated column ozone impacts was considered a major source of uncertainty in this assessment. Because of the existence of a carefully developed estimate of uncertainty in atmospheric inputs, the effect of this estimated uncertainty on health impacts was quantified.

The placement of the upper and lower uncertainty bounds reflects the potential for actual ozone changes to be either greater or less than predicted (see Figure 3-1 in Chapter 3). The upper and lower uncertainty bounds are established by adding 0.9 and -2.1 percent, respectively, to each derived value of percent column ozone change due to HSCT. A step-wise method was used to estimate these bounds (i.e., scaling uncertainty from 0 to 1,000 aircraft and then

holding these bounds constant from 2050 to 2100). The following equation is used to determine the ozone change used for the atmospheric uncertainty analysis:

(Equation 2-8)

$$HSCT_{2015+x} = [No\ HSCT_{2015} * (1 + \%_{\Delta}HSCT_{2050} * PSF_x)] + (No\ HSCT_{2015} * USF_x)$$

where,
x = years 0-35 (2015-2050)
HSCT = ozone levels in the presence of HSCT (Dobson units)
No HSCT = ozone levels in the absence of HSCT (Dobson units)
$\%_{\Delta}$HSCT = change in ozone levels due to HSCT (percent change in ozone is negative)
PSF = production scaling factor, a linear ramp-up from 1-1,000 jets between 2015 and 2050 (a percent expressed as x / 35).
USF = uncertainty scaling factor, a linear scaling of the uncertainty range between 2015 and 2033. The lower bound scales from 0.0 to -0.9 percent {-0.9% * (x / 18), for x = 0 to 18 and -0.9% for years thereafter} and the upper bound scales from 0.0 to 2.1 percent {2.1% * (x / 18), for x = 0 to 18 and 2.1% for years thereafter}.

2.6.2 Uncertainties associated with change in UVR estimates

Uncertainty involved in the estimation of weighted UV exposure at the surface is discussed and quantified below. Although this UV estimation uncertainty was not specifically modeled, expert opinion was solicited regarding the sensitivity of predicted health impacts to changes in UV transfer calculation parameters. Those sensitivities are discussed in Chapter 3. In general, the relationship between changes in ozone and changes in ground-level UVR is well known. Uncertainties contributed by estimating the change in UVR are relatively small compared with those inherent in other components of the analysis. The accuracy of any radiation model, including the TUV model (used in this analysis), depends on the quantity being estimated. In this evaluation, changes in UVR are generated by estimating the relative percent of UV changes stemming from a specific change in ozone, under the strong assumption that all other factors (e.g., air pollution, cloud cover) remain constant.

The key quantity in this estimation process is the sensitivity factor, often known as the "radiation amplification factor," or RAF.[14] The RAF is defined by:

$$(\Delta UV/UV) \sim - \text{RAF} \times (\Delta O_3/O_3). \qquad \text{(Equation 2-9)}$$

For example, the RAF for human erythema and UV index is approximately 1.1. Errors in UV are thus directly proportional to errors in the RAF. Of course, RAFs are not true constants, and the approach that the TUV model uses is to compute local RAFs from tables of ground-level UVR for a range of solar zenith angles, ozone column amounts, and surface elevations.[15]

Errors in estimating RAFs, and thus errors in estimating ground-level UVR, are dominated by uncertainties in the following:

1. Action spectra. The action spectra contribute by far the largest uncertainties. For example, a variety of action spectra can be used to weight the wavelengths of UVR that produce a given health effect. As discussed in UNEP (1998), for a given action spectrum, the RAFs for skin cancer in mammals range between 1.1 and 1.7, suggesting an uncertainty range of approximately 50 percent.

2. Ozone absorption. The ozone absorption spectrum in the critical 300-320 nm wavelengths is known to be accurate to better than 2 percent from many laboratory studies (De More *et al.* 1997).

3. Radiation model. Few systematic comparisons of RAFs from different radiation models have been performed. In the 1989 Ozone Assessment, Table 3.2-10 compares RAFs for different models and atmospheric conditions. Variations of a few percent are noted

[14] The RAF is commonly used to provide rough estimates of the response of surface UVR to changes in the total ozone column. The RAF concept is used in this evaluation for illustrative purposes only and a more accurate method of estimating ground-level UVR is used for the actual calculations that create the look-up tables discussed in Section 2.3. Background information on the use of RAFs is provided in Appendix D.

[15] A description of the effect that clouds and the altitude of an ozone perturbation could have on these values is provided in Appendix D.

(WMO 1989). Many other important model differences are possible (e.g., spectral resolution). Published comparisons of models and measurements show, in the best circumstances, agreement to approximately 10 percent for spectral irradiances and actinic fluxes (Koepke *et al.* 1998).

2.6.3 Uncertainties associated with change in health effect estimates

Health effects modeling contributes quantifiable uncertainties to the estimates of human health effects resulting from a fleet of HSCT in two major areas: (1) the dose-response relationships (expressed as a BAF) for the four endpoints of concern (i.e., cataract, BCC, SCC, and CMM), and (2) the future size, behavior, and distribution of the populations that will be affected. These sources of uncertainty are further described below. It should be noted that for this study, only estimated uncertainty in the BAF parameter was quantified. Qualitative discussions of the sensitivity of predicted impacts to other health effects modeling uncertainties are provided in Chapter 3.

2.6.3.a. Uncertainty in the BAF

Health effects modeling, which incorporates dose-response information in the form of a BAF is one source of uncertainty for change in health effect estimates. The model used in this analysis, the AHEF (described in Section 2.4), incorporates information on the dose-response relationships for cataract, BCC, SCC, and CMM through the use of a BAF (i.e., the slope of the dose-response relationship). Estimates of BAFs generated for SCC and BCC using the SCUP-h action spectrum are 2.5 ± 0.7 and 1.4 ± 0.4, respectively (deGruijl *et al.* 1993, Longstreth *et al.* 1998). This yields an uncertainty range of approximately 30 percent for changes in health effects estimates.

2.6.3.b. Uncertainty in population projections

The AHEF combines U.S. population projections with a number of other parameters to predict the absolute number of future skin cancer and cataract cases and/or deaths associated with a proposed fleet of HSCT. Projections of U.S. population size are obtained from the U.S. Census

Bureau grouped by state, age, sex, and race through 2025 (population by state) and 2050 (entire United States). These data then are further aggregated into latitude bands, as described in ICF (2000*a*). This process is used both in this evaluation and in all other EPA applications involving the AHEF.

The U.S. Census Bureau does not develop quantitative estimates of the uncertainty ranges accompanying the population projection groupings used by the AHEF (i.e., by state, age, sex, and race). However, the bureau does generate high and low estimates of the future population by state, and quantitative estimates of the uncertainty accompanying the annual population growth rate for the United States. The U.S. population is estimated to grow at a rate of 1 percent per year (Spencer personal communication). A ± 0.1 percent uncertainty range accompanies this annual estimate. This uncertainty range pertains only to the amount of yearly increase experienced by the U.S. population as a whole, however, and does not consider the uncertainty that may accompany the absolute estimate of the number of U.S. residents in a given year. In addition, it does not address the uncertainty surrounding the population groupings (i.e., age, state, sex, race) used by the AHEF.

Thus, applying this general estimate of uncertainty to the population groupings used by the AHEF would be difficult. For example, the growth rate of the total U.S. population may vary by ± 0.1 percent, but the uncertainty accompanying the growth rate of various ethnicities within this population may be much more or less than 0.1 percent. In addition, the uncertainties accompanying the absolute sizes of these subpopulations are unknown. However, several methodologies for testing uncertainty in population projections have been proposed. These methods are discussed in Section 3.4.3.a.

2.6.3.c. Latency

In this evaluation, latency refers to the lag time between UV exposure and the manifestation of skin cancer or cataract. Skin cancer latency and early life exposure have been identified as potentially important risk factors associated with increased susceptibility to CMM. Modeling this lag time accurately is difficult given the current state of knowledge about latency and its mechanisms (Madronich 1999). Thus, quantitatively estimating the uncertainty contributed by

this process is not possible at this time. However, the presence or absence of a formal modeling of latency is not thought to contribute significantly to the uncertainty accompanying the health effect estimates. The reasoning behind this expectation is as follows: The AHEF currently offers the option of weighting UV exposures by age and by type of exposure (e.g., peak-day exposure and annual exposure) summed over the lifetime of the individual, thus approximating a type of latency. When varying assumptions regarding latency were assumed, estimated health impacts were affected only moderately. The results of this analysis are presented in Section 3.4.3.b.

2.6.4 Other sources of uncertainty

Many uncertainties in this evaluation either cannot be quantified or are currently so poorly understood that an accurate estimate of their significance is not possible. For example, alterations in the composition of the future atmosphere, as well as uncertainties about the response of the ozone layer to changes in ODS emissions can combine with changes in HSCT fleet emission characteristics to contribute an unknown amount of uncertainty to change in ozone estimates. Similarly, laboratory techniques and instrumentation, changes in population size and composition, fluctuations in human UV exposure patterns, and a variety of other factors can greatly affect the uncertainty surrounding predictions of human health effects. These and other factors are briefly discussed below.

2.6.4.a. Contributions to unknown uncertainties in change in ozone estimates

The exact composition of the future atmosphere as a result of compliance with different ODS phaseout policies is unknown. As levels of atmospheric chlorine are reduced, the impact of NO_x species from the proposed HSCT fleet would change. In addition, future changes in climate could result in increases in atmospheric water vapor, which could in turn increase cloud cover.[16] The impacts of global warming on the composition of the future atmosphere also are unknown. These elements could introduce a variety of uncertainties into estimates of skin cancer and cataract incidence and/or mortality.

[16] See Appendix D for a brief discussion of the effects of cloud cover on ground-level UVR.

Uncertainties also can be contributed by assumptions regarding the future behavior of the ozone layer in response to the phaseout of ODS. When estimating future changes in ozone, accurately modeling the effects of various policy scenarios (e.g., the Montreal Protocol and its amendments) on ozone concentrations is important. In the future, some computer models predict that the phaseout of ODS will slow and eventually stop the rate of ozone depletion. Some of these models suggest that natural ozone-making processes will enable stratospheric ozone to return to 1979-1980 ozone conditions and eventually result in increased concentrations beyond those levels (see Chapter 12 in WMO 1998 for more detail). Because knowledge about the interaction of ozone with chemical species in the future atmosphere is still incomplete, no artificially created limit has been imposed on future ozone recovery in this evaluation. That is, in both the CSIRO input and the Montreal Adjustments baseline, ozone levels are allowed to recover beyond conditions observed in 1979-1980.[17]

In addition, improvements in engine design and technology may alter the emissions created by an HSCT fleet. Evolving knowledge regarding factors such as atmospheric transport, heterogeneous chemistry, climate change, and the representation of these factors in models, also may lead to changes in estimates of ozone impacts resulting from fleet emissions.

2.6.4.b. Contributions to unknown uncertainties in change in health effect estimates

Additional uncertainty can be contributed by the laboratory techniques and instrumentation used for deriving the action spectra used to weight UV exposure. Discrepancies between the wavelengths of UVR intended to be administered and the wavelengths actually received by the test organism can result in orders of magnitude differences in the measured response. In

---

[17] Whether this recovery scenario, called "ozone superabundance," is likely to occur is open to debate, particularly because of the potential for complex interactions between global climate change and stratospheric ozone dynamics. Model computations have predicted both future conditions of higher and lower amounts of ozone. Stratospheric temperature may be cooler due to increased emissions of greenhouse gases, and reactions that destroy ozone may consequently proceed more slowly. This scenario would lead to increases in ozone. Alternatively, the cooler temperatures could change stratospheric circulation and also may lead to increases in polar stratospheric clouds, which potentially could lead to decreases in ozone, possibly preventing or delaying ozone recovery.

addition, action spectra are derived using monochromatic light sources, which do not fully simulate the polychromatic light received directly from the Sun.

Changes in socioeconomic factors, population composition and size, and human UV exposure behavior also can have an impact on factors ranging from demand for air travel to the types of skin cancer most commonly observed. For example, population composition changes such as the expected increase in Hispanic populations, whose more pigmented skin decreases their skin cancer risk, could have significant effects on future U.S. skin cancer rates. Improvements in medical care and predictions of increased longevity for many population subgroups also could affect estimates of future skin cancer incidence and mortality significantly. In addition, this evaluation assumes that human exposure behavior remains constant through time and does not take into account innovations in sun protection technology (e.g., sunglasses, sunscreens), increases in public awareness of the effects of overexposure, and increased sensitization to the need for early treatment of suspicious lesions. Factors such as these cannot easily be quantified and are not addressed further in this evaluation.

These demographic and behavioral changes may also be augmented or offset by changes in surface UVR due to atmospheric constituents other than stratospheric ozone (e.g., changes in tropospheric ozone and aerosols from pollution, and changes in cloudiness stemming from climate change and pollution). These factors, as well as those described above, may in some cases result in UVR changes or health effect changes larger than those estimated to result from the operation of a fleet of HSCT.

Accurate prediction of future changes in human health effects would require consideration of the net effect of all factors described above. This challenge is beyond the ability of the current state of atmospheric and epidemiological science. In addition, direct measurements (e.g., of future UV levels or skin cancer incidence) cannot attribute explicitly observed changes to any specific factor, unless that factor is far more important than all the others combined. However, the principle of superposition can be used to examine the HSCT impact (i.e., one effect, in isolation) under the assumption that the other factors remain constant at current conditions. The validity of this principle is based on the assumption that the HSCT

impacts are independent of the other factors (e.g., behavioral changes will occur regardless of whether an HSCT fleet is in place).

2.7 Sensitivity of estimated health impacts to technological and operational change

When evaluating the number of excess cataracts or skin cancers estimated by the AHEF for the proposed HSCT fleet, it is important to consider the sensitivity of estimated health impacts to possible alterations in various operational, technological, and atmospheric parameters. A sensitivity analysis conducted along these lines can be a useful tool for decision-makers, as it can assist in identifying and focusing resources on factors that exert the greatest influence on ozone depletion and thus have the greatest ability to reduce expected health effects. For example, a sensitivity analysis may indicate that changes in fleet cruise altitude have significant impacts on ozone depletion whereas other changes might have only slight impacts. The NASA assessment contained an analysis of plausible variations in fleet size, fuel sulfur content, NO_x emission index, and altitude (e.g., the parameters listed in Table 2-4). The NASA analysis revealed that these changes could alter estimates of column ozone response by as much as -0.4 to +0.3 percent relative to the baseline scenario of 500 HSCT in 2015 and 1,000 HSCT in 2050 examined in that study (Table 2-4) (Kawa *et al.* 1999).

A perturbation of ±0.1 percent column ozone change around the central ozone estimate (approximately 17 percent of the central value) was selected as a representative perturbation to explore the sensitivity of estimated health impacts due to variation in various control parameters. Although this perturbation is smaller than the column ozone sensitivity to some of the technological and operational parameters examined in the NASA assessment, the results of this sensitivity study should provide a rough scaling factor between technological and operational change and changes in estimated health impacts.

To implement this sensitivity test, from 2015 to 2033 (i.e., from 0 to 500 aircraft), the magnitude of the perturbation was adjusted to reflect the growing number of HSCT in operation. The full perturbation of ±0.1 percent was used to evaluate HSCT impacts between 2033 and 2100 (i.e., 500 to 1,000 aircraft).

The following equation was used to apply the sensitivity bounds to the central value:

(Equation 2 -10)

$HSCT_{2015+x} = [No\ HSCT_{2015} * (1 + \%_{\Delta}HSCT_{2050} * PSF_x)] + (No\ HSCT_{2015} * SSF_x)$

where,

x = years 0-35 (2015-2050)

HSCT = ozone levels in the presence of HSCT (Dobson units)

No HSCT = ozone levels in the absence of HSCT (Dobson units)

$\%_{\Delta}$HSCT = change in ozone levels due to HSCT (percent change in ozone is negative)

PSF = production scaling factor, a linear ramp up from 1-1,000 jets between 2015 and 2050 (a percent expressed as x / 35).

SSF = sensitivity scaling factor, a linear scaling factor of the sensitivity range of ±0.1 percent between 2015 and 2033 {± 0.1% * (x / 18), for x = 0 to 18 and ±0.1% for years thereafter}.

Figure 2-5 indicates the sensitivity bound as the inner shaded region ("inner envelope"), whereas the uncertainty bound is the outer shaded region ("outer bound") around the central-value line. Table 2-4 lists NASA's findings regarding the sensitivities associated with changes in various parameters for a fleet of 500 aircraft. This evaluation assumes that these relationships remain constant from 500 to 1,000 aircraft.

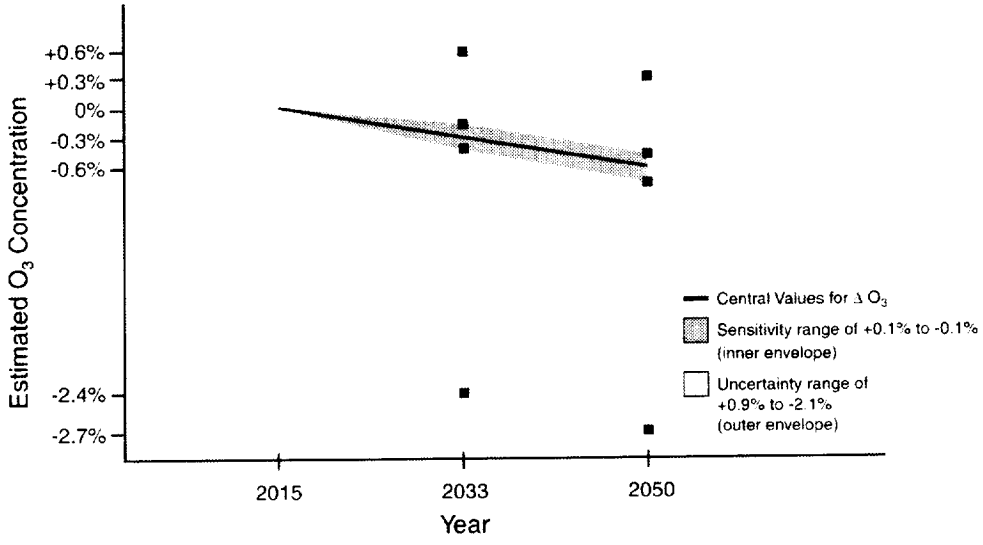

Figure 2-5. Sensitivity and uncertainty envelopes. This graph depicts the methods used to estimate the uncertainty inherent in generating ozone estimates as well as the methods used to quantify the sensitivity of the predicted ozone values to changes in various technical and operational parameters.

Table 2-4. Sensitivity of Ozone Estimates to Various Technological and Atmospheric Parameters

Parameter	Parameter Change Relative to Base Case	ΔO_3 Relative to Base (%)
Exhaust Emission		
Fuel Consumption	to 1,000 aircraft	-0.3%
Sulfur Content	to 0 to 0 with 4 x background	+0.3% +0.1%
EI_{NOx}	to 10 g/kg	-0.1%
Altitude	2 km below base case 2 km above base case	+0.2% -0.4%
Future Atmosphere		
Halogens	3 to 2 ppb	-0.1%
H_2O	base case -2 ppm base case +2ppm	-0.1% +0.1%
Aerosol	background to 4 x background	+0.1%
Temperature	Warm to cold	+0.1 to -0.1%*

*Temperature variation over the past two decades was used to generate this range of HSCT ozone loss. The Atmospheric and Environmental Research, Inc., (AER) model was used for this exercise (Kawa *et al.* 1999, p. 147)
Note: This table was originally derived for a fleet of 500 aircraft, but these values are assumed to remain constant from 500 to 1,000 aircraft for purposes of this evaluation (ICF 1999).
SOURCE: Kawa *et al.* 1999, Table 5-2, p.145.

Chapter 3. Results and Discussion

Chapter 3 presents results of the analyses performed to assess the impacts on human health of a proposed HSCT fleet and discusses these results. Section 3.1 first describes changes in stratospheric ozone concentrations due to HSCT and then compares the magnitude and seasonality of the HSCT-induced change with those expected from ODS emissions for a representative year (2033). Section 3.2 next describes the projected features of HSCT-induced UVR changes. Section 3.3 summarizes the calculated change in skin cancer incidence, skin cancer mortality, and cataract incidence from HSCT, relative to effects expected under adherence to the Montreal Adjustments of the Montreal Protocol. Section 3.4 presents and discusses the results of uncertainty analyses performed to provide information regarding the uncertainty in estimated health impacts. Section 3.5 presents the results of a sensitivity analysis performed to link changes in certain HSCT fleet technological and operational factors and the degree of reduction or exacerbation of human health impacts. A comparison of the estimated health impacts of HSCT with those of several past regulatory strategies for stratospheric protection is provided in Chapter 4.

3.1 HSCT impacts on stratospheric ozone concentrations

Using outputs from a previous application of the CSIRO model (see Section 2.2.1 for discussion), future changes in stratospheric ozone concentrations resulting from a fleet of HSCT were estimated. These results then were scaled linearly to a starting point of zero HSCT in service in 2015. The following subsections point out several features of these derived time-dependent column ozone patterns.

3.1.1 Annual percent change in ozone

A critical first step in the evaluation of HSCT impacts on human health is to generate a time-dependent series of annual estimates of the change in stratospheric ozone concentrations that would be produced by a growing fleet of HSCT. As described in Section 2.2.1, CSIRO outputs for the year 2050 were scaled based on the percent of the HSCT fleet in operation per year

from 2015 to 2050. From 2050 to 2100, the estimated HSCT-induced percent column ozone change is held constant at 2050 levels. Figure 3-1 presents the percent change in column ozone estimated to occur as a result of an HSCT fleet operating from 2015 to 2100. The positive change in ozone exhibited in the upper uncertainty bound suggests that ozone concentrations could show a net increase during the time frame in which the fleet is in operation. A net increase in ozone levels resulting from a fleet of HSCT, however, is considered less likely than a decrease in ozone levels.

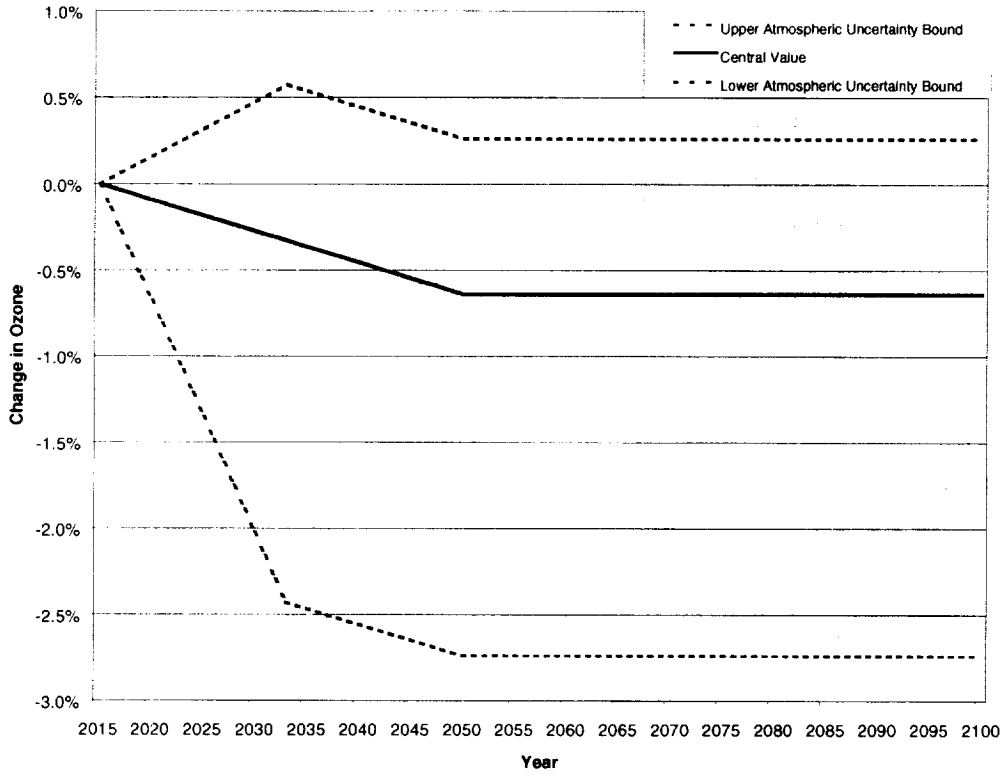

Figure 3-1. Annual percent change in ozone relative to the Montreal Adjustments atmospheric conditions resulting from a fleet of HSCT grown from 0 in 2015 to 1,000 in 2050 (40°-50°N latitude band). Lowest curve represents the lower uncertainty bound of -2.1 percent relative to the central value; middle curve is the central change in ozone value; highest curve is the upper uncertainty bound of +0.9 percent relative to the central value. Extrapolated from CSIRO simulation of the HSR program's Scenario 36 (Table 4-3, Kawa *et al.* 1999). See more detailed discussion of uncertainty in Section 2.6.1.

3.1.2 Seasonal patterns

In general, ozone depletion resulting from the operation of an HSCT fleet has been found to vary seasonally as temperature, circulation, and other changes influence atmospheric processes. Estimates generated by the CSIRO model predict the greatest ozone depletion during fall and winter months (i.e., from September to March) and the least depletion during spring and summer months (i.e., from April to August).[1] Figure 3-2 illustrates the seasonal fluctuations in the central-value ozone concentrations for the HSCT fleet per month in 2050. Central-value ozone changes produced by an HSCT fleet fluctuate seasonally from approximately -0.48 percent to -0.66 percent for the 20° to 30° latitude band.

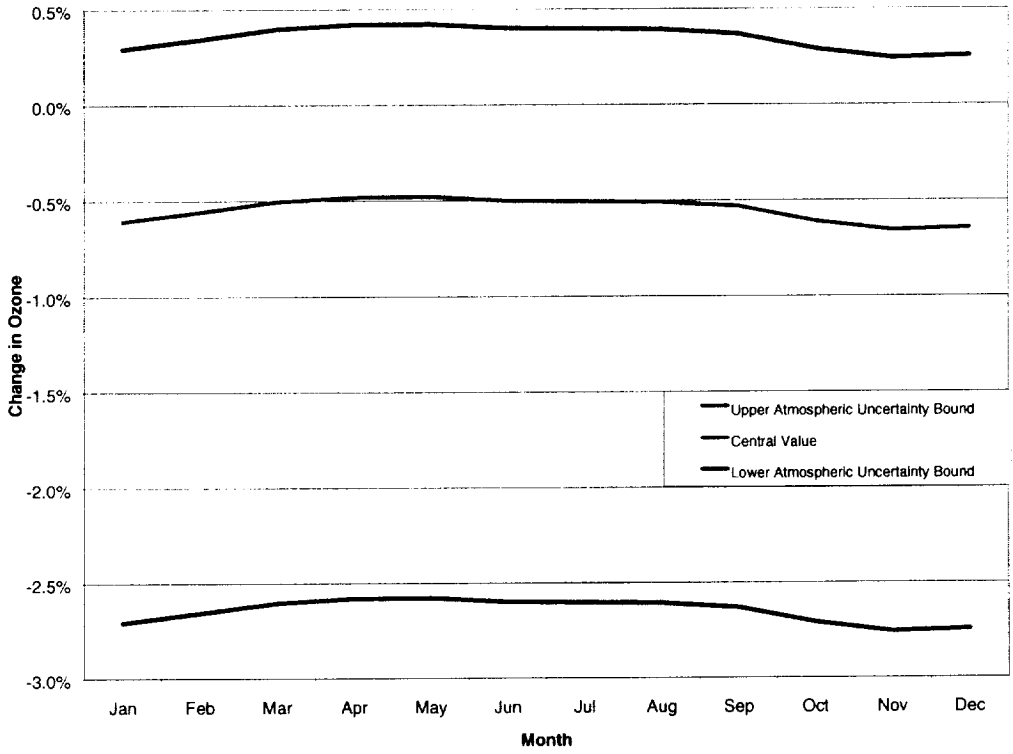

Figure 3-2. Percent change in ozone by month for 2050 resulting from a fleet of 1,000 HSCT. (For clarity, only the 20 to 30°N latitude band is presented.) The seasonal ozone trends observed in this figure are relevant to trends in latitudinal bands examined in this analysis. At higher latitudes the seasonal variation will differ.

[1] The NASA assessment performed an analysis of ozone seasonal distribution and trends for five 2-D models, including CSIRO (Kawa *et al.* 1999). This analysis compared the predicted seasonal behavior from the models with actual climatology data. NASA concluded that most of the models satisfactorily represented the parameters examined.

Because discussions concerning ozone depletion are based on ODS emissions, it is instructive to compare the seasonal patterns of ozone depletion resulting from these emissions with the seasonal patterns of ozone depletion that would result from a proposed fleet of HSCT. In general, ozone depletion resulting from the use of ODS (i.e., driven by estimates of equivalent effective stratospheric chlorine, or EESC[2]) occurs mainly in the winter and spring (i.e., January to June) with relatively wide seasonal fluctuations (Figure 3-3). Seasonal fluctuation in ozone depletion from HSCT, on the other hand, covers a much smaller range (i.e., the magnitude of values is more constant throughout the year, see Figure 3-3). Thus, in summer months (e.g., July) when little ozone depletion results from ODS emissions, ozone depletion resulting from a fleet of HSCT may constitute a larger percentage of overall depletion. Similarly, in winter months (e.g., February) when ODS-related ozone depletion is high, HSCT-related ozone depletion may contribute a smaller percentage of the overall depletion. In the example provided in Figure 3-3 for the year 2033, HSCT fleet impacts range between 6 and 11 percent of the total (ODS- plus HSCT-driven) ozone depletion occurring from January to June and between 17 and 35 percent of the total (ODS- plus HSCT-driven) ozone depletion occurring from July to December.

Figure 3-3 illustrates the seasonal impacts of ODS- and HSCT-related ozone depletion assuming full compliance with the Montreal Adjustments to the Montreal Protocol. The lightly shaded portion of the graph is the expected ozone depletion relative to atmospheric ozone in 1979-1980 due to ODS emissions for 2033, based on a separate analysis (calculations not presented).[3] The darkly shaded portion in each of the bars in Figure 3-3 represents the estimated incremental decrease associated with HSCT operation by month for 2033 (when half of the fleet is predicted to be in operation), as estimated by extrapolations performed on the CSIRO outputs described in Section 2.2.

[2] EESC is an expression of the ozone-depleting capability of a substance and its degradation products, expressed in terms of chlorine molecules. The EESC of substances that contain bromine can be calculated by using a bromine efficiency factor that relates the ozone-depleting efficiency of bromine to that of chlorine.

[3] ODS-induced ozone depletion was calculated as described in ICF (2000a), based upon ODS emissions projections assuming compliance with the Montreal Adjustments and empirical relationships between historical ODS emissions and observed ozone depletion, by latitude band.

3.1.3 Latitudinal patterns

In general, ozone depletion resulting from use of ODS also varies by latitude, with greater ozone depletion expected in colder northern regions (i.e., nearer the polar vortex) and less depletion expected toward the equator. An inspection of the three latitude bands (20° to 30°N, 30° to 40°N, and 40° to 50°N) used in this evaluation also indicates a trend of decreasing ozone depletion with decreasing latitude.

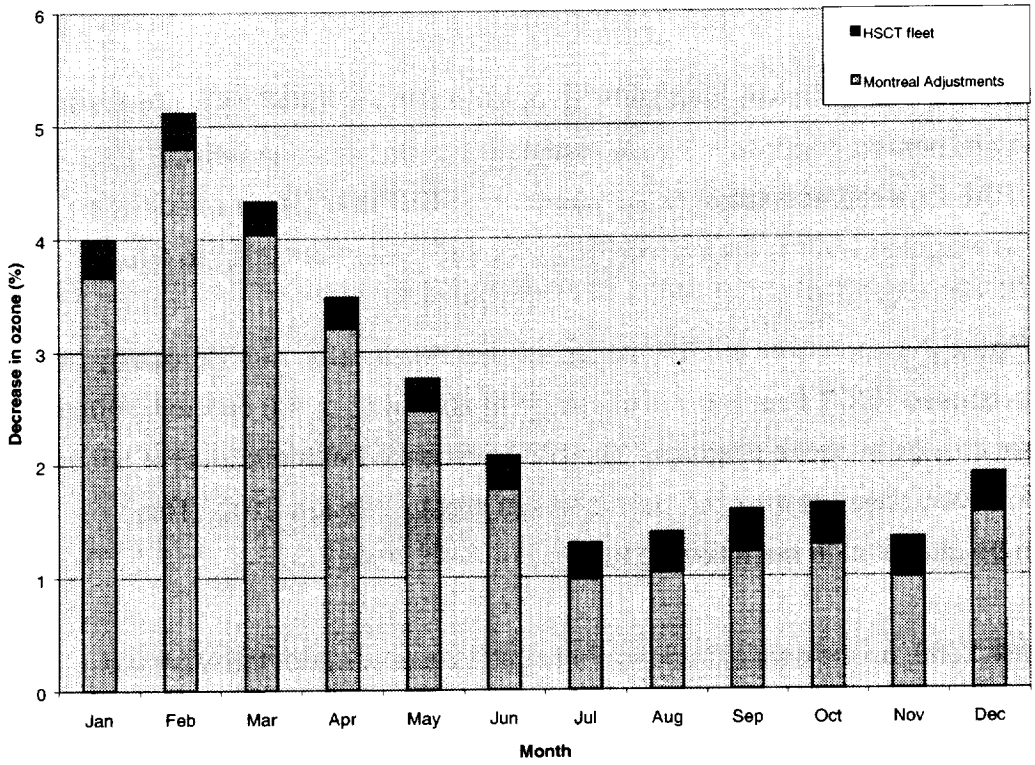

Figure 3-3. Comparison of ozone depletion due to ODS and HSCT in 2033 relative to 1979-1980 ozone conditions (40 to 50°N latitude band). The bottom of each column demonstrates the variable decrease in ozone throughout the months attributable to ODS-related depletion, with the greatest amount of depletion occurring in winter. The top portion of each column shows the incremental additional ozone depletion due to HSCT. See Section 3.1.2 for further discussion.

3.2 HSCT impacts on UVR

This section summarizes the estimated effects of an HSCT fleet on ground-level UVR. As described in Section 2.3, the TUV model was used to calculate UVR from changes in ozone inputs generated by the CSIRO model.

To illustrate the approach used, a sample calculation of the changes in ground-level UVR associated with a fleet of HSCT is provided. Extrapolated CSIRO data and a representative RAF are used in the discussion presented here. Although the results of this approach agree with the many output files generated by the TUV, these rough calculations are performed for descriptive purposes only and are not used directly to estimate incremental UVR. In particular, the TUV model used in this analysis is a more accurate tool for generating these incremental UVR estimates because the look-up tables created from the TUV estimate a series of local ground-level UVR values based on a wide variety of parameters including solar zenith angle, time of day, and day of month (whereas an RAF is a single average value).

Figure 3-4 presents the change in weighted UVR associated with an HSCT fleet. To produce this figure, the annual percent changes in ozone, estimated as described in Section 3.1.1, are multiplied by the RAF for a representative action spectrum (SCUP-h = 1.4) to calculate an average change in weighted UVR in the United States for each year from 2015 to 2050.

As illustrated in Figure 3-4, increases in UVR exhibit a linear relationship with increasing fleet size. When the proposed HSCT fleet is in full operation in 2050 (i.e., 1,000 operating aircraft), the annual percent change in ozone plateaus. The UVR associated with this level of annual ozone change, however, does not level off, but increases slightly through 2100. This phenomenon can be attributed to the following factors:

1. After 2050, ozone concentrations continue to recover under the Montreal Adjustments scenario, resulting in higher ozone levels ("superabundance," discussed in Section 2.6.4.a.).

2. The column ozone percent depletion due to the HSCT fleet of 1,000 aircraft is held constant after the year 2050.

3. The column ozone depletion associated with HSCT operation is a fixed percentage of the base ozone concentration; therefore, the absolute amount of

HSCT-induced ozone depletion increases as the base ozone concentration increases.[4]

4. This increased amount of ozone depletion leads to higher UVR values over time.

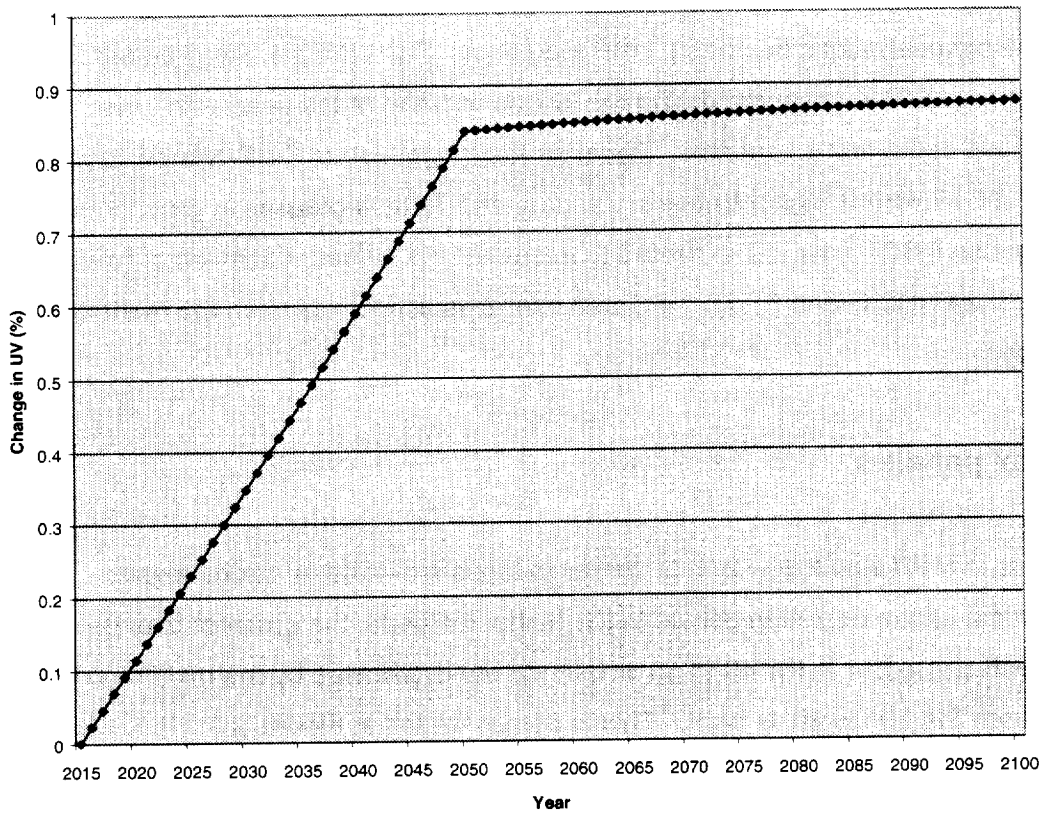

Figure 3-4. Annual change in UVR due to the implementation of an HSCT fleet from 2015-2100. Note that as the number of aircraft increases from zero in 2015 to 1,000 in 2050, the UV R increases linearly. Once the entire fleet is online in 2050, the slope of the change in UVR decreases.

In summary, the values of the percent change in UVR estimated to occur from 2050 to 2100 increase slightly over time as a result of the combined influence of the above factors. UVR is predicted to increase less than 0.05 percent from 2050 to 2100, in contrast to the more than 0.80 percent increase predicted to occur between 2015 and 2050. Thus, this slight increase in UVR after 2050 is judged to be a second-order effect of HSCT fleet operation attributable to the

[4]This analysis also was performed using absolute ozone change rather than percent ozone change; however, the difference between these methodologies is not significant since the results differ by less than 1.5 percent (see Section 2.2.2.a. and Appendix C for additional detail).

modeling approach (i.e., assuming a constant percentage decrease in ozone levels associated with HSCT operation after 2050).

3.2.1 Seasonal patterns

Seasonal changes in UVR are closely related to the ozone changes presented in Figure 3-2 because as ozone concentrations decrease, UVR increases. For example, the greatest percentage change in UVR is observed during the last six months of the year, with lower proportions observed in the first six months. Because the magnitude of ODS-related ozone depletion (i.e., EESC-driven) is higher between January and June, increases in ground-level UVR resulting from an HSCT fleet are expected to account for a higher proportion of total UV change (resulting from HSCT- and EESC-mediated ozone depletion) between the months of July and December.

3.2.2 Latitudinal patterns

Latitudinal patterns in UVR also follow trends similar to those exhibited by ozone levels. Because the greatest ozone depletion occurs in the higher latitudes, the greatest change in irradiance is expected to occur in the 40 to 50°N latitude band, followed by the middle 30° to 40°N band, and then the 20° to 30°N band. This is demonstrated in Figure 3-5.

3.3 HSCT impacts on human health

This evaluation attempts to assess the changes in skin cancer and cataract cases and/or deaths in the U.S. population that would occur over time as a result of changes in UV exposure that would be produced by operation of an HSCT fleet. The AHEF combines information on ozone change, UV exposure change, and dose-response information to quantify these changes. The following sections describe the total incidence and mortality due to the operation of an HSCT fleet, seasonal and latitudinal variations in human health effects, and the annual estimates of changes in human health effects.

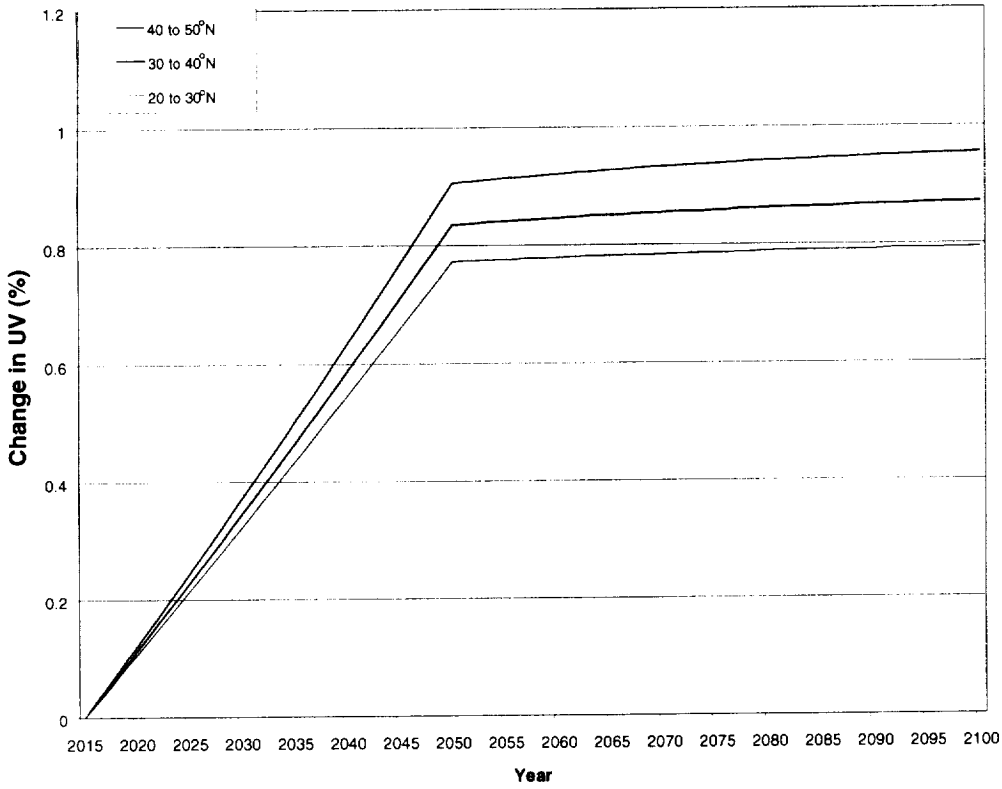

Figure 3-5. Annual latitudinal differences in UVR caused by an HSCT fleet (2015-2100). Lowest band represents the 20-30 N latitude band, middle band represents the 30-40°N latitude band and highest band represents the 40-50°N latitude band.

3.3.1 Total incidence and mortality due to HSCT operation

Table 3-1 presents the estimated increase in health impacts among the U.S. light-skinned population that would occur if an HSCT fleet were launched in 2015 and were to grow to an in-service fleet size of 1,000 by the year 2050 and operate at this constant size from 2050 through 2100. The health impacts presented are total skin cancer incidence, skin cancer mortality, and cataract incidence. Incidence and mortality estimates were performed for cohorts born between 1890 (i.e., dying in 1980) and 2100 (i.e., dying in 2190). Although individuals born after 2100 will receive additional UV exposures due to HSCT fleet operation, the model estimates increased human health impacts due to higher cumulative UV exposures only for individuals born through 2100.

The AHEF health effects estimates in Table 3-1 are presented for the central-value case. The values presented in parentheses in Table 3-1 are upper and lower bounds around the central value, based only on the uncertainty range accompanying estimated HSCT ozone impacts. To

include the uncertainty contributed by the health effects estimates, the values presented in the table, including those in parentheses, should be multiplied by a factor of 2 (see Section 3.4.4 for derivation of this factor). Sections 2.6 and 3.4 provide discussion of these uncertainty factors.

As shown for the central-value case, the greatest predicted increase in skin cancer incidence is for BCC (964,500 cases), and the greatest predicted increase in mortality is for CMM (4,500 deaths).

Table 3-1. Total Predicted Incremental Incidence or Mortality in the United States among People Born Between 1890 and 2100 due to HSCT Operation (thousands)

	CMM Incidence	CMM Mortality	BCC Incidence	SCC Incidence	NMSC Mortality	Cataract Incidence
Central Value	36 (-25 to 180)	4.5 (-3 to 23)	960 (-690 to 4,900)	523 (-380 to 2,700)	2.6 (-2 to 13)	360 (-270 to 1,900)

Note: Numbers presented in parentheses are upper and lower bounds around the central value, based only on the uncertainty range accompanying estimated HSCT ozone impacts. To include the uncertainty contributed by the health effects estimates, the values presented in the table, including those in parentheses, should be multiplied by a factor of 2 (see Section 3.4.4). Further discussion of these results is provided in Chapter 4.
CMM = Cutaneous Malignant Melanoma, **BCC** = Basal Cell Carcinoma, **SCC** = Squamous Cell Carcinoma, and **NMSC** = Non-Melanoma Skin Cancer (SCC + BCC).
SOURCE: Estimated for this report based on ICF 2000*a*.

3.3.2 Seasonal patterns

Increases in UV-related health effects are thought to be associated with repeated exposure to UVR and often are assessed by examining cumulative doses (ICF 2000*a*). This dose metric does not separate incremental health effects by season, recognizing that cumulative year-round UV exposure is thought to be a more accurate predictor of skin cancer and cataract than is an analysis of seasonal exposure trends. The method used in this study sums estimates of UV exposure across all days in a given year and presents incremental health effects on an annual basis.

3.3.3 Latitudinal patterns

Figures 3-6 and 3-7 present annual excess SCC and BCC incidence by latitude band associated with the proposed HSCT fleet. SCC and BCC were chosen for comparison because they provide a good snapshot of the AHEF results by latitudinal gradient. The total incidence and mortality estimates have been divided by the total affected population (i.e., light-skinned individuals) and then multiplied by 100,000. By expressing these estimates as rates per 100,000 individuals, the influence of different population sizes across latitudes is removed.

When examining the excess number of cases for each latitude band, it is important to remember that these incidence predictions are obtained as described in Equation 2-6. Of the three inputs to the equation (i.e., the BAF, the percent change in annual UVR, and the historical baseline incidence rate), the BAF stays constant across latitudes for a given health effect. Due to the fact that ozone changes predicted by the atmospheric models are largest at higher latitudes, the percent change in annual UVR for the HSCT fleet scenario is greatest in the north (40 to 50°N latitude band) and lowest in the south (20 to 30°N latitude band). In contrast, the historical baseline incidence rate for a given health effect is usually much higher at lower latitudes due to the normally higher UV radiation levels prevailing there.

For SCC, presented in Figure 3-6, the high estimated number of cases of excess skin cancer due to an HSCT fleet in the southern latitude band (20° to 30°N) is a result of the dominating influence of historical baseline incidence rates that are many times higher than the percent change in UVR for this region. The northern latitude band (i.e., 40° to 50°N) has a much smaller historical baseline incidence rate. Thus, despite the larger HSCT impacts on ozone and UVR at this latitude, excess skin cancer cases under the HSCT fleet scenario are smaller than those calculated for lower latitudes.

For BCC, presented in Figure 3-7, the large baseline incidence rates in the southern latitude band also produce the highest predicted incremental number of cases of this type of skin cancer. However, in contrast to SCC, historical baseline incidence rates for BCC vary only slightly between middle and northern latitudes, with northern incidence rates being slightly lower than middle latitude rates.

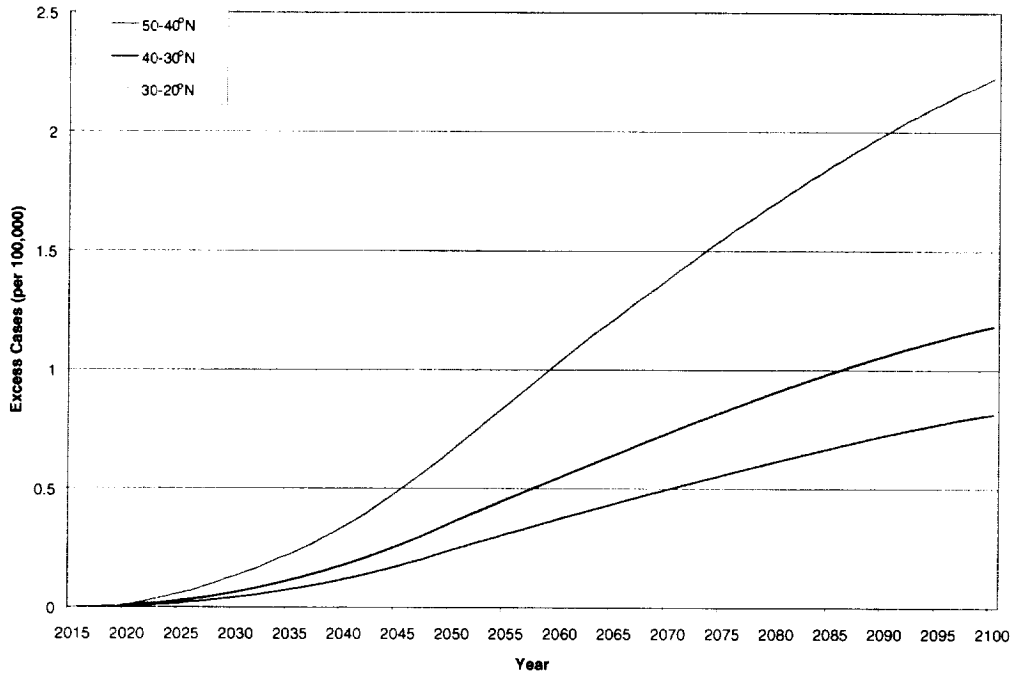

Figure 3-6. Annual estimates of excess SCC incidence per 100,000 by latitude. The lowest line represents the 40-50°N latitude band; the middle line represents the 30-40°N latitude band; the highest band represents the 20-30°N latitude band.

Because the equation used to estimate excess incidence holds the BAF constant, and because the historical baseline incidence rates in the two regions are not significantly different, estimates of excess incidence are more strongly influenced by estimates of percent change in UVR. Because the percent change in UVR is greater in the north than in the middle latitude band, the 40° to 50°N latitudinal band has a higher excess incidence rate for BCC than the 30° to 40°N band.

3.3.4 Estimates of annual changes in health effects

Estimates of annual changes in health effects illustrate the impact of a proposed HSCT fleet over time relative to the Montreal Adjustments baseline. Figures 3-8 through 3-13 present estimates for each health effect endpoint generated by the AHEF[5]. The shape of

[5] Note that in these health effects graphs, unlike the figures depicting changes in ozone, the "upper" uncertainty bounds (i.e., representing less ozone depletion compared to the central value) are the lower lines on the figures. Similarly, the "lower" uncertainty bounds, representing greater decreases in ozone, are the upper lines on these figures. This "shifting" of results is explained by the relationship between ozone concentrations and health effects. That is, increased levels of ozone lead to decreased levels of UVR at the Earth's surface and decreased incidence and mortality for human health effects.

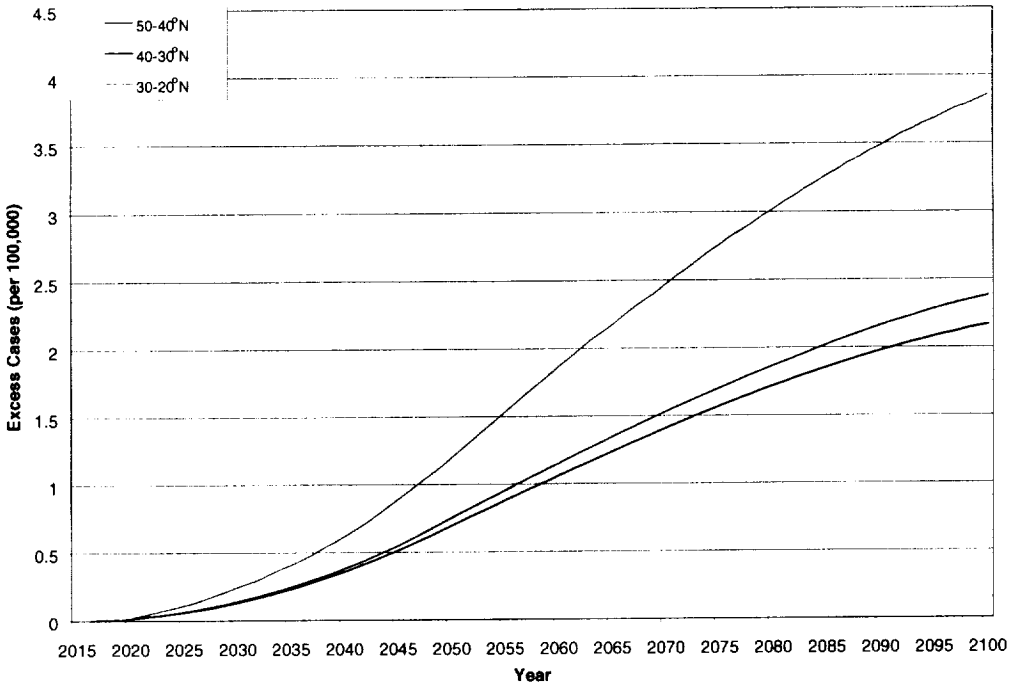

Figure 3-7. Annual estimates of excess BCC incidence per 100,000 by latitude. The lowest line represents the 30-40°N latitude band; the middle line represents the 40-50°N latitude band; the highest band represents the 20-30°N latitude band.

each of these figures is very similar for all of the examined health effects. In each, the central case exhibits a progressive increase in the predicted annual number of cases or deaths expected to affect the U.S. population. The changes in predicted health effects do not track the HSCT in-service schedule as closely as the ozone time series constructed for this study because changes in UV exposure resulting from the HSCT fleet can continue to affect human health for years after the HSCT fleet size has leveled off (i.e., manifestation of a health effect, as modeled in this study, is due to cumulative lifetime exposure). This continuing effect is a result of the decades-long latency periods associated with the various forms of skin cancer and cataract (Madronich 1999).

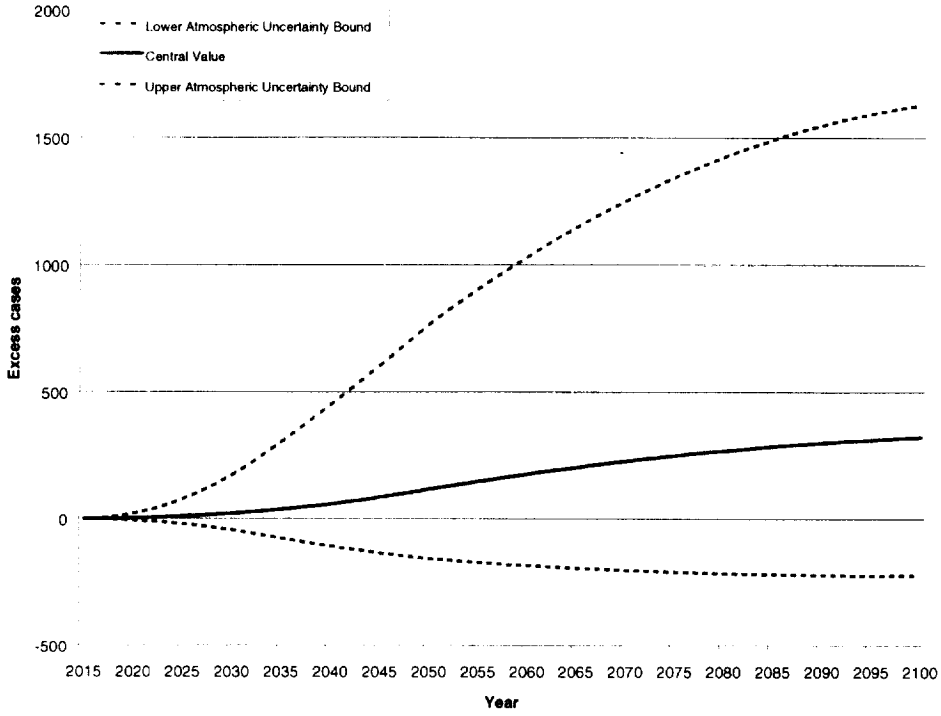

Figure 3-8. Annual estimates of excess CMM incidence for the U.S. resulting from an HSCT fleet (2015-2100) relative to Montreal Adjustments. Lowest curve represents the estimated health impacts when the smallest value of the estimated atmospheric input uncertainty range is used (upper uncertainty bound of +0.9 percent relative to the central value). Middle curve is the estimated health impacts from the central-value scenario. Highest curve is the estimated health impacts when the highest value of the estimated atmospheric input uncertainty bound is used (lower uncertainty bound of -2.1 percent relative to the central value). Uncertainty in estimated health effects due to one major source of uncertainty (column ozone impacts) is shown for illustration purposes. The indicated uncertainty range thus reflects only one source of uncertainty and should be considered a minimum. See Sections 2.6 and 3.4 for additional detail.

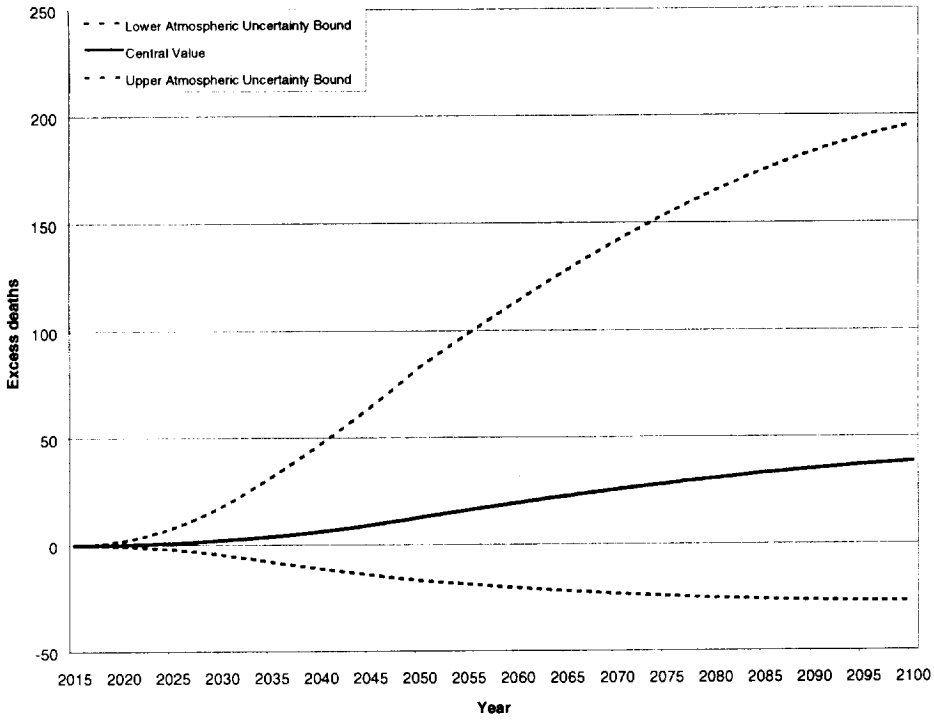

Figure 3-9. Annual estimates of excess CMM mortality for the United States resulting from an HSCT fleet (2015-2100) relative to Montreal Adjustments. See caption for Figure 3-8 for additional detail.

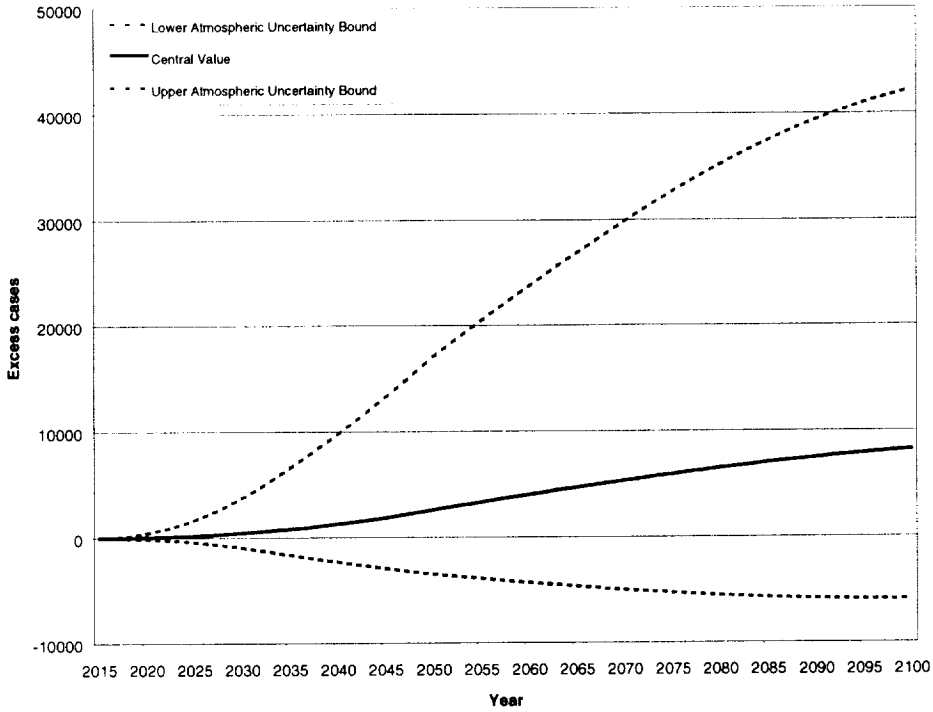

Figure 3-10. Annual estimates of excess BCC incidence for the United States resulting from an HSCT fleet (2015-2100) relative to Montreal Adjustments. See caption for Figure 3-8 for additional detail.

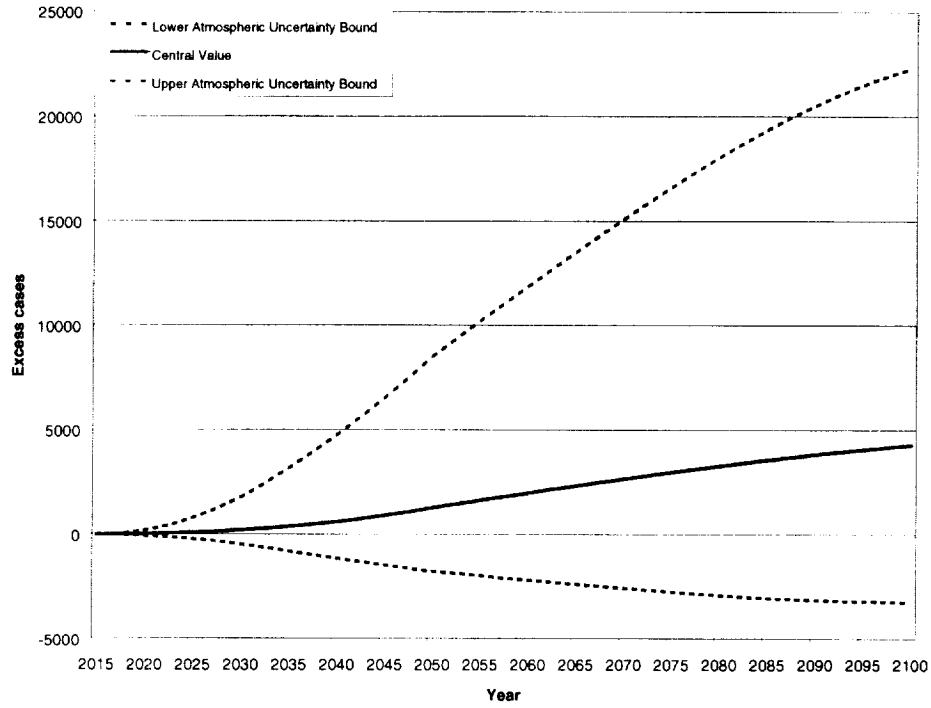

Figure 3-11. Annual estimates of excess SCC incidence for the United States resulting from an HSCT fleet (2015-2100) relative to Montreal Adjustments. See caption for Figure 3-8 for additional detail.

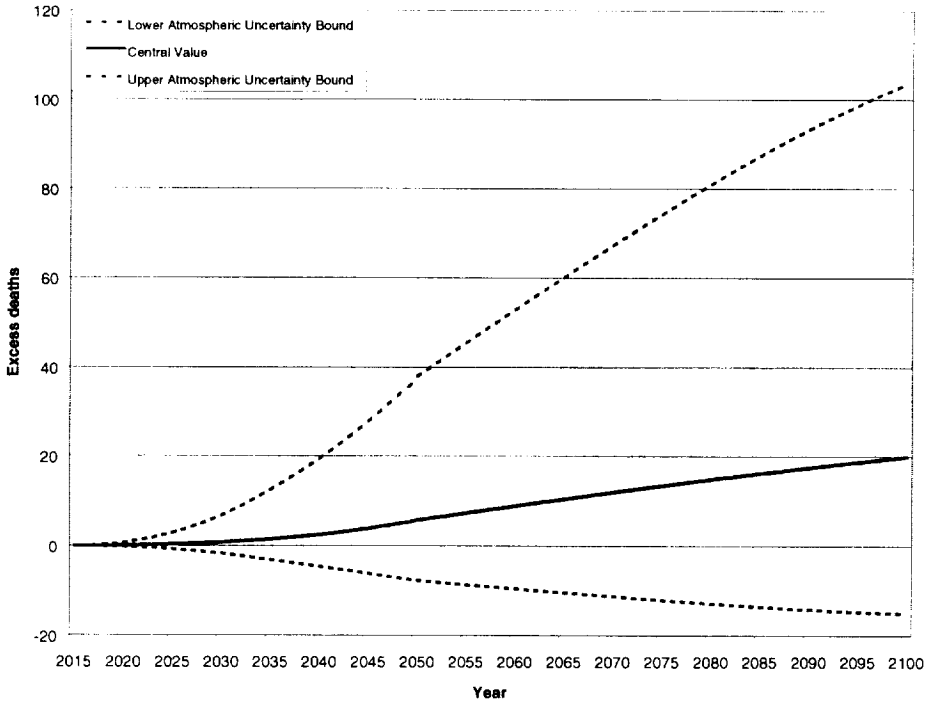

Figure 3-12. Annual estimates of excess NMSC mortality for the United States resulting from an HSCT fleet (2015-2100) relative to Montreal Adjustment. See caption for Figure 3-8 for additional detail.

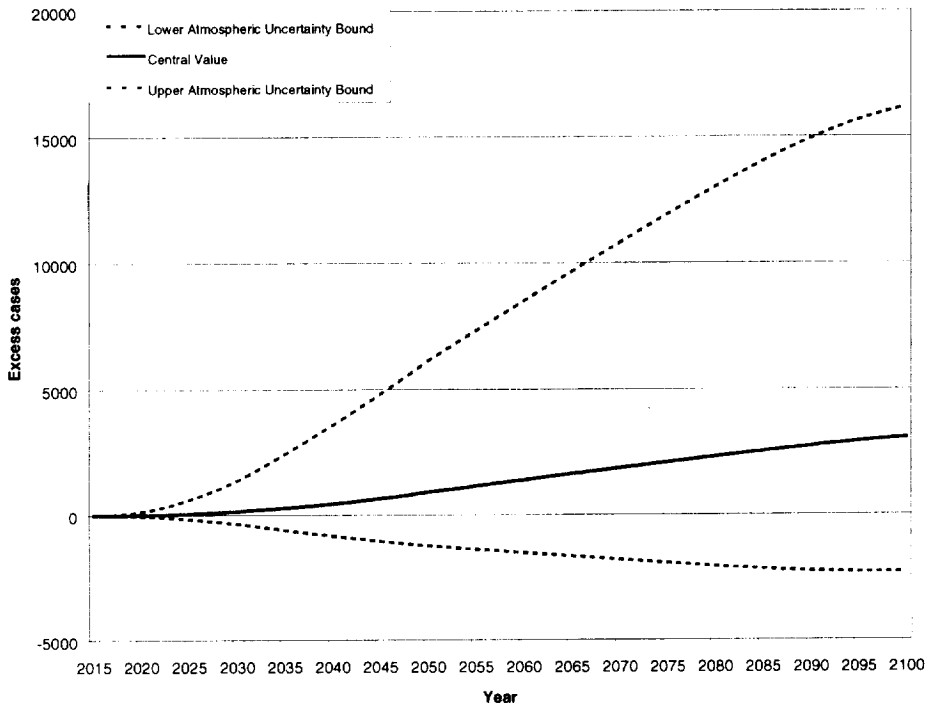

Figure 3-13. Annual estimates of excess cataract incidence for the United States resulting from an HSCT fleet (2015-2100) relative to Montreal Adjustments. See caption for Figure 3-8 for additional detail.

3.4 Uncertainty analyses

A series of quantitative and qualitative analyses were performed to analyze the uncertainty associated with a variety of parameters examined in this evaluation. Table 3-2 summarizes the quantitative uncertainty analyses, and Table 3-3 summarizes the qualitative analyses. See Section 2.6 for additional detail on the methodology used for these analyses.

In this study, an integrated (e.g., Monte-Carlo style) analysis of uncertainty in estimated HSCT health impacts was not performed. Instead, a combination of analyses and reasoning were used to roughly characterize the uncertainty in projections of health impacts attributable to HSCT-induced ozone depletion. For several major sources, estimated uncertainty was quantified, based on consultation with experts and/or the literature. For two of these major sources (i.e., BAFs and estimated changes in column ozone), the upper and lower bounds of the estimated uncertainty range were modeled. The results are presented in Table 3-2.

Table 3-2. Summary of Uncertainty Results for Total Predicted Excess Incidence or Mortality in the United States among People Born Between 1890 and 2100 due to HSCT Operation (thousands)

Scenario	CMM Incidence	CMM Mortality	BCC Incidence	SCC Incidence	NMSC Mortality	Cataract Incidence
HSCT Scenario (Central Case)	36	4.5	960	520	2.6	360
Atmospheric Uncertainty						
Upper Uncertainty Bound (+150%)	-25 *(-170%)*	-3.1 *(-170%)*	-690 *(-170%)*	-380 *(-170%)*	-1.8 *(-170%)*	-270 *(-170%)*
Lower Uncertainty Bound (-350%)	180 *(410%)*	23 *(410%)*	4900 *(410%)*	2700 *(410%)*	13 *(410%)*	1900 *(420%)*
Health Parameters Uncertainty						
HSCT (BAF+30%)	46 *(30%)*	5.8 *(30%)*	1300 *(30%)*	680 *(30%)*	3.4 *(30%)*	450 *(24%)*
HSCT (BAF-30%)	25 *(-30%)*	3.1 *(-30%)*	680 *(-30%)*	370 *(-30%)*	1.8 *(-30%)*	270 *(-24%)*

Note: Negative numbers indicate fewer cases or deaths relative to the Montreal Adjustments. Percent values correspond to percent change in incidence/mortality estimates from the HSCT scenario central value.

Table 3-3. Summary of Qualitative Uncertainty Analyses

Source of uncertainty	Expected sensitivity of health impacts to uncertainty in source
UVR Estimates	Linear, 5% change will result in ~5% change in results
Health Parameters	
Action Spectrum	Linear, 5% change will result in ~5% change in results
Population	A 10% change will result in ~5% change in result
Latency	Skews input to later generations, but absolute number of cases/deaths is not affected dramatically

Finally, the sensitivity of the model results was tested with regards to two assumptions made for this study: (1) the specification of the reference atmosphere and (2) the decision to characterize the HSCT column ozone impact as a fixed percentage of baseline atmospheric ozone (instead of as an absolute value). Discussion of reference atmosphere selection and sensitivity testing is provided in Section 2.5 and Appendix F. The analysis supporting the decision to use relative (versus absolute) ozone change is provided in Appendix C. Briefly, predicted impacts were found to be linearly sensitive to changes in to the assumed reference atmosphere. Predicted impacts were found to be fairly insensitive to how the HSCT column ozone impact is characterized (as a fixed percentage of baseline atmospheric ozone or as an absolute value); model results varied by only 1-2 percent depending on which method was used.

3.4.1 Uncertainties associated with change in ozone estimates

Uncertainty in estimated HSCT-induced health impacts due to quantified uncertainty in estimated HSCT-induced column ozone change is considerable (see Table 3-2). This large uncertainty range comprises not only the possibility for adverse health impacts of much larger magnitude than the central value, but also the possibility that the impacts may be *directionally* different: An atmosphere with HSCT-induced ozone change could lead to a *reduction* in skin cancer and cataract occurrences, relative to a reference atmosphere. This latter possibility arises from the uncertainty in the estimated column ozone response to HSCT. In addition to providing an estimate of how much larger than the central value the estimated HSCT ozone depletion could be, the NASA assessment concluded that there is a small possibility that the HSCT fleet could lead to an increase in column ozone. However, the NASA uncertainty range should be viewed as conservative, as it is considered less likely that an HSCT fleet will have a positive impact on ozone (ICF 1999).

The analysis summarized in Table 3-2 indicates that a decrease in HSCT ozone impact (i.e., an increase in column ozone) leads to a slightly larger percentage decrease in estimated health impact, or a *reduction* in health impacts relative to an atmosphere without HSCT. The increase in HSCT ozone depletion indicated by the lower bound of the estimated uncertainty range for the column ozone response leads to a roughly five-fold increase in adverse health impacts.

The column ozone uncertainty range is unique in several respects: (1) The uncertainty is relatively large; (2) There is uncertainty regarding both *magnitude* of column ozone change, as well as *direction*; and (3) This uncertainty, unlike uncertainty in the UV transfer and health effects modeling steps, affects the HSCT health impact estimate uniquely. Uncertainty in the other steps would affect both the HSCT health impact estimates as well as estimates of health effects under ODS policy scenarios, with which the HSCT effects are compared.

3.4.2 Uncertainties associated with change in UVR estimates

Estimated health impacts show an approximately linear response to changes in the RAF value associated with an action spectrum, at least for small changes in the action spectrum. Consequently, it is assumed that the uncertainty in estimated health impacts of HSCT attributable to the uncertainty in action spectrum values (discussed in Chapter 2, see Table 2-2)

is approximately 50 percent. The discussion in Chapter 2 also indicates that the UV radiative transfer modeling step induced approximately 5 percent uncertainty due to calculations relating to radiative transfer. Table 3-3 illustrates that the small uncertainties of the radiative transfer modeling step are expected to result in similarly small uncertainties in estimated health impacts.

3.4.3 Uncertainties associated with change in health effects estimates

Table 3-2 shows that changes of 30 percent in the BAF yield corresponding 30 percent changes in estimated health effects. Moreover, separate analysis (see Table 3-4) illustrates that when the choice of dose metric is changed from a cumulative lifetime UV exposure to exposure only during the first 20 years of life, the estimated health impacts shift by less than 10 percent (and the timing of predicted skin cancer incidence and mortality and cataract incidence also changes). Two additional sources of uncertainty in the health effects parameters, although they have not been quantitatively treated in this study, should be noted: uncertainty in population projections and uncertainty regarding latency. These are discussed below.

3.4.3.a. Uncertainty in population projections

Although no quantitative analysis is provided at this time, three methods are possible for determining the ranges of uncertainty around the central value that are attributable to population projection uncertainty. A description of each of these methods, along with the advantages and disadvantages of each, is presented below.

In the first method, population projection uncertainty is estimated by multiplying all age and cohort groups, past and future, by ±10 percent. Although this method is simple to perform, it is highly inaccurate because the age group distribution for future populations is not known, and past and near-future population estimates are not subject to this degree of uncertainty. Immigration and emigration rates by state further confound this uncertainty.

The second method of estimating population projection uncertainty would involve adjusting the size of each future cohort manually based on knowledge of state-by-state and county-by-county demographic information. This method focuses on the cohorts and age groups that realistically can be changed (i.e., future populations). However, it would take some time to analyze the

appropriate populations and adjustments, and then to manually alter the population file accurately.

Finally, the third method involves revisiting the original Bureau of Census projections used in the AHEF and obtaining the high and low population projections by state. From these disaggregated estimates, new U.S. population projection high and low estimates can be generated. This is the most accurate method, but it does not create an uncertainty range, but rather a set of high and low values. In addition, this method is extremely resource-intensive as high and low estimates must be collected by state and then combined in the appropriate manner.

Regardless of the method selected, some discussion of the expected impact of population changes on health effects estimates is possible. Changes in future population size do not lead to linear changes in a given health effect. Health effects of long-term changes in UVR estimated by applying incidence and mortality rates to populations are typically summed over historical, present, and future population cohorts. The characteristics of historical and present populations are fixed/known, whereas those of future populations are uncertain. Clearly, uncertainty in estimated health effects due to uncertainty in population projections would therefore only arise for estimates made for future population cohorts.

3.4.3.b. Latency

The treatment of latency[6] in health effects modeling is often a source of controversy, because little definitive research exists on the most accurate means of modeling the lag time between UV exposure and the manifestation of skin cancer or cataract. Although not a true measure of latency, Figure 3-14 presents the results of an AHEF simulation of changing the relationship between age of exposure and the development of UV-related health effects. It should be noted that the results illustrated in the figure are based on scenarios related to adherence to ODS emission reduction requirements under the Montreal Adjustments policy scenario, in the absence of HSCT. Enhanced exposures due to ODS-induced ozone depletion under the Montreal Adjustments policy scenario in this simulation reach their highest level around 2050.

[6] Latency can be defined as the length of time between the exposure to a stressor (e.g., UV-B radiation) and the response to that stressor (e.g., skin cancer) (ICF 2000*a*).

The figure depicts CMM mortality estimates using cumulative annual exposures computed either by weighting all exposures equally over a person's lifetime (the methodology used in this evaluation) or by considering only the exposures received between age 1 and age 20.

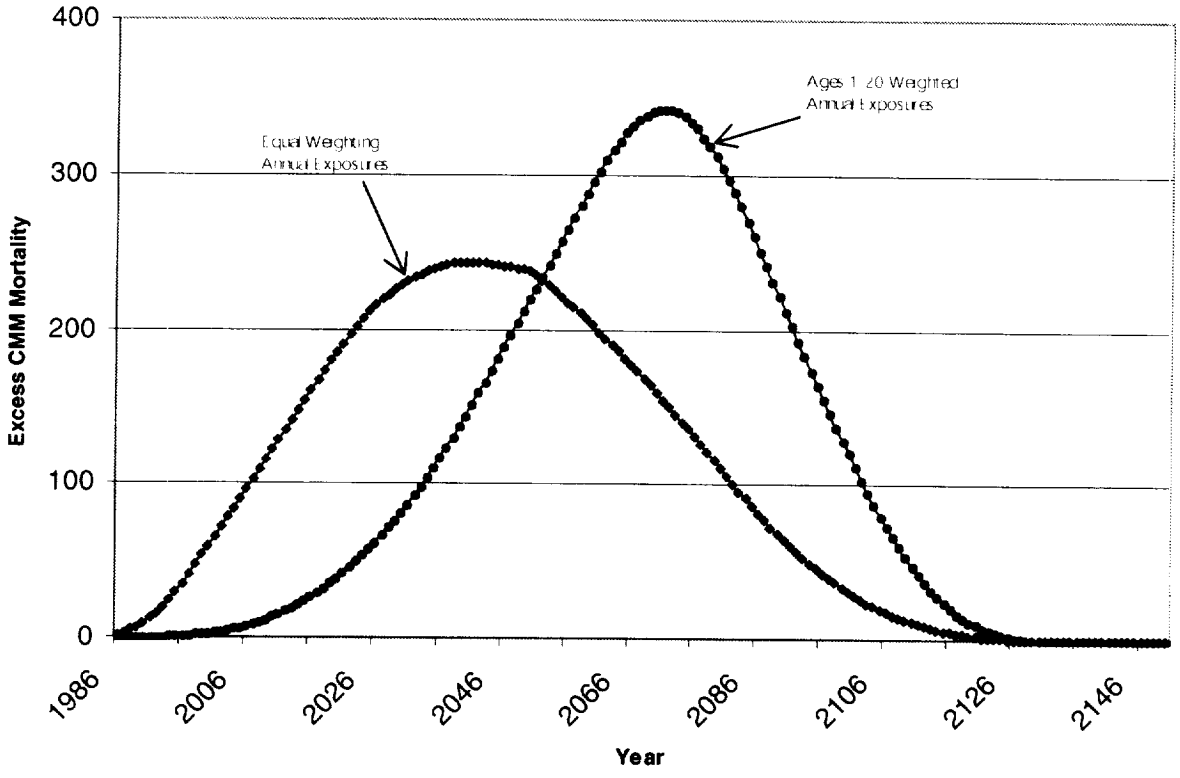

Figure 3-14. Excess CMM mortality for the Montreal Adjustments scenario for equal-age exposure weighting and weighting for exposures only for ages 1-20: cumulative annual exposure.

The results of this exercise suggest that by weighting and summing only early life exposures, the health risk of ozone depletion is shifted from current to future generations (i.e., individuals that would receive exposures prior to the age of 20). Again, this approach does not reflect a formal modeling of latency, which would involve an elaborate method for assigning different weights to exposures incurred at different ages. Rather, it results from the fact that additional health risks of UV exposure are computed by multiplying the percentage change in UV exposure by the associated BAF and the baseline rate of incidence or mortality – the bulk of which occurs among the elderly. This suggests that if early life exposures are more important in inducing CMM, the remaining health risks from ozone depletion will be borne largely by future generations.

It should be noted that aggregate incidence and mortality for the simulations in which only early-life exposures are weighted is slightly higher than the aggregate incidence and mortality in simulations in which all exposures through life are weighted equally (see Table 3-4). This difference is attributable to the shifting of ozone impacts to future, larger populations. As shown in Table 3-4, modeling only those exposures received between the ages of 1 and 20 produces a difference in the cohort group mortality estimates. However, the total mortality estimates differ by less than 10 percent.

Table 3-4. Summary of Results for the Montreal Adjustments Scenario for CMM Mortality for the SCUP-h Action Spectrum (thousands)
(Relative to 1979-1980 Average Column Ozone)

Cohort Group	Equal Age Weighting	Ages 1-20 Weighted*
1890-1980	9.1	2.1
1985-2010	6.3	13
2015-2050	1.2	3.6
2055-2100	0	0
Totals	17	18

*Approximated by giving exposures received between the ages of 1 and 20 a value of 1 and exposures received at all other ages a value of 0.

3.4.4 Summary of uncertainty analyses

Based on the limited analyses presented above, it can be estimated that the HSCT health impact is uncertain to a factor of approximately -1.7 to +4.1 around the central value due to uncertainties in estimated fleet atmospheric impacts. The health effects uncertainty considered quantitatively in this study can be summarized as follows: the uncertainties accompanying the action spectrum values (0.50), the UV radiative transfer modeling step (0.05), the BAF (0.30), and the choice of dose metric (0.10) (see Sections 3.4.2 and 3.4.3 for more detail). By evaluating these uncertainty values "in quadrature," the square root of the sum of squares results in a value of 0.6 (or a factor of 1.6) for uncertainty associated with health effects estimates (not including choice of dose metric).

This statistical method of generating the uncertainty factor assumes that all the contributing terms are independent variables. In this study, however, that is not the case. In fact, certain parameters are negatively correlated. For example, the variation imparted by the TUV model is inversely related to the estimated BAFs because both of these parameters are based on the

same set of fixed epidemiological values and thus as one increases, the other must decrease. The factor of 1.6 does not consider this relationship and thus, actual uncertainty is likely to be less than a factor of 1.6. However, to be conservative, a factor of 2 is used in this study as an estimate of the uncertainty contributed by health effects parameters.

It should be noted that the uncertainty intervals established for the atmospheric and health effects estimates do not reflect consideration of all sources of uncertainty. As discussed in Chapter 2, many other assumptions or sources of uncertainty have not been quantitatively considered. These additional sources include long-term, systematic changes in atmospheric opacity; changes in human UV exposure behavior; improvements in medical care; and increased longevity. For this analysis, assumptions based on best available knowledge have been made, but further quantitative tests are needed to understand the sensitivity of simulated results to each of the assumptions made. Further analyses that could improve our understanding of uncertainty include a more systematic evaluation of sensitivity to larger changes in the action spectrum and an integrated analysis of uncertainty in results arising from all sources of input or model uncertainty.

3.5 Sensitivity to technological and operational change

It is important to understand the sensitivity of expected health impacts to parameters over which technologists and operators may have some design discretion. Such information provides insight to policy makers and technologists as to the potential for mitigation of adverse environmental impacts through technological or operational means. A simple sensitivity analysis was completed to provide such insight into the estimation of health effects presented in this study. This section presents the results of the atmospheric sensitivity analysis, as outlined in Section 2.7.

When the estimated values of column ozone depletion were perturbed by ±0.1 percent (i.e., ±17 percent of the central value – the Northern-Hemisphere annual average; see Section 2.7), estimated skin cancer and cataract cases responded with a change of between 18 percent and 22 percent (see Table 3-5).

The test case of a ±0.1 percent change in column ozone inputs used in the present sensitivity calculation was a modest perturbation, in comparison with the atmospheric sensitivities to

engineering parameters demonstrated in the NASA assessment. The NASA analyses show that the simulated ozone impact is highly sensitive to changes in these parameters. As discussed by the NASA assessment, estimated column ozone depletion can shift by as much as -0.4 percent to +0.3 percent from the central-value estimate of -0.4 percent (annual average Northern Hemisphere depletion, based on a scenario of 500 HSCT in the year 2015).

Table 3-5. Atmospheric Sensitivity in Total Predicted Excess Incidence or Mortality in the United States among People Born between 1890 and 2100 due to HSCT Operation (thousands)

	CMM Incidence	CMM Mortality	BCC Incidence	SCC Incidence	NMSC Mortality	Cataract Incidence
Lower Sensitivity Bound (-17%)	28 *(-218%)*	3.6 *(-21%)*	760 *(-21%)*	410 *(-22%)*	2.0 *(-21%)*	290 *(-20%)*
HSCT Scenario	36	4.5	960	520	2.6	360
Upper Sensitivity Bound (+17%)	42 *(19%)*	5.3 *(19%)*	1,100 *(18%)*	620 *(18%)*	3.1 *(18%)*	430 *(20%)*

Note: Negative numbers indicate fewer cases or deaths relative to the Montreal Adjustments. Percent values correspond to percent change in incidence/mortality estimates from the HSCT scenario central value.

Some important specific sensitivities explored in the NASA assessment relate to assumed particle production by HSCT, aircraft cruise altitude, and size of the proposed HSCT fleet. Elimination of particle production reduces ozone loss by 0.3 percent, assuming a volcanically clean atmosphere. Reducing the cruise altitude by 2 km reduces the fleet's adverse column ozone impact (increases estimated column ozone response by +0.2 percent); increasing the cruise altitude by the same amount adds 0.4 percent to the estimated column ozone depletion.

Based on the simple sensitivity test performed here and consideration of the results of the NASA sensitivity runs, it appears that there is considerable sensitivity of estimated health impacts to changes in engineering parameters. The results of the simple sensitivity test described here can be used to roughly scale the scope of engineering parameter perturbations considered in the NASA assessment to the range of corresponding responses in estimated health effects. That is, based upon the results of the sensitivity test presented here, it can be coarsely estimated that a 2 km reduction in cruise altitude would not only decrease the projected column ozone impact by roughly half, but also would decrease the estimated health impacts by a similar proportion. By the same token, increasing the cruise altitude could be expected to not only double the projected column ozone depletion, but also roughly double the estimated adverse health impacts.

Chapter 4. Synthesis

Estimated human health impacts associated with predicted column ozone changes from a hypothetical HSCT fleet have been discussed in this study. Impacts estimated were total skin cancer incidence, skin cancer mortality, and cataract incidence expected among the U.S. light-skinned population if an HSCT fleet were launched in 2015, grew to a fleet size of 1,000 aircraft by the year 2050, and stayed in constant operation (i.e., at fleet size 1,000) from 2050 through 2100. This chapter provides a discussion of this study, in the context of previous international stratospheric protection control measures for ozone-depleting substances (ODS) such as chlorofluorocarbons (CFCs). Section 4.1 first provides background on specific features of these previous measures. Next, the estimated health impacts from HSCT-induced ozone depletion developed in this study are compared with health effects associated with the earlier control measures. Section 4.1 also highlights the past stringency of stratospheric protection measures taken by the international community and individual nations. Section 4.2 discusses the applicability of the methods and results used in this study to scenarios other than the single HSCT fleet scenario evaluated in this report.

4.1 Findings in context of past ODS regulatory activities

4.1.1 Description of the Montreal Protocol: Amendments and adjustments

As discussed in Chapter 1, the Montreal Protocol, signed in 1987, was designed to phase out levels of CFCs and other ODS such as halons and methyl chloroform. The agreement stipulated a freeze on CFC production and consumption at 1986 levels within one year following the signing of the Protocol. The agreement targeted a 50 percent reduction on the production of CFCs by 1998 for developed countries and by 2008 for Article 5 (developing) countries. The agreement also established later production freezes on halons, other halogenated compounds, carbon tetrachloride, and methyl chloroform.

As of March 2001, the Protocol has been amended or adjusted five times to increase the array of controlled chemicals and the stringency of the control measures. Key features of the original Protocol, and its five subsequent amendments or adjustments, are summarized in Appendix G.

The Protocol still serves as the chief forum for the establishment of effective global control measures for protecting the stratosphere (i.e., ozone layer). Several of these amendments and adjustments are discussed in the following paragraphs.

Three years after the initial signing of the Protocol, the production and import of ODS was further regulated. The London Amendments in 1990 stipulated the complete phase-out of CFCs, hydrochlorofluorocarbons (HCFCs), and carbon tetrachloride by the year 2000 for developed countries and by the year 2010 for developing nations. It also specified the complete phase-out of methyl chloroform by 2005 for developed countries and by 2015 for developing countries.

In 1992, the phase-out schedule was accelerated again, under the Copenhagen Amendments. Developed countries agreed to ban the manufacture of CFCs, carbon tetrachloride, and methyl chloroform by 1996. Similarly, a complete production ban on halons was scheduled to occur by 1994, instead of 2000. The amendments also set an accelerated timetable for the reduction of HCFCs and hydrobromofluorocarbons (HBFCs) for developed countries.

The Montreal Adjustments were agreed to in 1997, and entered into effect in June 1998. These adjustments brought a total phase-out of methyl bromide for developed countries by 2005 and for developing countries by 2015. This agreement also established an HCFC phase-out schedule for developing countries.

Today, 175 countries have ratified the Montreal Protocol, and 48 have ratified the Montreal Adjustments. The Parties to the Protocol also meet regularly to proactively protect stratospheric ozone through additional initiatives such as the Beijing Amendments of 1999, which are discussed in more detail in Section 4.1.3.

4.1.2 Comparison of HSCT with ODS policy scenarios

Chapters 2 and 3 of this report describe the human health impacts associated with predicted column ozone changes from a hypothetical HSCT fleet, as estimated in this study. These estimates were for total skin cancer incidence, skin cancer mortality, and cataract incidence expected among the U.S. light-skinned population for the HSCT fleet scenario described previously. Table 4-1a summarizes the central-value estimates associated with HSCT. The results in Table 4-1a are identical to the results presented in Table 3-1 of Chapter 3. For comparison, previous estimates of human health impacts under the ODS policy scenarios described above in Section 4.1.1 are also presented in Table 4-1b.

Table 4-1a. Estimated Incremental U.S. Health Impacts due to HSCT Fleet among People Born between 1890 and 2100 (thousands of cases)

Numbers in parentheses are upper and lower bounds, based only on the uncertainty range in estimated HSCT ozone impacts. All values, including those in parentheses, are subject to an additional uncertainty (approximately a factor of 2) due to uncertainties related to the estimation of biological effects of UVR. See text for additional discussion of uncertainty.

	CMM Incidence	CMM Mortality	BCC Incidence	SCC Incidence	NMSC Mortality	Cataract Incidence
HSCT	36 (-25 to 180)	4.5 (-3 to 23)	970 (-690 to 4,900)	520 (-380 to 2,700)	2.6 (-2 to 13)	360 (-270 to 1,900)

CMM = Cutaneous Malignant Melanoma, **BCC** = Basal Cell Carcinoma, **SCC** = Squamous Cell Carcinoma, **NMSC** = Non-Melanoma Skin Cancer (SCC + BCC)

As explained previously, for all (both HSCT and ODS policy) scenarios, incidence and mortality estimates were created for model cohorts in the U.S. light-skinned population born between 1890 and 2100. The same UVR and health effects models were used for all scenarios, and health effects estimates were based on consideration of the same baseline data and simulation period. The methods used to estimate the ozone responses to ODS policy scenarios (Table 4-1b) are described elsewhere (ICF 2000*a*). Briefly, for each ODS policy scenario, ODS physical and chemical properties, ODS emission histories, and ODS emission projections were used to calculate EESC loading. Previously developed empirical relationships between known atmospheric EESC conditions and stratospheric ozone distributions (from Nimbus-7 satellite data) by month and latitude band for the years 1978-1993 were used to project stratospheric

ozone response to EESC trends for each ODS policy. The empirical relationships based on Nimbus-7 data have been discussed elsewhere (WMO 1995, WMO 1999). Uncertainty in estimates of future ozone depletion from ODS scenarios are discussed elsewhere (WMO 1999).

Table 4-1b. Estimated Excess U.S. Health Impacts among People Born between 1890 and 2100 under Several Ozone-Depleting Substance (ODS) Policy Scenarios (thousands of cases)

	CMM Incidence	CMM Mortality	BCC Incidence	SCC Incidence	NMSC Mortality	Cataract Incidence
Montreal Protocol (row a)	6,300	820	160,000	80,000	380	140,000
London Amendments (row b)	330	41	8,100	4,100	18	3,500
Copenhagen Amendments (row c)	160	20	4,000	2,000	8.3	1,700
Montreal Adjustments (row d) [1]	130	17	3,300	1,600	6.9	1,400

CMM = Cutaneous Malignant Melanoma, **BCC** = Basal Cell Carcinoma, **SCC** = Squamous Cell Carcinoma, **NMSC** = Non-Melanoma Skin Cancer (SCC + BCC)

"MONTREAL PROTOCOL" of 1987: Freeze of CFC production and consumption at 1986 levels; 50% reduction in CFC production by 1998 (for developed countries) and 2008 (for Article 5 (developing) countries); later production freezes on halons, other halogenated compounds, carbon tetrachloride (CCl_4), and methyl chloroform (CH_3CCl_3).

"LONDON AMENDMENTS" of 1990: Complete phase-out of CFCs, hydrochlorofluorocarbons (HCFCs), and CCl_4 by 2000 (developed countries) and by 2010 (Article 5 countries); complete phase-out of CH_3CCl_3 by 2005 (developed countries) and by 2015 (developing countries).

"COPENHAGEN AMENDMENTS" of 1992: Accelerated phase-out of CFCs, CCl_4, and CH_3CCl_3 by 1996 and halons by 1994 (developed countries); and accelerated reduction of HCFCs and hydrobromofluorocarbons (HBFCs) (Article 5 countries).

"MONTREAL ADJUSTMENTS" of 1997: Complete phase-out of methyl bromide by 2005 (developed countries) and 2015 (Article 5 countries); HCFC phase-out schedule (Article 5 countries).

SOURCE: ICF 2000*a*. See text for additional discussion.

[1] The Parties to the Protocol meet regularly to consider further measures to protect stratospheric ozone. In 1999, the Parties to the Protocol agreed upon the "Beijing Amendments." As of June, 2001, this Amendment had not yet been ratified.

Rows (a) through (d) of Table 4-1b show the number of "excess" health effects cases that were estimated to occur under each policy scenario relative to 1979-1980 levels of ozone depletion.[2] For example, row (a) shows that according to previous model studies, about 6.3 million "excess" cases of CMM (i.e., in excess of baseline incidence of this malady) in the U.S. light-skinned population would have occurred under an atmosphere reflecting worldwide compliance with the controls set forth in the original 1987 Montreal Protocol. Subsequently, row (d) shows that if all Parties (i.e., nations) to the Montreal Protocol fully implement the Protocol, including all amendments and adjustments (through the Montreal Adjustments), approximately 130,000 cases of CMM, in excess of baseline CMM rates, would still occur in the U.S. light-skinned population.

A key manner in which the data in Table 4-1b can be read is to indicate the incremental health benefits (i.e., avoided health impacts) achieved by each set of amendments and adjustments to the Montreal Protocol. For example, data in rows (c) and (d) of the table indicate that an increase in the stringency of the Montreal Protocol through the Montreal Adjustments was expected to decrease CMM incidence by approximately 30,000 cases when compared to health impacts under the Copenhagen Amendments (i.e., by subtracting row (d) from row (c)). By comparison, data in Table 4-1a indicates that the simulated incremental increase in CMM incidence, due to operation of an HSCT fleet is about 36,000 additional cases relative to an atmosphere in compliance with the Montreal Adjustments but in the absence of this fleet. This increase can be compared to the approximately 30,000 avoided cases of CMM achieved through the Montreal Adjustments. This comparison suggests that the adverse human health impacts associated with operation of the proposed fleet of HSCT may be of similar magnitude to the health benefits expected from recent international stratospheric protection agreements under the Montreal Protocol.

It should be reiterated that there is some uncertainty in the HSCT estimates presented in these tables. The estimated HSCT health impact is uncertain to a factor of -1.7 to +4 about the central value due to uncertainties in estimated fleet atmospheric impacts. This uncertainty range is shown parenthetically in Table 4-1a, indicating the upper and lower uncertainty bounds

[2]As explained in Section 2.5 and Appendix F of this report, the "baseline" level of stratospheric ozone used in this study was set equivalent to 1979-1980 ozone levels held constant through time to simulate no further ozone depletion.

around the estimated central value. The estimated health impact associated with ODS-induced ozone depletion are also uncertain due to uncertainties in atmospheric impacts, as described elsewhere (WMO 1999). The estimates of HSCT health impacts and estimates of health impacts under ODS policy scenarios in both tables should all be considered uncertain to a factor of approximately 2 due to uncertainties in the estimation of biological effects of UVR. The development of these uncertainty factors is discussed in detail in Chapter 3.

Also, as discussed in Chapter 3, some possibility of mitigating the impacts of HSCT on column ozone and UV-related health effects may exist. The sensitivity of estimated column ozone response to HSCT design parameters such as cruise altitude and fuel sulfur content was assessed in Kawa *et al.* (1999). This assessment indicated significant sensitivity of ozone impact to changes in these design parameters. For example, decreasing fleet cruise altitude reduced the average annual Northern Hemisphere column ozone impact by 50 percent. Elimination of fuel sulfur content decreased the column ozone response by 75 percent. As discussed in Chapter 3, reduced ozone impacts of this magnitude are projected to lead to approximately proportional reductions in estimated health impacts.

Estimates of baseline rates of the maladies considered in this report are presented in Table 4-2. These values are based on: (1) the assumption that 1979-1980 atmospheric conditions are maintained throughout the period of consideration, (2) national cancer statistics (Scotto *et al.* 1983), and (3) Census Bureau information on population over this time period. In the absence of any ozone depletion, these baseline rates are extremely large because UVR is a human carcinogen (IARC 1992). Stratospheric ozone depletion is expected to lead to health impacts at levels above these background rates.

Table 4-2. Estimated U.S. Baseline Health Impacts among People Born Between 1890 and 2100 (thousands of cases)

	CMM Incidence	CMM Mortality	BCC Incidence	SCC Incidence	NMSC Mortality	Cataract Incidence
Baseline Atmosphere	18,000	2,200	190,000	55,000	1,200	250,000

CMM = Cutaneous Malignant Melanoma, **BCC** = Basal Cell Carcinoma, **SCC** = Squamous Cell Carcinoma, **NMSC** = Non-Melanoma Skin Cancer (SCC + BCC).

SOURCE: Estimated for this report based on ICF 2000*a*.

Several additional issues should be highlighted, including the past stringency of stratospheric protection measures taken by the international community and individual nations (Section 4.1.3) and the applicability of the methods and results used in this study to scenarios other than the single HSCT fleet scenario evaluated in this report (Section 4.2).

4.1.3 Other stratospheric protection actions within and beyond Montreal Protocol requirements

The strong resolve of the Parties to prevent stratospheric ozone depletion is indicated by the text of the Montreal Protocol and by implementation actions already taken around the world. For example, the preambulatory text of the Montreal Protocol suggests a strict approach to controlling substances that deplete the ozone layer. "The Parties are...," it states,

> "...determined to protect the ozone layer by taking precautionary measures to control equitably total global emissions of substances that deplete it, with the ultimate objective of their elimination on the basis of developments in scientific knowledge, taking into account technical and economic considerations and bearing in mind the developmental needs of developing countries..." (Source: Preamble to the Montreal Protocol).

Despite harsh economic realities associated with initiatives to decrease ozone depletion, the Parties are carrying out significant measures to implement the Montreal Prococol. In fact, control measures established by the Montreal Protocol have led to pervasive transformations in multiple industries. As an example, in the 1980s, CFCs were entrenched in the U.S. economy, with more than $100 billion worth of equipment relying on these compounds, with no acceptable alternatives commercially available for many applications. CFC applications included refrigeration and air conditioning systems in automobiles, buildings, and supermarkets; cleaning equipment for electronic components and medical instruments; and factories producing foam cushions, insulation, and packaging. In spite of major anticipated economic impacts, the Parties agreed to a ban on the production and consumption of CFCs throughout the industrialized world as of January 1, 1996, except for essential uses such as for certain

laboratory and analytical requirements and as propellants in metered-dose inhalers for treatment of asthma and chronic obstructive pulmonary disease (Cook 1996).

The Parties to the Protocol have demonstrated their strong willingness to be proactive in implementing this international agreement by collaboratively establishing control measures for substances that have limited current applications, but the potential for substantially increased use. For example, in the most recent amendment to the Protocol ("Beijing Amendment" of 1999), the Parties agreed to ban the production and consumption of chlorobromomethane (CBM), an ODS with an estimated ODP of 0.12 and atmospheric lifetime of approximately 3 months.

In addition to the control measures set forth in the Montreal Protocol and its amendments and adjustments, individual nations have instituted domestic requirements that are not otherwise required under the Protocol. Parties to the Protocol must align their domestic regulations with the control measures of the Protocol. Any Party, however, may adopt more stringent governmental control measures than those specified by the Protocol (Article 2, Paragraph 11, Montreal Protocol). Accordingly, several Parties have in fact instituted significant controls on ODSs which exceed the measures required by the Protocol.

Parties that have instituted programs or regulations that place more stringent controls on ODS include the United States and the nations in the European Community. Examples of such programs or regulations include the following.

- A regulation issued by the European Commission banning the sale and use of most CFCs, halons, hydrobromofluorocarbons, and other ODS; and bans on the use of HCFCs in certain applications, within the European Community. The regulation also mandates the recovery and disposal of ODS in refrigeration, solvent, and fire protection equipment.

- Refrigerant recycling rules in the United States. §§ 608 and 609 of the CAA require EPA to develop and implement regulations to minimize ODS emissions from

refrigeration and stationary and mobile air conditioning equipment during service, maintenance, and disposal. Under the CAA §§ 608 and 609, EPA published several regulations in the 1990s that mandate: service practices that maximize recycling of ODS during the service, maintaining, and disposal of air conditioning and refrigeration equipment; certification requirements for recycling and recovery equipment, technicians, and businesses that purify reclaimed ozone-depleting refrigerants; repair of substantial leaks in certain types of stationary air conditioning and refrigeration equipment; and establishment of safe disposal requirements to ensure removal of ozone-depleting refrigerants from goods that enter the waste stream with the charge intact (e.g., cars, home refrigerators, and room air conditioners).

The results of the HSCT health impacts analysis appear to indicate that the impacts of the HSCT fleet scenario may be of similar magnitude to the impacts that have been avoided by previous actions by the Parties to the Protocol. While not an indication that any action on HSCT would be taken under the Montreal Protocol, ICAO, or domestic agencies, it is important to consider the nature of ongoing efforts to protect stratospheric ozone in decisions on future development of stratospheric flight.

4.2 Applicability of results to other scenarios

The present study has evaluated a single conceptual scenario for a large fleet of long-range supersonic commercial transport aircraft. The results of this study should be considered highly specific to the single scenario modeled in this evaluation. This is because the emissions inventory constructed to represent the chemical inputs to the atmosphere from this fleet were based upon specific aviation traffic and market scenario projections, narrowly defined projected performance and emission characteristics of the NASA Technology Concept Airplane (TCA), and other factors (Kawa *et al.* 1999). The emissions, cruise altitude, and flight routes of a stratospheric fleet are sensitive to assumptions made in constructing scenarios such as those used in the NASA assessment of atmospheric impacts of HSCT. Simulated atmospheric impacts, in turn, are sensitive to the fleet's emissions, cruise altitude, and flight routes. Finally, UV exposure and health response are sensitive to the atmospheric impacts arising from the

fleet scenario. Thus, the results of this study, based upon many scenario-specific assumptions, should be considered specific to the scenario considered in the study.

It may be possible to scale the results of this study to smaller HSCT fleet sizes or small HSCT aircraft sizes, as long as flight routes, cruise altitudes, and emission characteristics are largely similar to the fleet simulated in this study. However, results of this study should not be directly extrapolated to estimate the health impacts from substantially different future stratospheric aviation scenarios (e.g., a fleet of business jets that fly in the stratosphere). Some correction for differences in flight routes or engine emission characteristics might be developed based on sensitivity studies that already have been carried out for previous assessments (IPCC 1999, Kawa *et al.* 1999). However, the scaling procedure would become more complex (Madronich 1999).

In short, the methodology or sequence of modeling tools used in the present study should be applicable to a wide range of future stratospheric aviation scenarios. However, for substantially different fleet scenarios (e.g., different aircraft, different routes, different altitudes, different emissions characteristics), the atmospheric impacts would likely have to be re-assessed, including re-evaluation of uncertainties in atmospheric impacts. In addition, as the scientific knowledge of stratospheric chemistry and dynamics, background atmosphere, global atmospheric change, and human health effects evolves, the models and assumptions used in future analyses should be updated accordingly.

Chapter 5. References

Andrady D.L., S.H. Hamid, X. Hu, and A. Torikai (1998), Effects of increased solar ultraviolet radiation on materials, *Photochemistry and Photobiology B: Biology* 46: 93-103.

Anonymous (2000), Darpa Eyes Supersonic Quiet Recce Aircraft. Aviation Week and Space Technology, April 3, 2000, p. 39.

Armstrong B.K., A. Kricker and D.R. English (1997), Aetiology and pathogenesis of skin cancer, *Aust J Dermatol* 58 (Suppl): S1-S6.

Baughcum, S.L. (1997), Requirements and evaluation criteria for supersonic cruise emissions standard. Working paper from ICCAIA, presented at the ICAO/CAEP/Working Group (WG) 3 meeting, January 15-16, 1997, Seville, Spain.

Caldwell M.M., L.O. Bjorn, J.F. Bornman, S.D. Flint, G. Kulandaivelu, A.H. Teramura, and M. Tevini (1998), Effects of increased solar ultraviolet radiation on terrestrial ecosystems, *Photochemistry and Photobiology B: Biology* 46:40-52.

Cook, E. (editor) (1996), Ozone protection in the United States: Elements of success. World Resources Institute, Washington, DC: 120.

Cutchis, P. (1974), Stratospheric ozone depletion and solar UV radiation on Earth. Science 184(4132): 13-19.

De Fabo, E.C. and F.P. Noonan (1983), Mechanism of immune suppression by ultraviolet irradiation *in vivo*. I. Evidence for the existence of a unique photoreceptor in skin and its role in photoimmunology. *J. Exp. Med.* 158:84-98.

de Gruijl, F.R., H.J.C.M. Sterenborg, P.D. Forbes, R.E. Davies, C. Cole, G. Kelfkens, H. van Weelden, H. Slaper, and J.C. van der Leun (1993), Wavelength dependence of skin cancer induction by ultraviolet irradiation of albino hairless mice, *Cancer Research*, 53 (1): 53-60.

de Gruijl, F.R, and J.C. Van der Leun (1993), Influence of ozone depletion on the incidence of skin cancer: quantitative prediction, in *Environmental UV Photobiology*, A.R. Young, L.O. Bjorn, J. Moan, and W. Nultsch (eds.), Plenum Press, New York: 1-39.

De More, W. B., S. P. Sander, D. M. Golden, R. F. Hampson, M. J. Kurylo, C. J. Howard, A. R. Ravishankara, C. E. Kolb, and M. J. Molina (1997), Chemical Kinetics and Photochemical Data for Use in Stratospheric Modeling, JPL Publication 97-4, Jet Propulsion Laboratory, National Aeronautics and Space Administration, Pasadena.

Elwood M. and J. Jopson (1997), Melanoma and sun exposure: an overview of published studies, *International Journal of Cancer* 73:198-203.

EPA (U.S. Environmental Protection Agency) (1987), Regulatory Impact Analysis: Protection of Stratospheric Ozone, U.S. Environmental Protection Agency, Washington, DC.

EPA (U.S. Environmental Protection Agency) (1987), Assessing the Risks of Trace Gases That Can Modify the Stratosphere. EPA 400/1-87. Office of Air and Radiation, Washington, DC. Eight volumes.

EPA (U.S. Environmental Protection Agency) (1988), Regulatory Impact Analysis: Protection of Stratospheric Ozone. Prepared by the U.S. Environmental Protection Agency, Stratospheric Protection Program, Office of Program Development, Office of Air and Radiation.

EPA (U.S. Environmental Protection Agency) (1997), EPA Strategic Plan. EPA/190-R-97-002, September 1997. U.S. Environmental Protection Agency, Washington, DC: 108.

Epstein, J.H. (1996), Nonmelanoma skin cancer, *Comprehensive Therapeutics* 22:179-182.

Gerstle, J.H. (1996), Emission standards for SST. Working Paper 17, presented to the ICAO/CAEP Working Group (WG) 3 meeting, May 30-31, 1996, Washington, DC.

Hader D.-P., H.D. Kumar, R.C. Smith, and R.C. Worrest (1998), Effects on aquatic ecosystems, *Photochemistry and Photobiology B: Biology* 46: 53-68.

IARC (International Agency for Research on Cancer) (1992), IARC Working Group on the Evaluation of Carcinogenic Risks to Humans. Monographs on Cancer Risks, Volume 55: Solar and Ultraviolet Radiation. Lyon, 11-18 February 1992. 316 pp.

ICF Consulting (1999), Summary of the Meeting on Next Generation Supersonic Civil Transport Risk Assessment Methods , Prepared for Stratospheric Protection Division, Office of Air and Radiation, U.S. Environmental Protection Agency, by ICF Consulting, Washington, DC. November 18-19, 1999, and Addendum, February 9, 2000.

ICF Consulting (2000*a*), Human health benefits of stratospheric ozone protection. Revised Draft Report Prepared by ICF Consulting for U.S. EPA, Stratospheric Protection Division. Office of Air and Radiation, Washington DC. February 29, 2000.

ICF Consulting (2000*b*), Summary of the Second Meeting on Next Generation Supersonic Civil Transport Evaluation Methods , Prepared for Stratospheric Protection Division, Office of Air and Radiation, U.S. Environmental Protection Agency, by ICF Consulting, Washington, DC. August 8, 2000.

IPCC (Intergovernmental Panel on Climate Change) (1999), Aviation and the Global Atmosphere. J.E. Penner, D.H. Lister, D.J. Griggs, D.J. Dokken, and M. McFarland, editors. Cambridge University Press: 373.

Italian American Cataract Study Group (1991), Risk Factors for age-related cortical, nuclear and posterior subcapsular cataracts, *American Journal of Epidemiol*ogy 133: 542-553.

Javitt J.C., and H.R. Taylor (1995), Cataract and latitude, *Documenta Ophthalmologica* 88:714-718.

Kawa, S.R., et al., (1999), Assessment of the Effects of High-Speed Aircraft in the Stratosphere: 1998. NASA Technical Paper (TP) 1999-209237. National Aeronautics and Space Administration (NASA), Washington, DC: 150 and appendices.

Kirk, J. T. O., B. R. Hargreaves, D. P. Morris, R. Coffin, B. David, D. Fredrickson, D. Karentz, D. Lean, M. Lesser, S. Madronich, J. H. Morrow, N. Nelson, and N. Scully (1994), Measurements of UV-B radiation in two freshwater lakes: an instrument intercomparison, *Archiv für Hydrobiologie* 43: 71-99.

Klein, B.E.K., J.K. Cruickshanks, and R. Klein (1995), Leisure time, sunlight exposure and cataracts, *Documenta Ophthalmologica* 88: 295-305.

Koepke, P., A. Bais, D. Balis, M. Buchwitz, H. De Backer, X. de Cabo, P. Eckert, P. Eriksen, D. Gillotay, A. Heikkila, T. Koskela, B. Lapeta, Z. Litynska, J. Lorente, B. Mayer, A. Renaud, A. Ruggaber, G. Schauberger, G. Seckmeyer, P. Seifert, A. Schmalwieser, H. Schwander, K. Vanicek, and M. Weber (1998), Comparison of Models Used for UV Index Calculations, *Photochemistry and Photobiology (B:Photobiology)* 67: (6) 657-662.

Kricker A. (1992), Sun exposure and non-melanocytic skin cancer, Dissertation, University of Western Australia, Perth.

Lantz, K. O., R. E. Shetter, C. A. Cantrell, S. J. Flocke, J. G. Calvert, and S. Madronich (1996), Theoretical, actinometric, and radiometric determinations of the photolysis rate coefficient of NO_2 during MLOPEX II, J. *Geophysical Research* 101: 14613-14629.

Longstreth, J.D., F.R. de Gruijl, M.L. Kripke, S. Abseck, F. Arnold, H.I. Slaper, G. Velders, Y. Takizawa, and J.C. van der Leun (1998), Health risks, *Photochemistry and Photobiology B: Biology* 46:20-39.

McKenzie, R. L., K. J. Paulin, and S. Madronich (1998), Effects of snow cover on UV irradiances and surface albedo: A case study, *Journal of Geophysical Research* 103: 28785- 28792.

McKinlay, A.F. and Diffey, B.O. (1987), A reference action spectrum for ultraviolet-induced erythema in human skin, in *Human Exposure to Ultraviolet Radiation: Risks and Regulations.* W.R. Passchier and Bosnjakovic, B.F.M. (Eds); Elsevier, Amsterdam.

Madronich, S. (1992), Implications of recent total atmospheric ozone measurements for biologically active ultraviolet radiation reaching the Earth's surface, *Geophysical Research Letters* 19: 37-40.

Madronich, S. (1993a), The atmosphere and UV-B radiation at ground level, in *Environmental UV Photobiology*, A.R. Young, L.O. Bjorn, J. Moan, and W. Nultsch (eds.), Plenum Press, New York: 1-39.

Madronich, S. (1993b), UV radiation in the natural and perturbed atmosphere, in *Environmental Effects of UV (Ultraviolet) Radiation* (M. Tevini, ed.), Lewis Publisher, Boca Raton: 17-69.

Madronich, S. and F. R. de Gruijl (1993), Skin cancer and UV radiation, *Nature*, 366: 23.

Madronich, S., E. Weatherhead, and S. Flocke (1996), Trends in UV radiation, *Int. J. Environ. Sci.* 51: 183-198.

Madronich, S., R. E. McKenzie, L. O Björn, and M. M. Caldwell (1998), Changes in biologically active ultraviolet radiation reaching the Earth's surface, *Journal of Photochemistry and Photobiology B:Biology* 46: 5-19.

Madronich (1999), Some comments on the methods used to estimated the effects of HSCTs on atmospheric ozone, surface UV radiation, and skin cancer incidence. Paper presented at a workshop held by EPA, "Meeting on Next Generation Supersonic Civil Transport Risk Assessment Methods," November 18-19, 1999 at ICF Consulting, Washington, DC.

NAS (National Academy of Sciences) (1975), Environmental Impact of Stratospheric Flight. Biological and Climatic Effects of Aircraft Emissions in the Stratosphere. Climatic Impact Committee: 348.

NASA (National Aeronautics and Space Administration) (1999), Models and Measurements Intercomparison II, Langley Research Center, Hampton, VA, NASA/TM-1999-209554.

NRC (National Research Council) (1997), U.S. Supersonic Commercial Aircraft --Assessing NASA's High Speed Research Program. Report prepared by the Committee on High Speed Research, Aeronautics and Space Engineering Board, Commission on Engineering and Technical Systems. National Academy Press, Washington, DC. 151 pp.

Pitts, D.G., A.P. Cullen, and P.D. Hacker (1977), Ocular effects of ultraviolet radiation from 295 to 365 nm, Invest. Ophthalmol. Visual Sci. 16(10): 932-939.

Public Health Service (1996), National Skin Cancer Prevention Education Program: At-A-Glance, 1996, U.S. Department of Health and Human Services, Rockville, MD, NTIS PB97-198048.

Scott, W.B. (1999), Ukraine OKs Sale of TY-160s as Space Launch Platform. Aviation Week and Space Technology, January 11, 1999, pp. 444-445.

Scotto, J., T.R. Fears, and J.F. Fraumeni Jr. (1983), Incidence of nonmelanoma skin cancer in the United States, U.S. Department of Health and Human Services, (NIH) 82-2433, Bethesda, MD.

Setlow, R.B., E. Grist, K. Thompson, and A.D. Woodhead (1993), Wavelengths effective in induction of malignant melanoma, *Proc. Natl. Acad. Sci. USA* 90: 6666-6670.

Shaw, R.J., L. Koops, and R. Hines (1997), Progress toward meeting the propulsion technology challenges for a 21st century high-speed civil transport. NASA TM 113161, ISABE-97-7045.

Shetter, R. E., A. H. McDaniel, C. A. Cantrell, S. Madronich, and J. G. Calvert (1992), Actinometer and Eppley radiometer measurements of the NO_2 photolysis rate coefficient during MLOPEX, *Journal of Geophysical Research 97*: 10349-10359.

Shetter, R.E., C. A. Cantrell, K. O. Lantz, S. J. Flocke, J. J. Orlando, G. S. Tyndall, T. M. Gilpin, S. Madronich, J. G. Calvert (1996), Actinometric and radiometric measurement and modeling of the photolysis rate coefficient of ozone to $O(^1D)$ during Mauna Loa Observatory Photochemistry Experiment 2, *Journal of Geophysical Research* 101: 14631-14641.

Sparaco, P. (1998), Dassault Explores SuperSonic Business Jet Perspectives. Aviation Week and Space Technology, October 19, 1998. pp. 62-65.

Spencer, G. (2000), Personal communication with Greg Spencer of the US Census Bureau.

Stamnes, K., S. Tsay, W. Wiscombe, and K. Jayaweera (1988), A numerically stable algorithm for discrete-ordinate-method radiative transfer in multiple scattering and emitting layered media, *Appl. Opt.* 27: 2502-2509.

Stolarski, R.S., S.L. Baughcum, W.H. Brune, A.R. Douglass, D.W. Fahey, R.R. Friedl, S.C. Liu, R.A. Plumb, L.R. Poole, H.L Wesoky, and D.R. Worsnop. *1995 Scientific Assessment of the Atmospheric Effect of Stratospheric Aircraft.* NASA Reference Publication 1381, Washington, DC, 1995.

Tafoya G.B., J.M. Gale, R.D. Ley (1997), Photorepair of ultraviolet radiation (UVR)-induced pyrimidine dimers in lens epithelial DNA of *Monodelphis domestica. Photochem Photobiol* 1997 Jan;65(1):125-8

UNEP (United Nations Environment Programme) (1989, 1991, 1994, 1998), Environmental effects of ozone depletion, *UNEP Environmental Effects Panel Report*, United Nations Environmental Programme, Nairobi, Kenya.

UNEP (United Nations Environment Programme) (1992), Methyl Bromide: Its Atmospheric Science, Technology, and Economics – Montreal Protocol Assessment Supplement," 1992.

UNEP (United Nations Environmental Programme) (1998), Environmental Effects of Ozone Depletion: 1998 Assessment: 193.

UNEP (United Nations Environment Programme) (2000), Handbook for the International Treaties for the Protection of the Ozone Layer. Fifth Edition (2000). Ozone Secretariat, United Nations Environment Programme. Available from UNEP, PO Box 30552, Nairobi, Kenya. Web site: <http://www.unep.org/ozone>.

USSA (1976), "U.S. Standard Atmosphere," National Oceanic and Atmospheric Administration (NOAA), National Aeronautics and Space Administration (NASA), United States Air Force, Washington, D.C.

Vohralik, P.F, L.K. Randeniya, I.C. Plumb, and K.R. Ryan (1998), Use of correlations between long-lived atmospheric species in assessment studies, *Journal of Geophysical Research* 103: 3611-3627.

Wall, R. (2000), Darpa Envisions New Supersonic Designs. Aviation Week and Space Technology, August 28, 2000, p. 47.

Wall, R., and W.B. Scott (2000), Northrop Grumman Gets Quiet Supersonic Work. Aviation Week and Space Technology, November 13, 2000.

West S.K., B. Munoz, O.D. Schein, D.D. Duncan, G.S. Rubin (1998), "Racial differences in lens opacities - The Salisbury Eye Project," *American Journal of Epidemiology*, 148: 1033-1039.

West, S.K. and C.T. Valmadrid (1995), "Epidemiology of risk factors for age-related cataract," *Surveys Ophthalmology*, 39: 323-335.

West S.K., D.D. Duncan, B. Munoz, G.S. Rubin, L.P. Fried, K. Bandeen-Roche, O.D. Schein (1998), "Sunlight exposure and risk of lens opacities in a population-based study," *JAMA*, 280: 714-718.

WMO (World Meteorological Organization) (1989, 1991, 1995, 1998, 1999), Scientific assessments of ozone depletion, *Global Ozone Research and Monitoring Project*, World Meteorological Organization, Geneva, Switzerland.

Appendix A - Overview of Evaluation Methodology

The schematic presented below provides a graphical summary of the methodology used in this evaluation. Atmospheric inputs to the process are listed along the left-hand side and the various process stages are described along the bottom.

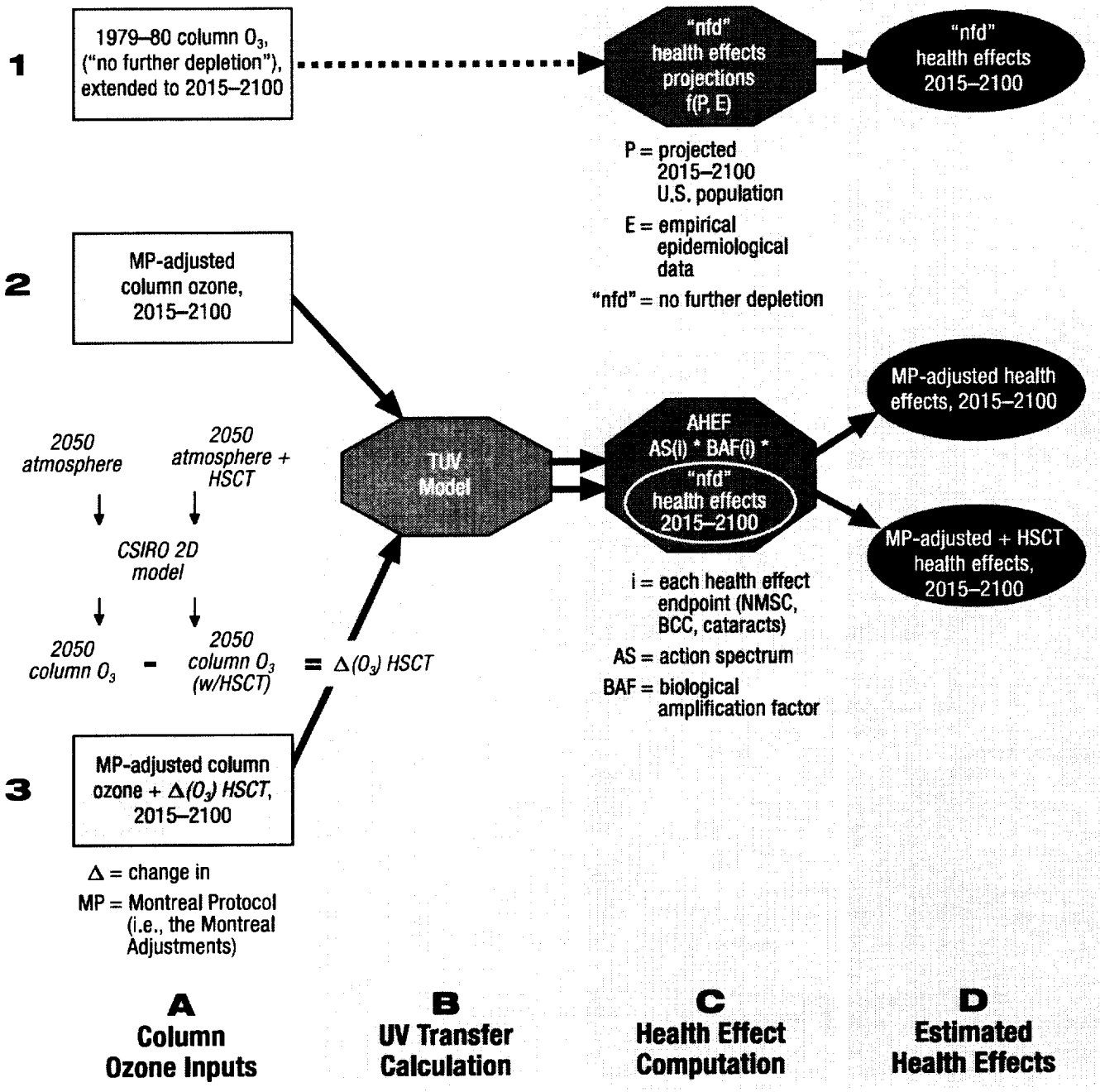

Appendix B – Description of the CSIRO Model

The CSIRO model is a two-dimensional (2-D) numerical chemical-transport model of the atmosphere. Like other numerical models of the atmosphere, the CSIRO model simulates transport and chemical interactions of trace gases (such as ozone) to obtain their spatial and seasonal distributions.

The CSIRO model analyzes ozone changes from 90°S to 90°N in 5-degree intervals and from ground level to 80 km with a vertical resolution of approximately 2 km. To generate ozone estimates, the model combines information on atmospheric chemistry (e.g., diffusion, mixing, production, and loss patterns) for various chemical species (NASA 1999).

Model transport is provided by a combination of zonal mean diabatic[1] circulation and appropriate diffusion terms. These terms are based on observed temperatures and ozone mixing ratio profiles. Zonal and monthly mean temperatures were calculated on an 8-year average using National Meteorological Center values obtained from the 1992 Models and Measurements database (Prather and Remsberg 1993 as cited in NASA 1999) and were not adjusted for zonal asymmetry (Kawa *et al.* 1999, NASA 1999).

Improvements in eddy diffusion terms have allowed for enhanced representation of tropical and mid-latitude mixing. Mixing ratios of N_2, O_2, and CO_2 are held constant throughout the model atmosphere. Tropospheric water concentrations are determined according to either Oort (1983 as cited in Kawa *et al.* 1999) climatology or SAGE-II model results from Prather and Remsberg (1992 as cited in NASA 1999). Stratospheric water concentrations are allowed to vary from a volume mixing ratio of 3×10^{-6} established at the tropopause. Rainout and surface deposition rates for certain transported chemical families also are included in the model (NASA 1999). No rainout is assumed within 3 km of the tropopause (Kawa *et al.* 1999), and an upper tropospheric source of NO_y also is provided (NASA 1999).

The model includes a solar radiation module that uses ray-tracing techniques to allow for the curvature of the Earth and includes the method of Meier *et al.* (1982 as cited in NASA 1999) to provide fully interactive multiple scattering calculations. The solar radiation module examines 158 wavelengths from 175 to 180 nm, as defined by the World Meteorological Organization (1986 as cited in NASA 1999).

The family-based chemical module examines 67 different species and 213 reactions. The model also considers hydrolysis processes occurring with sulphuric acid aerosols but does not consider heterogeneous reactions such as those occurring in polar stratospheric clouds (NASA 1999). Production and loss terms for long-lived species are updated every 10 days via a diurnal calculation that establishes the 24-hour behavior of all examined species (Vohralik *et al.* 1998).

[1] This term refers to solar-driven heating or cooling of an air parcel due to physical processes such as latent heat release and radiative effects.

References

Kawa, S.R., et al., (1999). Assessment of the Effects of High-Speed Aircraft in the Stratosphere: 1998. NASA Technical Paper (TP) 1999-209237. National Aeronautics and Space Administration (NASA), Washington, DC. 150 pp. plus appendices.

NASA (1999), *Models and Measurements Intercomparison II*, National Aeronautics and Space Administration, Langley Research Center, Hampton, VA, NASA/TM-1999-209554.

Vohralik, P.F, L.K. Randeniya, I.C. Plumb, and K.R. Ryan (1998), Use of correlations between long-lived atmospheric species in assessment studies, *Journal of Geophysical Research*, 103, 3611-3627.

Appendix C – Methodological Sensitivity: Use of Relative Versus Absolute Ozone Change

In this evaluation, ozone concentration estimates were obtained from the CSIRO model in Dobson units for a fleet of 1,000 HSCT in 2050 and for zero HSCT in the year 2050. The analysis presented in this evaluation used both of these CSIRO runs to calculate a fixed percentage change in ozone for the year 2050. This percent change then was scaled according to the HSCT "in-service" fleet production schedule for the years 2015 to 2100 and applied to a Montreal Adjustments ozone scenario that assumes zero HSCT. Section 2.2.2 provides additional detail on this methodology.

Meeting participants at a workshop held to discuss preliminary results of this effort inquired whether performing this scaling operation using absolute Dobson units rather than the percent change in ozone would have a material effect on the predicted health effects (ICF 2000*b*). To answer this question, the absolute difference between the two sets of CSIRO ozone estimates for 2050 was obtained by subtracting the monthly ozone estimates. This absolute number then was scaled from 2015 to 2100 according to the HSCT in-service fleet production schedule. The adjusted incremental ozone estimates then were applied to the Montreal Adjustments ozone scenario described above and input to the AHEF to determine the effect of the methodology on the human health impact estimates.

The sensitivity of the health effect results to these two methods of estimation is presented in Table C-1 as the central value incidence and mortality estimates for the HSCT scenario using both relative and absolute changes in ozone.

Table C-1. Relative vs. Absolute Results for Total Predicted Excess Incidence or Mortality in the United States among People Born between 1890 and 2100 due to HSCT Operation (thousands)

Scenario	CMM Cases	CMM Deaths	BCC Cases	SCC Cases	NMSC Deaths	Cataract Cases
Relative Scaling*	36	4.5	970	520	2.6	360
Absolute Scaling	35 *(1.3%)*	4.4 *(1.5%)*	960 *(0.9%)*	520 *(0.7%)*	2.5 *(1.4%)*	360 *(1.3%)*

* This is the method currently used in the HSCT evaluation.
Note: Percent values correspond to percent change in incidence/mortality estimates from the HSCT scenario central value.

Only small differences (less than 1.5 percent) are observed between the incidence and mortality rates predicted as a result of the percent scaling technique versus the Dobson unit scaling technique. Thus, the results of the HSCT evaluation are judged to be relatively insensitive to the method used to scale ozone estimates, and the percent technique currently in place will continue to be used.

Reference

ICF Consulting (2000*b*), Summary of the Second Meeting on Next Generation Supersonic Civil Transport Evaluation Methods , Prepared for Stratospheric Protection Division, Office of Air and Radiation, U.S. Environmental Protection Agency, by ICF Consulting, Washington, DC. August 8.

Appendix D – Background Information on RAFs

The RAF is a sensitivity coefficient indicating how surface UVR, weighted by the appropriate action spectrum, responds to changes in the total ozone column. Because of the weighting by action spectra, different biological action spectra have different RAF values. The RAF is a critically important number because it relates changes in ozone directly to changes in surface UVR.

The RAF is a simple and convenient number allowing a quick estimation of the sensitivity to ozone changes. However, the RAF is not a true constant, even for a single action spectrum, and it can depend on various atmospheric conditions such as total ozone column amount, amount of ozone change, solar zenith angle, and possibly other factors (see below). Although representative RAF values are useful for quick discussion purposes, a more accurate calculation must use RAFs that are re-calculated for the specific conditions. Or equivalently (as done in this work), the irradiance changes can be computed directly from pre-calculated tables of UVR as a function of the ozone column and solar zenith angle.

The RAF is obtained by computing the UV irradiance for a given ozone column amount, Ω, e.g., using the erythemal action spectrum $B_{ery}(\lambda)$,

$$UV(\text{erythemal}) = \int F(\lambda, \Omega)\, B_{ery}(\lambda)\, d\lambda$$

where $F(\lambda, \Omega)$ is the spectral irradiance at the surface. Now suppose this calculation is repeated for two different ozone column values, say Ω_1 and Ω_2, yielding the weighted irradiances UV_1 and UV_2, respectively. If the ozone changes are very small, say on the order of 1 percent or so, the RAF is simply the (percent) increase in UVR for a 1 percent decrease in the ozone column:

$$RAF \sim -\left[(UV_2 - UV_1)/UV_1\right] / \left[(\Omega_2 - \Omega_1)/\ \Omega_1\right].$$

For larger changes, it has been shown (Madronich 1993) that weighted irradiances scale with ozone column following a power equation, with the power being the RAF:

$$UV_2/UV_1 \sim (\Omega_2/\ \Omega_1)^{-RAF}$$

In this case, the RAF is computed from:

$$RAF \sim -\log(UV_2/UV_1) / \log(\Omega_2/\ \Omega_1)$$

which for small changes is identical to the previous (percent) definition.

Unpublished calculations by S. Madronich have shown that the power rule arises naturally for action spectra that decay exponentially in the ozone-sensitive 300-330 nm spectrum. Indeed, if the action spectrum decays exponentially in this band, e.g.,

$$B(\lambda) \propto \exp[-\beta\lambda]$$

and given that the ozone absorption cross section $\sigma_{O3}(\lambda)$ also is approximated by an exponential decay in this band,

$$\sigma_{O_3}(\lambda) \propto \exp[-\alpha \lambda]$$

then the RAF is given, to reasonable approximation, simply by the ratio of the two decay slopes:

$$RAF \approx \beta/\alpha$$

In other words, the sensitivity of UVR to ozone changes is directly proportional to the steepness of the action spectrum decay.

Effect of clouds on RAF values

Clouds can reduce surface UVR significantly. However, clouds have only a small effect on the spectral distribution of surface UVR; i.e., clouds are essentially white at these wavelengths. Thus, as long as cloud cover remains constant, the percent changes in surface UVR calculated for a given ozone depletion should be nearly the same for cloudy and cloud-free skies. This expectation was confirmed by detailed calculations of the RAF for cloudy and clear conditions, reported in Table 3.2-10 of one of the earlier ozone assessments (WMO 1989). This table shows that the RAF (for DNA damage, but entirely analogous for erythema) is essentially unchanged by the presence of clouds.

Altitude of ozone perturbation

In the present calculations, the change in ozone column is applied as a constant scaling factor at all altitudes (shape preserving), and the resulting UVR changes are interpolated from look-up tables of UV irradiances as functions of solar zenith angle and total ozone column. In principle, not only the total ozone column change, but also the altitude at which ozone perturbations occur, can have some effect because of the coupling between ozone absorption and scattering by air molecules. For high sun, tropospheric scattering increases photon path length substantially, so that tropospheric ozone is, on a molecule-by-molecule basis, more effective in absorbing UVR than is stratospheric ozone (e.g., Brühl and Crutzen 1989). For low sun, the reverse is known to occur (e.g., see Figures 12 and 13 in Madronich 1993), so that stratospheric ozone molecules are more effective. In practice, these considerations are important only when the ozone perturbations occur in the lower to middle troposphere and are relatively insensitive to the exact height of perturbations that occur the stratosphere, i.e., well above the region where scattering occurs.

The following figure shows the magnitude of this effect. The thick curves (solid for overhead sun, dashed for solar zenith angle = 60 degrees) show the RAF for erythemal radiation, when ozone perturbations are applied at different altitudes. The enhanced absorption by tropospheric ozone is obvious below approximately 10 km. Changes occurring near 20 km (i.e., near the HSCT flight corridors) have an RAF near 1.12, while uniform column changes (thin vertical lines) result in a slightly larger RAF, approximately 1.17. For 60 degrees solar zenith angle, the uniform column change yields RAF ~ 1.12, while perturbations at 20 km yield RAF ~ 1.09, again in fairly good agreement.

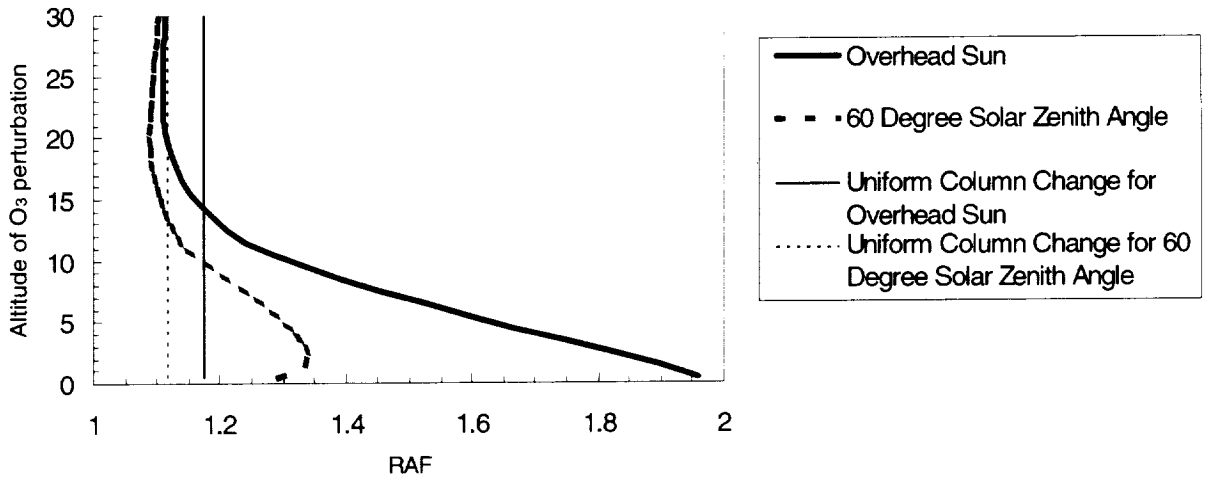

References

Brühl, C. and P. J. Crutzen (1989). On the disproportionate role of tropospheric ozone as a filter against solar UV-B radiation, *Geophys. Res. Lett.*, vol. 16, pp. 703-706.

Madronich, S. (1993). UV radiation in the natural and perturbed atmosphere, in *Environmental Effects of UV (Ultraviolet) Radiation* (M. Tevini, ed.), Lewis Publisher, Boca Raton, pp. 17-69.

WMO (1989). *Scientific Assessment of Stratospheric Ozone: 1989*, (D. Albritton and R. Watson, eds.) World Meteorological Organization Report No. 20.

Appendix E – Information and Future Directions for Cataract Methodology

Origin of current BAFs for cataract incidence

The current BAFs for cataract are based on the work of Hiller *et al.* (1983), in which a multivariate logistic risk function was used to describe the correlation between the prevalence of senile cataract, the flux of UV-B, and a variety of other risk factors. Hiller and her colleagues used data on 2,225 people aged 45-74 from the ophthalmological subsection of the 1971-1972 National Health and Nutrition Examination Survey (NHANES). This population was divided into two groups: those who either had cataract or were aphakic (i.e., had a lens removed) and those with neither cataract or aphakia. Of the 2,225 people in the selected population, 413 (18.6 percent) were placed in the cataract/aphakia group. UV data were developed by the National Oceanic and Atmospheric Administration (NOAA) for the 35 NHANES locations based on a statistical analysis of data from Robertson-Berger meters located at 10 of the NHANES sites. Subsequent validation of the estimates at 6 locations indicated differences of about 7 percent between the observed and estimated mean daily flux values. Hiller *et al.* (1983) modeled their data using the following logistic risk function:

$$P = \frac{1}{1 + e^{-(a+b_1X_1+\ldots+b_kX_k)}}$$

where P is the probability of having a cataract and X_{1-k} are the risk factors examined. In addition to UV, the risk factors examined were age, race, sex, education, diabetes, systolic blood pressure, and residence (urban versus rural). Hiller and her colleagues developed standardized regression coefficients under three conditions: as a function of each factor individually (univariate), as a function of each factor plus age (bivariate), and as a function of all risk factors simultaneously (multivariate).

The logistic function is commonly used in epidemiology when it is clear that age has a significant (and presumably independent) influence on risk (i.e., risk changes with age irrespective of exposure). However, such a specification also has drawbacks in that the dose-response curve created from the Hiller *et al.* (1983) data is non-linear. Thus, different BAFs must be used for each age cohort because of the changing slope of the curve. The following figure shows the dose-response relationships between UVR exposure and risk (prevalence) for the three age cohorts examined in the NHANES study: 42-54, 55-65, and 65+. The BAFs for these cohorts are 0.3, 1.3, and 4.3, respectively. Using this data, an age-weighted mean BAF that can be applied to an entire population is about 1.5.

Selection of the current action spectrum for cataract incidence

In order to derive a BAF, a weighting scheme must first be selected that assigns varying importance to different wavelengths of UV light according to their effectiveness in inducing a certain response. Often, this scheme takes the form of an action spectrum, in which monochromatic light at different wavelengths is administered to a test organism and each wavelength's effectiveness at inducing a specific health effect (e.g., tumors) is recorded.

By contrast, in the Hiller *et al.* (1983) cataract study, Robertson-Berger (R-B) meters at various NHANES sites measured light directly from the sun, weighting it as it was received from the natural source. This weighting scheme was discovered to be very similar to that derived for the erythema action spectrum. However, no biological connection is felt to exist between cataract formation and the incidence of erythema (sunburn), and it was believed that insufficient evidence existed at that time (i.e., 1983) to create an action spectrum based exclusively on cataract induction in laboratory animals. Thus, the Setlow DNA damage action spectrum, modified for human skin and renamed DNA-h, was suggested as a possible action spectrum to weight the wavelengths of solar radiation thought to be most effective in inducing cataract (Setlow *et al.* 1993).[2] Once an action spectrum is selected, it is integrated over the spectrum in question to generate one number, called the RAF. The RAF is used to weight the actual UV doses administered, which then are plotted against the response observed at each effective dose on a logarithmic scale. The slope of this curve is the BAF.

Use of the current RAF, obtained from the DNA-h action spectrum, to predict cataract incidence was questioned by participants at the August HSCT meeting (ICF 2000*b*). In response to these questions, the following changes are proposed with respect to the selection of the action spectrum, RAF, and dose-response curve used to derive the BAF for cataract incidence.

Interim solution

Pitts *et al.* (1977) have generated an action spectrum in rats for cataract incidence. A recent review of the original document discussing this derivation process reveals that this action spectrum is suited for use in the current application because it does in fact extend into the UVA wavelength range. Thus, the RAF from the Pitts *et al.* (1977) action spectrum will be used in the AHEF to weight future UV doses and thus estimate BAFs for future cataract incidence. The Robertson-Berger meter RAF and the BAFs obtained from the Hiller *et al.* (1983) study will continue to be used to estimate past cataract incidence. Using the updated BAF for cataract incidence will improve the predictions as compared with the prior methodology.

Future solution

The Salisbury Eye Project (West *et al.* 1998) measures cataract incidence (all major types) from a subset of the U.S. population. Once this project has concluded, its data will be used to generate a linear dose-response curve. UV doses for this curve will be weighted using the RAF from the Pitts *et al.* (1977) action spectrum. Because the curve will be generated using a linear function, only one BAF will be applied to all age cohorts.

[2] The AHEF uses the DNA-h spectrum to derive the BAF for cataract incidence.

References

Hiller, R., R. Sperduto, and F. Ederer (1983), "Epidemologic associations with cataracts in the 1971-1972 National Health and Nutrition Examination Survey," American Journal of Epidemiology, vol. 118, no. 2, pp. 239-249.

ICF Consulting (2000*b*), Summary of the Second Meeting on Next Generation Supersonic Civil Transport Evaluation Methods , Prepared for Stratospheric Protection Division, Office of Air and Radiation, U.S. Environmental Protection Agency, by ICF Consulting, Washington, DC. August 8.

Pitts, D.G., A.P. Cullen, and P.D. Hacker (1977), "Ocular effects of ultraviolet radiation from 295 to 365 nm," Invest. Ophthalmol. Visual Sci., vol. 16, no. 10, pp. 932-939.

Setlow, R.B., E. Grist, K. Thompson, and A.D. Woodhead (1993), "Wavelengths effective in induction of malignant melanoma," Proc. Natl. Acad. Sci. USA, vol. 90, pp. 6666-6670.

West S.K., B. Munoz, O.D. Schein, D.D. Duncan, G.S. Rubin (1998), "Racial differences in lens opacities - The Salisbury Eye Project," American Journal of Epidemiology, vol. 148, pp. 1033-1039.

West S.K., D.D. Duncan, B. Munoz, G.S. Rubin, L.P. Fried, K. Bandeen-Roche, O.D. Schein (1998), "Sunlight exposure and risk of lens opacities in a population-based study," *JAMA*, vol. 280, pp. 714-718.

Appendix F – Sensitivity to Choice of Reference Scenario

In this study, it has been assumed that the appropriate "reference" atmospheric scenario for expressing the health impacts of HSCT-induced stratospheric ozone depletion is one that reflects worldwide compliance with the stratospheric ozone control provisions of the Montreal Protocol, as amended through the "Montreal Adjustments" of that Protocol (i.e., the "Montreal Adjustments" reference scenario). A description of the Montreal Protocol and its amendments and adjustments is provided in Appendix G. The use of the reference atmospheric scenario is described in Section 2.5 and illustrated schematically in Figure 2-4.

Sensitivity tests indicate that modeled HSCT health impacts exhibit limited sensitivity to the specification of the reference scenario. Two sensitivity tests were performed that illustrate this sensitivity. First, the atmospheric ozone values of the Montreal Adjustments reference scenario were perturbed by ± 20 percent of the monthly differences between the Montreal Adjustments scenario and the 1979-1980 reference scenario ozone levels in 2015. This difference represents the greatest possible error that could be associated with the Montreal Adjustments baseline. The values for 2015 were selected because in later years the differences between the scenarios decrease as ozone levels are expected to recover. The ± 20 percent monthly differences for 2015 were then applied through 2050. Then, the ozone impacts resulting from a fleet of HSCT (developed as described in Section 2.2.2.a and 2.2.2.b) were applied to the perturbed reference scenario, and incremental health effects of HSCT relative to the perturbed reference scenarios were calculated as described in Section 2.5. The results of these simulations were then compared with the health impacts estimated relative to the "unperturbed" Montreal Adjustments reference scenario.

When the atmospheric ozone of the reference scenario was increased by 20 percent of the difference between the two baseline scenarios, estimated health impacts decreased by approximately 1.5 percent. Similarly, when reference scenario ozone was decreased by 20 percent of the difference, estimated health impacts increased by approximately 1 percent (except for cataract incidence, which increased by 2 percent). Table F-1 summarizes the results of these sensitivity tests.

Table F-1. Sensitivity of Reference Scenario Selection in Determining Total Predicted Excess Incidence or Mortality in the United States among People Born between 1890 and 2100 due to HSCT Operation (thousands)

Scenario	CMM Cases	CMM Deaths	BCC Cases	SCC Cases	NMSC Deaths	Cataract Cases
HSCT Scenario (Relative to the Montreal Adjustments)	36	4.5	970	520	2.6	360
HSCT (2015 Baseline Difference + 20%)	35 *(-1.6%)*	4.4 *(-1.6%)*	950 *(-1.5%)*	520 *(-1.4%)*	2.5 *(-1.5%)*	360 *(-1.3%)*
HSCT (2015 Baseline Difference - 20%)	36 *(1.0%)*	4.5 *(1.0%)*	970 *(0.8%)*	530 *(0.7%)*	2.6 *(1.0%)*	370 *(2.0%)*

Note: Negative numbers indicate fewer cases or deaths relative to the Montreal Adjustments. Percent values correspond to percent change in incidence/mortality estimates from the HSCT scenario central value. Negative percentages reflect lives saved as a result of increased ozone concentrations.

Second, an AHEF model simulation was performed in which atmospheric ozone amounts representative of 1979-1980 conditions were used as the reference scenario. The incremental health effects from HSCT relative to this reference scenario were estimated, and again compared with the health impacts estimated relative to the "unperturbed" Montreal Adjustments reference scenario. Incremental HSCT health impacts produced by the AHEF model using the 1979-1980 reference scenario were approximately 5 percent greater than those produced using the Montreal Adjustments reference scenario. This sensitivity analysis represents the greatest possible change in health effects that could be attributed to miscalculation in the baseline. Table F-2 summarizes the results of this sensitivity test.

Table F-2. Sensitivity of Reference Scenario Selection in Determining Total Predicted Excess Incidence or Mortality in the United States among People Born between 1890 and 2100 due to HSCT Operation (thousands)

Scenario	CMM Cases	CMM Deaths	BCC Cases	SCC Cases	NMSC Deaths	Cataract Cases
HSCT Scenario (Relative to the Montreal Adjustments)	36	4.5	970	520	2.6	360
HSCT (Relative to 1979-80 Baseline)	37 *(5.0%)*	4.7 *(5.0%)*	1,000 *(4.8%)*	550 *(4.6%)*	2.7 *(4.9%)*	390 *(7.6%)*

Note: Percent values correspond to percent change in incidence/mortality estimates from the HSCT scenario central value.

Appendix G – Summary of ODS Policy Controls

In Tables G-1 through G-4, this appendix presents the ODS phaseout schedules for both non-Article 5 (developed) and Article 5 (developing) countries under each of the policy scenarios discussed in Table 4-1 (i.e., the original Montreal Protocol, the London Amendments of 1990, the Copenhagen Amendments of 1992, and the Montreal Adjustments of 1997). In each table, phaseouts are presented as percentages of a given base year.

Table G-1. Original Montreal Protocol (1987)

Controls for Non-Article 5 Nations

	CFCs	Halons
Base Year	**1986**	**1986**
Controls		
Year	**Percent of Base Year**	**Percent of Base Year**
July 1, 1989	100%	---
1990	100%	---
1991	100%	---
1992	100%	100%
1993	80%	100%
1994	80%	100%
1995	80%	100%
1996	80%	100%
1997	80%	100%
1998	50%	100%

Controls for Article 5 Nations

	CFCs	Halons
Base Year	**1996**	**1996**
Controls		
Year	**Percent of Base Year**	**Percent of Base Year**
July 1, 1999	100%	---
2000	100%	---
2001	100%	---
2002	100%	100%
2003	80%	100%
2004	80%	100%
2005	80%	100%
2006	80%	100%
2007	80%	100%
2008	50%	100%

Table G-2. London Amendments (1990)

Controls for Non-Article 5 Nations

	CFCs	Halons	Carbon Tetrachloride (CCl_4)	Methyl Chloroform (CH_3CCl_3)
Base Year	**1986**	**1986**	**1989**	**1989**
Controls				
Year	**Percent of Base Year**	**Percent of Base Year**	**Percent of Base Year**	**Percent of Base Year**
July 1, 1989	100%	---	---	---
1990	100%	---	---	---
1991	100%	---	---	---
1992	100%	100%	---	---
1993	100%	100%	---	100%
1994	100%	100%	---	100%
1995	50%	50%	15%	70%
1996	50%	50%	15%	70%
1997	15%	50%	15%	70%
1998	15%	50%	15%	70%
1999	15%	50%	15%	70%
2000	0%	0%	0%	30%
2001	0%	0%	0%	30%
2002	0%	0%	0%	30%
2003	0%	0%	0%	30%
2004	0%	0%	0%	30%
2005	0%	0%	0%	0%

Table G-2, continued

Controls for Article 5 Nations

	CFCs	Halons	Carbon Tetrachloride (CCl_4)	Methyl Chloroform (CH_3CCl_3)
Base Year	**1996**	**1996**	**1999**	**1999**
Controls				
Year	**Percent of Base Year**	**Percent of Base Year**	**Percent of Base Year**	**Percent of Base Year**
July 1, 1999	100%	---	---	---
2000	100%	---	---	---
2001	100%	---	---	---
2002	100%	100%	---	---
2003	100%	100%	---	100%
2004	100%	100%	---	100%
2005	50%	50%	15%	70%
2006	50%	50%	15%	70%
2007	15%	50%	15%	70%
2008	15%	50%	15%	70%
2009	15%	50%	15%	70%
2010	0%	0%	0%	30%
2011	0%	0%	0%	30%
2012	0%	0%	0%	30%
2013	0%	0%	0%	30%
2014	0%	0%	0%	30%
2015	0%	0%	0%	0%

Table G-3. Copenhagen Amendments (1992)

Controls for Non-Article 5 Nations

	CFCs	Halons	Carbon Tetrachloride (CCl_4)	Methyl Chloroform (CH_3CCl_3)	HCFCs*	Methyl Bromide (CH_3Br)**
Base Year	**1986**	**1986**	**1989**	**1989**	**1989 (3.1%)**	**1991**
Controls						
Year	**Percent of Base Year**	**Percent of Base Year**	**Percent of Base Year**	**Percent of Base Year**	**Percent of Base Year**	**Percent of Base Year**
July 1, 1989	100%	---	---	---	---	---
1990	100%	---	---	---	---	---
1991	100%	---	---	---	---	---
1992	100%	100%	---	---	---	---
1993	80%	100%	---	100%	---	---
1994	25%	0%	---	50%	---	---
1995	25%	0%	15%	50%	---	100%
1996	0%	0%	0%	0%	100%	100%
1997	0%	0%	0%	0%	100%	100%
1998	0%	0%	0%	0%	100%	100%
1999	0%	0%	0%	0%	100%	100%
2000	0%	0%	0%	0%	100%	100%
2001	0%	0%	0%	0%	100%	100%
2002	0%	0%	0%	0%	100%	100%
2003	0%	0%	0%	0%	100%	100%
2004	0%	0%	0%	0%	65%	100%
2005	0%	0%	0%	0%	65%	100%
2010	0%	0%	0%	0%	35%	100%
2015	0%	0%	0%	0%	10%	100%
2020	0%	0%	0%	0%	0.5%	100%
2030	0%	0%	0%	0%	0%	100%

* The baseline HCFC consumption, or HCFC cap, was calculated as the total ODP-weighted HCFC consumption in 1989 plus 3.1 percent of the ODP-weighted CFC consumption in 1989.

** The methyl bromide freeze did not apply to post-harvesting uses (i.e. quarantine and pre-shipment).

Table G-3, continued

Controls for Article 5 Nations

	CFCs	Halons	Carbon Tetrachloride (CCl_4)	Methyl Chloroform (CH_3CCl_3)
Base Year	**1996**	**1996**	**1999**	**1999**
Controls				
Year	**Percent of Base Year**	**Percent of Base Year**	**Percent of Base Year**	**Percent of Base Year**
July 1, 1999	100%	---	---	---
2000	100%	---	---	---
2001	100%	---	---	---
2002	100%	100%	---	---
2003	80%	100%	---	100%
2004	80%	100%	---	100%
2005	50%	50%	15%	70%
2006	50%	50%	15%	70%
2007	15%	50%	15%	70%
2008	15%	50%	15%	70%
2009	15%	50%	15%	70%
2010	0%	0%	0%	30%
2011	0%	0%	0%	30%
2012	0%	0%	0%	30%
2013	0%	0%	0%	30%
2014	0%	0%	0%	30%
2015	0%	0%	0%	0%

Note: The Copenhagen Amendments did not change the Article 5 control schedule.

Table G-4. Montreal Adjustment (1997)

Controls for Non-Article 5 Nations

	CFCs	Halons	Carbon Tetrachloride (CCl_4)	Methyl Chloroform (CH_3CCl_3)	HCFCs*	Methyl Bromide (CH_3Br)**
Base Year	**1986**	**1986**	**1989**	**1989**	**1989 (2.8%)**	**1991**
Controls						
Year	**Percent of Base Year**	**Percent of Base Year**	**Percent of Base Year**	**Percent of Base Year**	**Percent of Base Year**	**Percent of Base Year**
July 1, 1989	100%	---	---	---	---	---
1990	100%	---	---	---	---	---
1991	100%	---	---	---	---	---
1992	100%	100%	---	---	---	---
1993	80%	100%	---	100%	---	---
1994	25%	0%	---	50%	---	---
1995	25%	0%	15%	50%	---	100%
1996	0%	0%	0%	0%	100%	100%
1997	0%	0%	0%	0%	100%	100%
1998	0%	0%	0%	0%	100%	100%
1999	0%	0%	0%	0%	100%	75%
2000	0%	0%	0%	0%	100%	75%
2001	0%	0%	0%	0%	100%	50%
2002	0%	0%	0%	0%	100%	50%
2003	0%	0%	0%	0%	100%	30%
2004	0%	0%	0%	0%	65%	30%
2005	0%	0%	0%	0%	65%	0%
2010	0%	0%	0%	0%	35%	0%
2015	0%	0%	0%	0%	10%	0%
2020	0%	0%	0%	0%	0.5%	0%
2030	0%	0%	0%	0%	0%	0%

* The baseline HCFC consumption, or HCFC cap, is calculated as the total ODP-weighted HCFC consumption in 1989 plus 2.8 percent of the ODP-weighted CFC consumption in 1989.

** The methyl bromide freeze does not apply to post-harvesting uses (i.e., quarantine and pre-shipment).

Table G-4, continued

Controls for Article 5 Nations

	CFCs	Halons	Carbon Tetrachloride (CCl_4)	Methyl Chloroform (CH_3CCl_3)	HCFCs	Methyl Bromide (CH_3Br)*
Base Year	**1996**	**1996**	**1999**	**1999**	**2015**	**Average of 1995-1998**
Controls						
Year	**Percent of Base Year**	**Percent of Base Year**	**Percent of Base Year**	**Percent of Base Year**	**Percent of Base Year**	**Percent of Base Year**
July 1, 1999	100%	---	---	---	---	---
2000	100%	---	---	---	---	---
2001	100%	---	---	---	---	---
2002	100%	100%	---	---	---	100%
2003	80%	100%	---	100%	---	100%
2004	80%	100%	---	100%	---	100%
2005	50%	50%	15%	70%	---	80%
2006	50%	50%	15%	70%	---	80%
2007	15%	50%	15%	70%	---	80%
2008	15%	50%	15%	70%	---	80%
2009	15%	50%	15%	70%	---	80%
2010	0%	0%	0%	30%	---	80%
2011	0%	0%	0%	30%	---	80%
2012	0%	0%	0%	30%	---	80%
2013	0%	0%	0%	30%	---	80%
2014	0%	0%	0%	30%	---	80%
2015	0%	0%	0%	0%	---	0%
2016	0%	0%	0%	0%	100%	0%
2040	0%	0%	0%	0%	0%	0%

* The methyl bromide freeze does not apply to post harvesting uses (i.e., quarantine and pre-shipment).

REPORT DOCUMENTATION PAGE

Form Approved
OMB No. 0704-0188

1. AGENCY USE ONLY (*Leave blank*)	2. REPORT DATE	3. REPORT TYPE AND DATES COVERED
	September 2001	Final Contractor Report

4. TITLE AND SUBTITLE

Human Health Effects of Ozone Depletion From Stratospheric Aircraft

5. FUNDING NUMBERS

WU-714-01-20-00
Interagency Agreement
Reference #80938647,
NASA Reference #C-30039-J

6. AUTHOR(S)

U.S. Environmental Protection Agency

7. PERFORMING ORGANIZATION NAME(S) AND ADDRESS(ES)

U.S. Environmental Protection Agency
Global Programs Division
1200 Pennsylvania Avenue, NW (6205J)
Washington, DC 20460

8. PERFORMING ORGANIZATION REPORT NUMBER

E-13018

9. SPONSORING/MONITORING AGENCY NAME(S) AND ADDRESS(ES)

National Aeronautics and Space Administration
Washington, DC 20546-0001

10. SPONSORING/MONITORING AGENCY REPORT NUMBER

NASA CR—2001-211160

11. SUPPLEMENTARY NOTES

This work was supported by NASA under RTOP 714-01-20-00 and by other contributions from the EPA. Project Manager, Chowen Wey, Vehicle Technology Center, NASA Glenn Research Center, organization code 0300, 216-433-8357.

12a. DISTRIBUTION/AVAILABILITY STATEMENT

Unclassified - Unlimited
Subject Category: 51 Distribution: Nonstandard

Available electronically at http://gltrs.grc.nasa.gov/GLTRS

This publication is available from the NASA Center for AeroSpace Information, 301-621-0390.

12b. DISTRIBUTION CODE

13. ABSTRACT ***(Maximum 200 words)***

This report presents EPA's initial response to NASA's request to advise on potential environmental policy issues associated with the future development of supersonic flight technologies. Consistent with the scope of the study to which NASA and EPA agreed, EPA has evaluated only the environmental concerns related to the stratospheric ozone impacts of a hypothetical HSCT fleet, although recent research indicates that a fleet of HSCT is predicted to contribute to climate warming as well. This report also briefly describes the international and domestic institutional frameworks established to address stratospheric ozone depletion, as well as those established to control pollution from aircraft engine exhaust emissions.

14. SUBJECT TERMS	15. NUMBER OF PAGES
Healthy impacts of supersonic aircraft	138
	16. PRICE CODE

17. SECURITY CLASSIFICATION OF REPORT	18. SECURITY CLASSIFICATION OF THIS PAGE	19. SECURITY CLASSIFICATION OF ABSTRACT	20. LIMITATION OF ABSTRACT
Unclassified	Unclassified	Unclassified	